ANALYSIS OF CHARACTERISTICS OF RANDOM MICROSTRUCTURES OF NANOMATERIALS

Thomas Bobga Tengen

A thesis submitted to the Faculty of Engineering and the Built Environment, University of the Witwatersrand, Johannesburg, in fulfilment of the requirements for the degree of Doctor of Philosophy.

Johannesburg 2008

DECLARATION

I declare that this thesis is my own unaided work. It is being submitted to the Degree of Doctor of Philosophy to the University of the Witwatersrand, Johannesburg. It has not been submitted before for any degree or examination to any other University.

……..…….
(Signature of Candidate)

…….. day of …….. year…….
day month year

ABSTRACT

Predicting and manipulating materials macroscopic properties from the knowledge of their microstructure characteristics are attracting significant attention in the field of Materials Science and Engineering. Nowadays, Nanoscience and Nanotechnology are engaged in these studies. Nanomaterials constituents, called herein unambiguously microstructures, have inherently random features/characteristics. In the research reported in this thesis the tools of stochastic processes and stochastic differential equations theory have been used as they offer a sound approach to understanding and analysing microstructures characteristics. This research adopts the approach of first delineating the necessary mathematical formulations, followed by their applications.

Substantial number of atoms at nanomaterial Grain Boundaries, GBs, lowers the material thermal stability leading to grain growth. The growth of individual grain size, ***d***, in a nanomaterial is apprehended to be jointly caused by Grain Boundary Migration, GBM, and Grain Rotation-Coalescence, GRC, mechanisms. A model is established that includes the previously ignored GRC in the expression for increment of ***d*** and, further, considering the fact that the energy required to activate GBM increases during grain growth. The stochastic counterpart of the expression is obtained by adding two fluctuation terms; to account for the random fluctuations in ***d*** caused by GBM and GRC. Results show that nanomaterials low stabilities are also due to their grains' high rotational mobilities at low grain size dispersion, CV(d). Using information about microstructure size evolution, its probability density function, pdf, is determined using the generalised Fokker-Planck-Kolmogorov equation. Results demonstrate that the type of scaling state pdf depends on the nature of the fluctuation terms. Grain growth parameters are calibrated in such a way that the pdf evolves lognormally throughout.

Microstructure-property dependence has for long been given by the Hall-Petch to Reverse Hall-Petch relationship, HP-RHPR, (a relationship between mechanical property and mean grain size, E(d), only). A modified model for this dependence is established using complete information about microstructure size distribution. Results suggest that both E(d) and CV(d) are central in designing materials with

required properties. Reasons for conventional, homologous and anomalous temperature dependences of yield stress are revealed.

Thus, implementing desired stochastic “properties” of microstructures entails designing required materials mechanical properties.

To my father

Ba Jacob Tengen

and my mother

Na Nahbula Prescila Kontan

ACKNOWLEDGEMENT

I gratefully acknowledge the assistance of my supervisor, Prof. RADOSLAW IWANKIEWICZ, for his untiring efforts, valuable guidance and insight to see the work through. My greatest appreciations equally go Professor KRZYSTOF JAN KURZYDLOWSKI and Dr. TOMASZ WEJRZANOWSKI for their readiness to scientifically collaborate and exchange data. My endless thank to the Dean, Prof. Jerzy Szawlowski, of the Faculty of Material Science and Engineering, Warsaw University of Technology, Poland, for twice inviting me to pay study visits to his faculty, providing me with access to all the research facilities in the faculty and taking care of my subsistence while in Poland. Thanks to the South African National Research Foundation (NRF) for the financial assistance.

I am grateful to the entire members of staff of the School of Industrial, Mechanical and Aeronautical Engineering, University of the Witwatersrand; and Faculty of Materials Science and Engineering, Warsaw University of Technology, for their academic encouragement and assistance through this work. Thanks to Prof. Harold Campbell, Dr Jimoh O. Pedro and Mrs Sujee Kay (proof reading).

My acknowledgment also goes to my parents, Ba Jacob Tengen and Na Prescila Nkontan; my brother, Tengen Edwin Vola; my cousins, Ernest Gadinga Nti, Valentine Dobgima Nti, Godfrey Nyamalum Nti; my Friend, Tembe Wilfred Bakala and all fellow Cameroonian brothers and sisters in South Africa for their moral, material and financial supports. I wish to thank all members of the family of Ba GWAGU for their financial support throughout my academic life, Nyoni Cathrine Nahsala, Nicoline Fuhjem, Kahboh Emilia,, Denis Wagua, Chief Bernard Mbancho (proof reading), Robert Tingo, Dr. Chamba Lawrence, Muzang Thierry Mayor, Maxwell Vubangsi and Nelsoft Communications.

Not the least, thanks to all postgraduate students of the School of Industrial, Mechanical and Aeronautical Engineering, University of the Witwatersrand, for their flexibility and readiness to discuss academic.

CONTENTS

LIST OF FIGURES

LIST OF TABLES

LIST OF SYMBOLS AND ACRONYMS

Coefficient of Variation	CV
Coefficient of Variation of grain size or grain size dispersion	CV(r)
Curvature driven **G**rain **B**oundary **M**igration mechanism	GBM
Feature on microstructure at cross-section located at ω and at time t	X(ω,t)
Grain Boundary	GB
Grain Boundaries	GBs
Grain boundary mobility	M(r,T)
Increment of Weiner (continuous) Process	dW(t)
Increment of stochastic counting process	dN(t)
Increment of number of Coalescence events or mechanisms	
Of grains within infinitesimal time interval	dN(r,t)
Material mean yield stress	σ
Material mean yield stress	σ (E(r),CV(r))
Material mean yield stress due to simultaneous GBM-GRC	
at temperature T Kelvin	$\sigma_{Tot,T}$
Material mean yield stress due to GBM only at temperature T Kelvin	$\sigma_{Mig,T}$
Material mean yield stress due to GRC onlyat temperature T Kelvin	$\sigma_{Rot,T}$
Mean grain size	E(r)
Mean grain size	E(d)
Misorientation angle driven **G**rain **R**otation **C**oalescence mechanism	GRC
Probability Density Function	pdf
Rate of Coalescence events of grain	v(r,t)
Severe Plastic Deformation	SPD

REPORT FORMAT

This report is made up of two major parts. The first part introduces the project that has to be carried out and the background knowledge necessary to comprehend and undertake the project. The second part deals with the applications of knowledge presented in the first part which is another effort aimed at the interpretation and manipulation of the materials properties.

PART ONE

MATHEMATICAL FORMULATIONS

1 MOTIVATIONS AND BACKGROUND

From classical theories, small objects are considered to be smooth (homogeneous continuum) while big ones are rough and angular (heterogeneous). But the local observation of any material microstructures reveals fine details within infinitely small range of length scale. These details usually become increasingly apparent if the magnification of the observing microscope is ever-increasing. The details may vary with different materials under consideration. Within a single material, the variations may not be spatially uniform. Within infinitely small range of length scale (nanoscopic/mesoscopic range of length scales), but well above the discrete atomic levels present in any material, the internal constituents of a material (termed in this report as the material microstructures) usually possess characteristics which uniquely describe the particular material. These characteristics are, for example, measures, dimensions, the manner in which the constituents respond to strain rate, to strain hardening and to deformation mechanisms by **G**rain **B**oundary (GB) diffusion, by dislocation glide, by grain interior diffusion and by grain interior dislocation motion. These internal characteristics are termed "microstructure characteristics" in this report. Since the fine details reveal "random fine structure(s)" or "random microstructure(s)", these characteristics are obviously random too; and hence, the name "characteristics of random microstructure(s) of nanomaterials."

Conventional engineers make use of macroscopic properties like energy, strain and stress. These macroscopic properties arise as a result of "averaging in some sense" of the characteristics or properties that are generated from structures at mesoscopic/nanoscopic range of length scales. To better understand and to interpret with some degree of certainty the macroscopic properties, one has to first understand the exact nature of these mesoscopic characteristics that generate the macroscopic properties. Another most important issue is "how to relate the various microstructure characteristics within any material so as to yield the observed macroscopic property".

The overall mechanical properties of a material can be quite different due to the fact that the internal microstructures can be quite different at various ranges of length scales that these microstructures might be formed. For example, nanomaterials with finer sizes of constituent particles/grains possess more enhanced mechanical properties as compared to conventional materials with coarser particles/grains. Furthermore, nanomaterials produced through different processing routes to the same mean grain size may be different in their grain size dispersion and as such may exhibit different materials properties. And different nanomaterials having different mean grain sizes and grain size dispersions (different nanomaterials) may have the same materials properties. Hence, understanding the microstructures and their distributions in materials should help in obtaining the (microstructure) characteristics that generate the (macroscopic) engineering properties. An important point is that these macroscopic properties are not only determined by the (physical, mechanical, etc) properties of the constituents, but also by the constituents' morphology, i.e. by their topological (concerning shape) and metric (concerning volume) properties.

Since several observations have been made which reveal that the process of refining the sizes of the internal constituents of materials is accompanied by the instability of the materials' properties as the grains/constituents tend to grow more pronouncedly, a good knowledge of these grain growth processes should be crucial to the understanding of the evolution of the engineering properties. As such, microstructures evolutions and their impact on the evolution of the engineering properties will be dealt with.

Central to the analysis of the microstructure-property relation in materials is the Hall-Petch relationship, HPR, that expresses the yield stress, σ, of a material as function of the size, $\boldsymbol{r}$, of the constituent particles given for constant K as, [1,2]

$$\sigma = \sigma_0 + K\mathbf{r}^{-1/2} \tag{1.1}$$

The above expression indicates that as the sizes of the microstructures reduce the

strength of the material increases. But due to the fact that the material strength does not increase indefinitely as the grain sizes decrease and coupled with observations that refining the material beyond some refinement critical mean grain size leads to decreasing material property as the grain sizes decrease, the HPR relationship/expression is supposed to be modified. Zhao, [3], derived a **single modified** expression, HP-RHPR, that represents the size-property dependence (both HPR and Reverse-HPR) throughout the entire range of deformation to be

$$\sigma(\mathbf{r}) = \sigma_0^{'} + A\mathbf{r}^{-1/2} - B(\mathbf{r}^{-1/2})^2 - C(\mathbf{r}^{-1/2})^3 \qquad (1.2)$$

where $\sigma_0^{'} = \sigma_0 + K_t$ is the conventional yield stress, $A=K=K_d$ is the Hall-Petch Relationship proportionality constant, $B = K_t[2hH_m / RT_r]$, $C = K_d[2hH_m / RT_r]$, K_t is a constant, h is atomic diameter in the case of metal, H_m is the bulk melting enthalpy, R is ideal gas constant, T_r is the room temperature, $K_d > 100K_t$ and $\sigma_0 > 10K_t$. Hence, since the materials properties depend on random microstructures that can correctly be described by some probability distribution, there are also similar needs to analyse the distribution of the materials properties in the materials. This distribution of the materials properties is dealt with in the later part of this report.

In order to undertake experimental investigations on materials microstructures, cutting planes maybe made randomly through the materials, and the microstructures are then randomly sectioned. Observing particles or grains of similar shape in a material (in space) could produce quite heterogeneous shape profile while those of differing shapes could produce a homogeneous shape profile. Efforts to resolve such controversial observations thoroughly are being dealt with under stereology. Stereology deals with the process of reconstructing three-dimensional information from two-dimensional images. If the number of objects under study is very large, coupled with the fact that the microstructure sizes, shapes and orientations are random in nature, then statistical analysis makes

sense and is indeed necessary. But statistical analysis is limited as it is assumed in it that the statistics of a section of the material is the statistics of the entire material (i.e. it deals with representative Volume element or *continuum theory*). It therefore, makes sense to reformulate the problems within the stochastic framework that uses field variables and as such can handle spatial variations easily. Knowledge of stochastic theory is presented in the later part of this report.

As it can be noticed, microstructures play important roles in this project. Thorough examination of a single microstructure (polyhedral tessellation) in material or space reveals that it is made up of some random features. The topological randomness of the microstructure of random polyhedral tessellations means that, [4,5], the number of the corners or vertices, C, the length of edges, E, and the number of faces, F, are random variables satisfying the self-consistency relations. For an isolated polyhedron, the relationship between these variables may be given by the Euler's formula, [4,5,6], as

$$C - E + F = 2 \tag{1.3}$$

and for any subdivision of the material into a finite number, N, of polyhedrons (grains) and irrespective of the number of edges connected at each corner; it is stated [4-9] that:

$$C - E + F + N = 1 \tag{1.4}$$

It follows, then, that sizes and shapes are connected. Stoyan, [10], called this connection as form. Thus, shapes and sizes may be investigated simultaneously. In analysing this connection (in analysing form), it is desirable to have parameters that can be interpreted physically or biologically. Since in most cases one cannot expect that the form-parameters uniquely determine figure in the sense that reconstruction is possible, one cannot also expect that the microstructure characteristics obtained as a result of these form parameters should uniquely reveal macroscopic properties. It should be noted that the shape of figure X is

always independent of its location, orientation in a plane and scales changes do not change shape. Example of a shape parameter is a function *f(x)*, [10]

$$f(X) = \frac{area \text{ of X}}{(perimeter \text{ of X})^2} \tag{1.4}$$

Recall that the effort of the present project is to interpret and/or manipulate materials properties from the knowledge of the internal microstructures. The knowledge of Geometric Measure Theory (or fractals) should also be helpful in the analysis of microstructure characteristics and material properties. Fractals are mathematical models for very irregular and very detailed sets with their topological dimensions smaller than the Hausdorff dimensions. Most macroscopic properties of materials are analysed by studying behaviours along the **G**rain **B**oundarie**s** (GBs). The boundaries (coastlines) of irregular sets in R^2 may be fractals, [10], and not the entire set as both the topological and fractal dimensions of the entire set are equal to 2. In nature, one often observes structures and phenomena with similar behaviour [11,12] like those of fractals. Adding to the list of examples given by Stoyan, [10], are the "boundaries" of rough and irregular objects such as the microscopic examinations of materials constituent structures. Of course, the behaviour of natural phenomena resembles that of mathematical fractal only up to a certain scale (i.e. infinite refinement is impossible in nature). But this should not create any difficulty in applications because frequently, what are of practical interests are just the scale and the accessibility to measurement in which the real objects have fractal-like behaviour, [10]. Hence, the theory of fractals (or geometric measure theorems), when applied with a lot of cautiousness, can help in the study and analysis of random microstructures (or form). For example, Lebesgue measure, a fractal characteristic, plays a useful role during the characterisation of microstructure. It is defined as the *n*-dimensional "volume", where "*n*" is a positive number. The "measures" of random material microstructure features, e.g. grain size, are described by some probability distributions. Thus, the stochastic features of microstructures are related to measures through the probability distributions.

2 MICROSTRUCTURE CHARACTERIZATIONS

Since the inherent features of nanostructures/microstructures are random, this chapter is devoted to outlining the tools that can be used for the local characterization (description) of materials' constituent structures, the corresponding properties or characteristics and the stochastic characterizations of these features. This should be the gateway into the analysis of practical results as different characterisation techniques offer different approaches to analysing the experimental data or the different characterisation techniques determine the extents to which data can be analysed. For example, if the local profile of a particle is reported by the Voronoi polygon of the particular particle or by the fractal measure of the particular particle, then a stochastic counterpart of this description has to be established before any further analysis. This is because different particles in the materials have different profiles, and as such the particle profile in the material is random. Thus, the analyst must always asks himself/herself of the characterisation techniques that were deployed during experimentations

In order to develop "any" model of (heterogeneous) material microstructures such that it can be applicable to problems in solid mechanics, one must always base the approach on physical realities. These physical realities are the features and properties of the material microstructures that are obtainable from experiments. It is, without loss of generality, logical to develop models for composite and/or polycrystalline materials as these two classes encompass most materials commonly used today.

2.1 Geometric Characterizations

The characterisation of a particle is the act of communicating the description of the essential multidimensional features/properties of the particle or a collection of particles. This may start with the characterization of the local geometry in random parking of particles that describe the geometry of a group of particles that

surround a particular particle. The particles may have various sizes and shapes. A complete description of an irregular parking is given by specifying the location, size, shape and orientation of each particle. But since this is a tedious task which is time consuming and practically impossible, the applicable approach is to characterize the geometrical structure of the irregular parking stochastically. This can be done by stochastic description of the Voronoi polygons that surround each particle. The description of the shapes of the Voronoi polygons contains information that gives the radial distribution function for the particle's neighbours and the geometric shapes formed by groups of neighbouring particles.

2.1.1 Voronoi Polygon

The Voronoi Polygon of a particle is that region of space which is closer to that particular particle centre than to any other particle centre, [5,13,Fig.2.1]. Mathematically, let a realisation of random point fields be given by a countable set of randomly distributed points $\{r_i\} \in \Re^3$, $i = 1,2,...$, and to each point r_i assign a set A_i such that, [5]

$$A_i = \left\{ r_z \in \Re^3 : |r_z - r_i| \le |r_z - r_j|,\ i \neq j \right\} \tag{2.1}$$

then the family of sets $\{A_i\}$ is known as the Voronoi tessellation in R^3 generated by the random points r_i, $i=1,2,\ldots$ The Voronoi polygon in R^3 is completed in such a way that it is bounded by planes that are perpendicular bisectors between neighbouring particles centres. It is stated that for a Voronoi polygon the edges are lines that are equidistant from three particles centres, the vertices are points that are equidistant from four particle centres and its number of faces gives the number of the particle's neighbours, [13]. Note that the neighbouring grains might or might not touch each other. If the random point field $\{r_i\}$ is a homogeneous point field then the tessellation is the well known Poisson-Voronoi-tessellation.

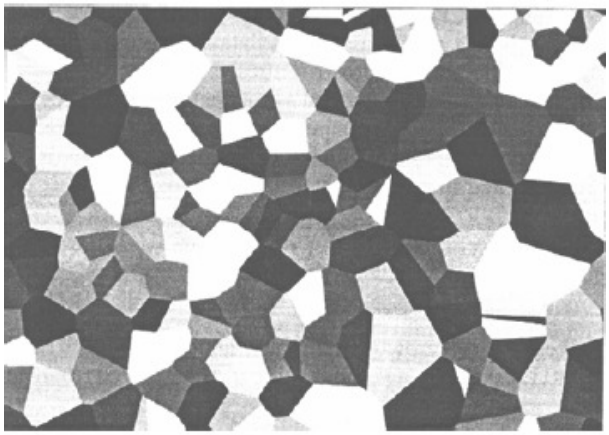

Figure 2.1 *Simulation of planar Poisson Voronoi tessellation,* [5]

2.1.2 Communicating local description of a particle profile

After describing the Voronoi polygon, the next issue is then the detailed local description of a particle profile that may be achieved mathematically**.** The representation of particle *profile* in polar coordinate has the form, [14],

$$R(\theta) = a_0 + \sum_{n=0}^{\infty} (a_n \cos n\theta + b_n \sin n\theta) \tag{2.2}$$

the representation of *extended surface* has the form

$$G(r,\theta) = \sum_{n=0}^{\infty}\sum_{m=0}^{\infty} (a_{m,n} \cos n\theta + b_{m,n} \sin n\theta) J_n(\gamma_{m,n} \frac{r}{R_v}) \tag{2.3}$$

and the representation of *3-D bulky* particle is

$$R(\theta,\varphi) = \sum\sum (a_{m,n} \cos m\theta + b_{m,n} \sin m\theta) P_n^{\,m}(\cos\varphi) \tag{2.4}$$

where the (a_n ,b_n) are Fourier coefficients and not shape function because they vary anisotropically. The equivalent radius, R_0, is defined as, [14],

$$R_0^{\,2} = a_0^{\,2} + \frac{1}{2}\sum_{n=1}^{\infty}(a_n^{\,2} + b_n^{\,2}) \tag{2.5}$$

where πR_0^2 is the area of the profile and a_0 is the mean radius. Stoyan, [10], states that if the contour of a figure is represented by a radius-vector function $r_X(\vartheta)$, then the area A(x) and perimeter U(x) are given by

$$U(X) = \int_0^{2\pi} [r^2(\vartheta) + r'^2(\vartheta)]^{1/2} \, d\vartheta \tag{2.7}$$

$$A(X) = \frac{1}{2}\int_0^{2\pi} r^2(\vartheta) d\vartheta \tag{2.8}$$

This leads to the following statistical relationship about the figure

$$\sigma^2(r) = \frac{A}{\pi} - \bar{r}^2 \tag{2.9}$$

where A is the area of the figure, $\bar{r}$ is the mean radius and σ^2 is the variance. Thus, comparing (2.5) and (2.9), it follows that the variance is given by

$$\sigma^2(r) = \frac{1}{2}\sum_{n=1}^{\infty}(a_n^{\,2} + b_n^{\,2}) \tag{2.10}$$

Knowing that a particle profile may be represented in polar coordinate form as given above that can be easily manipulated mathematically; the next target is how to communicate the description of the measured particle profile. To communicate the local description of a particle profile, Beddow, [14], suggests the use of a set of mathematical descriptors and a corresponding set of verbal descriptors. Beddow, [14], further suggests that the features should be given as moment of distributions that can be represented in the form of the moment vector (or matrix). The result is matrix operation of the form, [14]

$$\underset{\text{Measurement Vector}}{\mathbf{M}} = \underset{\text{Basis Set}}{\mathbf{B}} \; X \; \underset{\text{Characterization Vector}}{\mathbf{C}} \qquad (2.11)$$

The basis set should be made up of standard figures against which all other sizes or shapes of profiles could be compared, the feature or measurement vector is obtained from the experimental data and the characterisation vector is obtained as a result of the matrix operation (2.11) above. The basis set is compiled in such a way that succeeding columns are made up of standard figures such as circle (1^{st} column), cardioids (2^{nd} column), lemniscates (3^{rd}), equilateral triangle (4^{th}), square (5^{th}), pentagon, hexagon, etc. Each term in the characterisation vector describes the proportion to which the profile being analysed corresponds to the symmetry of a circle (a_1), a cardioids (a_2), and so on.

2.1.3 Stereological procedure

In order to conduct experimental investigations of microstructure features, observations are frequently made on the material surfaces after cutting the material randomly or on a probe line randomly placed on it. The same observation of an anisotropic material in space may produce different results depending on how the material is placed or on the orientation of the cross-section. Kanatani, [15], defines Stereology as the art of estimating "multidimensional" geometrical characteristics of microstructure from “partial observation” of the material, such as from observation of cross-sections or thin slices. Kanatani [15] then suggests that to engage in stereological project the individual undertaking the task should possess the ability to investigate average quantities; to estimate size distribution; and to estimate structural anisotropy due to internal distribution of line tissues and surfaces.

Estimating averaging quantities

The Average density quantities (average because they are given as per unit values) that can be estimated more easily are, [15],

V_v – volume of a specific phase per unit volume of material,

A_v – area of a specific internal surface structure per unit volume,

L_v – length of specific internal tissue per unit volume,

A_A – area of specific phase per unit area,

L_A – length of intersection with the internal surface structure per unit area,

N_A – number of intersections with internal line tissue per unit area,

L_L – length of intercept made by a specific phase per unit length, and

N_L – number of intersections with the internal surface structure per unit length.

The quantities are related to each other. For example, [15],

$$L_V = 2N_A \text{ and } A_V = \frac{4L_A}{\pi} = 2N_L \tag{2.12}$$

Estimating size distribution

Most often the experiments report on the equivalent radius, and as such, one deals with the equivalent radius (i.e. spherical in shape) of particle. Since many of these particles with different sizes are randomly distributed in a material, it is necessary to know the distribution of their sizes. The "distribution density" F(R) may be defined such that F(R)dR is the number of randomly distributed spheres of radii between R and R+dR in a unit volume of material. From the observation of a random cross-section on the material, the observed distribution density f(r) may be defined such that f(r)dr is the number of cross-sections of radii between r and r+dr in unit area of the plane. Then, F(R) and f(r) are related through the integral equation, [15],

$$f(r) = 2r \int_r^{R_{max}} \frac{F(R)dR}{\sqrt{r^2 - R^2}} \quad \Leftrightarrow \quad F(R) = \frac{R}{\pi} \int_R^{R_{max}} \frac{d(f(r)/r)}{\sqrt{r^2 - R^2}} \ldots\ldots(1) \tag{2.13}$$

Their corresponding (cumulative) distribution functions are, [15],

$$\phi(r) = 2\overline{R}N - 2\int_{r}^{R_{\max}} \sqrt{R^2 - r^2}\, d\Phi(R) \;\Leftrightarrow\; \Phi(R) = N - \frac{1}{\pi}\int_{R}^{R_{\max}} \frac{d\phi(r)}{\sqrt{r^2 - R^2}} \qquad (2.14)$$

where N is the number density and $\overline{R}$ is the mean radius of particles.

Estimating structural anisotropy

Since the microstructures features are random in nature, structural anisotropy may be characterised by the distribution density. The distribution density is expressed in terms of the "fabric tensor" and is also related to observed data by the "Buffon transform". Thus, the determination of the distribution density reduces to inverting the Buffon Transform.

a) **Definite model of anisotropy in mathematical sense (estimation of distribution density** *f(n)***)**

Internal line tissues or surfaces of differing shapes may be distributed in the materials. Let these line tissues (or surfaces) be hypothetically dissected into infinitesimal small line (or surface) segments that may be given by unit vectors **n** indicating their orientations. Note that **n** and **–n** both indicate the same orientation. As such one of them may be chosen randomly with the probability of ½. Kanatani, [15], suggests that the "distribution density" f(n) should be defined such that f(n)dΩ(n) is the total length of those line segments (or respectively the total area of those surface segments), in unit volume of the material, whose orientation are inside the differential solid angle dΩ(n) around **n.** If the distribution is isotropic then f(n)=const. Kanatani, [15], states that $C = \int f(n)d\Omega(n)$ is the total density i.e. $\int f(n)d\Omega(n) = L_V$ or respectively $\int f(n)d\Omega(n) = A_V$

b) **Determination of parameters of *f(n)***

The "spherical harmonics" expansion of *f(n)* in the Cartesian tensor notation is given as, [15]

$$f(n) = \frac{c}{4\pi}[1 + D_{ij}n_i n_j + D_{ijkl}n_i n_j n_k n_l + ...] \tag{2.15}$$

Define the moment tensor by

$$N_{ij} = \frac{1}{c}\int n_i n_j f(n) d\Omega(n), \qquad N_{ijkl} = \frac{1}{c}\int n_i n_j n_k n_l f(n) d\Omega(n) \tag{2.16}$$

where the tensors $\boldsymbol{D_{ij}, D_{ijkl}, \ldots}$ are "**deviator tensors**" and $\boldsymbol{N_{ij}, N_{ijkl}, \ldots}$ are "***fabric tensors***" of the distribution f(n). Then, there exists relationships between D_{ij}, D_{ijkl}, …and the N_{ij}, N_{ijkl},… through the Buffon transform.

Buffon Transform: Let the material be randomly dissected by a cutting plane with unit surface normal *m*, and let *N(m)* be the *number* of intersections with line tissues per unit area of the cutting plane. Then, the Buffon Transform states that the relationship between *N(m)* and the distribution density *f(n)* of the line tissues is in the form, [15]

$$N(m) = \int |m \cdot n| f(n) d\Omega(n) \tag{2.17}$$

If *N(m)* is the *length* of intersections with surfaces per unit area of the cutting plane, then the expected value of *N(m)* is related to *f(n)* by Buffon Transform, [15], as

$$N(m) = \int |m \times n| f(n) d\Omega(n) \tag{2.18}$$

2.2 Geometric Measure Theory: Mesoscopic Characteristics or Properties

The following section outlines some of the concepts and formulae of Geometric Measure Theory that are useful in analysing microstructures and their corresponding characteristics. It should be emphasized that under this major subsection the term "material" may stand for the entire nanomaterial and the term "microstructures" then represents the nanomaterial constituent particles. Furthermore, the name "material" may be used in the place of a nanomaterial constituent particle in which case the term "microstructures" then stands for the features on the constituent particle. Mathematically speaking, microstructures are subsets of a material, though a microstructure can still be made up of smaller subsets.

Local observations of materials microstructures reveal fine details within an infinitely small range of length scale, but well above the discrete atomic level present in any material. The fine details become more and more apparent as the magnifications of the observing microscopes become ever increasing. It has been demonstrated in the previous section that the local detailed features/profiles of a microstructure can be communicated in the polar coordinate form. Another level of characterisation that deals with the complete description of the local profile of a microstructure, as well as combining these local profiles of different microstructures to obtain the profile/shape of the entire material involves the use of the knowledge from Geometric Measure Theory. To apply the theorems of the Geometric Measure Theory, in the report, the description of the particle profile is termed "measure" and the corresponding property of that particle (or that measure) is termed dimension. Both measure and dimension of a microstructure can furthermore be called the microstructure characteristics. It is thus necessary to present some of the knowledge about measure and dimension as conveyed from the Geometric Measure Theory point of view.

2.2.1 Mathematical measures of microstructures or the entire nanomaterials

Mathematical measure of (nano)-material may be defined as a way of ascribing a numerical "size" to material, such that if the material is decomposed into a finite or countable number of pieces (the "pieces" are, for example, nano-sized grains or microstructures) in a reasonable way, then the size of the whole material is the sum of the sizes of the constituent microstructures, [derived from 11,12] i.e.

$$\mu(A) = \mu\left(\bigcup_i A_i\right) \leq \sum_i \mu(A_i) \tag{2.19}$$

with equality if the $\{A_i\}$ do not overlap. The μ(A) is called the measure of the material A, and μ(A) is the size of the material A measured in some way. Note that similar definitions hold for individual microstructures. In the microstructure case and in 2-D for example, the equivalent radius ("size" of the microstructure) may be obtained from the sum of the length of the edges, and in 3-D for example, the sum of the "size" or area of the faces is related to the volume of the grain from which the equivalent radius can be obtained as well.

The importance of both experimental findings and the mathematical interpretations/manipulations of those findings to advancements in sciences and technologies cannot be over emphasised. Since Lebesgue measure is easily obtainable from experiments and it is directly related to Hausdorff measure which is mathematically tractable, there is a need to present next, these two types of measures and the relationship between them.

Lebesgue Measure, L^n, is a natural extension to a large class of "n-dimensional volume". As a definition [derived from 11,12], let

$A = (x_1, x_2, x_3, .., x_n) \in \Re^n$, $\quad a_i < x_i < b_i$ then

$Vol^n(A) = (b_1 - a_1)(b_2 - a_2)(b_3 - a_3)...(b_n - a_n)$ and

$$L^n(A) = \inf\left\{\sum_{i=1}^{\infty} Vol^n(A_i) : \mathrm{A} \subseteq \bigcup_{\mathrm{i}=1}^{\infty} \mathrm{A}_\mathrm{i}\right\} \tag{2.20}$$

where $\{A_i\}$ is a covering of A, A_i is parallelepiped or the Voronoi polygon and $L^n(A)$ is the Lebesgue measure of the material A. A collection of microstructures, $\{A_i\}$, is a cover (δ-cover) of the material A if A is the subset of the "countable" union of the A_i (with $|A_i| \leq \delta$ for δ-cover). Saying that A is a subset of the countable union of the A_i means that the "size" of A is less than or equal to the size of the countable union (or combination) of the A_i

Hausdorff Measures, H^n: Adopting from Stoyan's definition of fractals, [10], the n-dimensional Hausdorff measure of a material A may be defined, where the microstructures that are δ-covers are closed discs $b(x_i, r_i)$ (i.e. the microstructures are spherical in nature), as

$$H_\alpha^n(A) = \omega_n \lim_{\delta \downarrow 0} \inf\left\{\sum_{(i)} r_i^n : \mathrm{A} \subset \bigcup_{(i)} b(x_i, r_i), \quad \mathrm{r_i} < \delta\right\} \tag{2.21}$$

where $\omega_n = \pi^{n/2} \Big/ \Gamma(1+\frac{n}{2})$; $\omega_0 = 1, \ \omega_1 = 2, \ \omega_2 = \pi$

Relationship between Lebesgue, $L^n(a)$, and Hausdorff, $H^n(a)$, measures is given by, [11,12],

$$H^n(A) = c_n L^n(A) = 2^{-n} v_n L^n(A) \tag{2.22}$$

where $c_n = \pi^{\frac{1}{2}n} \Big/ \left[2^n \left(\frac{n}{2}\right)!\right]$ is the volume of n-dimensional spherical microstructure of diameter 1. Thus, the following interpretations are given to these n-dimensional Hausdorff measures, [11,12],

$H^0(A)$ = number of microstructures in A,

$H^1(A)$ = length of smooth curve A,

$H^2(A)$ =(¼)*π* area(A), if A is a smooth surface, and

$H^3(A)$ = (4/3*)π *Vol (A).

2.2.2 Dimension of a microstructure/material

Though "dimension" provides only limited information, it can be used to measure irregular microstructures/material. This is because it is mathematically tractable, it can also be estimated by experiments and it has been proven that the dimension of an object is related to other features of the objects. It is acknowledged that it is possible to define dimension of a (nano)-material in many ways. Different definitions may give different values of dimensions for the same material, and may also have very different properties. Two materials of the same dimensions may not be equal. Upper box-counting and Hausdorff dimensions are of interest because in practice all the definitions of dimensions take values between these two dimensions and if the two extreme values are equal, then all others will assume this common value. A similar fact that will be dealt with in detail in PART TWO of this report is that it is possible to produce nanomaterials through different processing routes. Different processing routes may result in the same mean grain size but with different grain size dispersion (i.e. results in different material) and hence different material property. Two different materials may possess the same property. Thus, it can be acknowledged that "the process of defining dimension of a material" is similar or related to "the fabrication of nanomaterials through different processing routes", and "the dimension of material" is related to "grain size distribution parameters such as mean grain size and grain size dispersion". The exact nature of the relationship or the correlation is opened to further research.

The box counting dimension: Draw a mesh of side δ and count the number $N_\delta(A)$ that overlaps the material for various δ (hence the name "box-counting").

The dimension is the logarithmic rate at which $N_\delta(A)$ increases as $\delta \to 0$, and may be estimated by the gradient of the graph of $\log N_\delta(A)$ against $-\log\delta$ as

$$Dim_B A = \lim_{\delta \to 0} \frac{\log N_\delta(A)}{-\log \delta} \tag{2.23}$$

The number of mesh or cubes of sides δ that intersect a material is an indication of how spread out or irregular the material is when examined at that scale δ. Thus, dimension reflects how rapidly the irregularity develops as $\delta \to 0$. Note that the mesh or cube of side δ is a rough approximation of a microstructure profile of "size" is δ. Thus, the box-counting dimension is the dimension of an approximated profile compared to the Hausdorff dimension which is that of a more detailed profile.

Hausdorff dimension of a material A with Hausdorff measure $H^s(A)$ is defined as

$$Dim_H(A) = \inf\left\{n : H^n(A) = 0\right\} = \sup\left\{n : H^n(A) = \infty\right\} \tag{2.24}$$

Dimension of self-similar microstructures: If $A = \bigcup_{i=1}^{m} A_i$ where each A_i is geometrically similar to A but scaled by a factor c_i then provided that the A_i do not overlap "too much", it follows that

$$Dim_H A = n \text{ if } \sum_{i=1}^{m} c_i^{\,n} = 1 \tag{2.25}$$

For random fractals (i.e. randomly distributed self-similarity of the microstructures) and with the mean calculated according to the distribution of the similarities, then the Hausdorff dimension of the material A is "n" if the following condition adapted from Stoyan, [10], holds,

$$Dim_H A = n \quad \text{if} \quad \mathbf{E}\left(\sum_{j=1}^{m} c_j^n\right) = 1 \tag{2.25}$$

2.2.3 Local properties of dimensions and measures; and dimension decompositions

Much of the theories of Hausdorff and parking dimensions depend on the local properties of suitably defined measures. Thus, the so-called "lower local dimension" of measure is the basic working tool since it is closely related to the Hausdorff dimension of the measure by, [11,12],

$$Dim_H \mu = \sup\{s : \underline{\dim}_{loc}\mu(x) \geq s \text{ for } \mu - a.a \;\; x\} \tag{2.26}$$

The dimension of measures can be expressed as dimension of the material as, [11,12],

$$Dim_H \mu = \inf\{\dim_H A : A \text{ is a Borel set with } \mu(x) > 0\} \tag{2.28}$$

The local dimension describes the power law behaviour of $\mu\{\mathrm{B(x,r)}\}$ for small r (i.e. the power law behaviour of the measure of the microstructure). Thus, if a measure μ has local dimension α, then μ can be expressed as $\mu\{\mathrm{B(x,r)}\} = \mathrm{r}^{\alpha}$. To define the local dimension of a measure μ, let μ be finite Borel regular measure of R^n, so that $0<\mu\ (R^n)<\infty$. Then, the lower and upper local dimensions are respectively given by [11,12]:

$$\underline{\dim}_{loc}\mu(x) = \liminf_{r\to 0} \frac{\log \mu(\mathbf{B}(x,r))}{\log r} \tag{2.29}$$

$$\overline{\dim}_{loc}\mu(x) = \limsup_{r\to 0} \frac{\log \mu(\mathbf{B}(x,r))}{\log r} \tag{2.30}$$

where *B(x,r)* is an open ball centred at x with radius r (i.e. it is the region of space occupied by a microstructure of equivalent radius r located at x). The local dimension exists if the values of equations (2.29) and (2.30) are equal. It should be noted that the local dimension of μ at a point *x* is small if μ is "highly concentrated" near x, it is infinite if x is outside the support of μ i.e. $\underline{\dim}_{loc}\mu(x) = \overline{\dim}_{loc}\mu(x) = \infty$ if $\mu(B(x,r)) = 0$ for some $r > 0$ and it is zero if x is an atom of μ.

Materials with some kind of self-similarity of the internal microstructures have constant local dimension and are said to have exact lower dimension, i.e. $\underline{\dim}_{loc}\mu(x) = s = \text{constant}$ for μ-a.a. *x*. Materials or measures that do not have exact lower dimension (i.e. do not have self-similar internal microstructures) can be decomposed into measures or representative volume elements that are of exact lower dimensions s for a range of s.

Let $\underline{E}_{\le s} = \{x : \underline{\dim}_{loc}\mu(x) \le s\}$ then $Dim_H \underline{E}_{\le s} \le s$. Also let $\mu_s = \mu\big/_{\underline{E}_{\le s}}$ then $\mu_s(A) = \sup\{\mu(A \cap E)$ such that E is a Borel set with $Dim_H E \le s\}$. Define $\hat{\mu}$ by $\hat{\mu}([0,s]) = \mu_s(R^n) \Rightarrow \hat{\mu}([0,s]) = \mu(\underline{E}_{\le} s)$, then $\hat{\mu}$ is called the dimension measure of μ since $\hat{\mu}(A)$ records the μ-measure of the group of microstructures with (lower) local dimension in the set of real numbers *A*. Dimension disintegration formula, [11],

$$\mu_s(A) = \int_{[0,s]} v_t(A)\, d\hat{\mu}(t), \quad v_t - \text{probability measure with } 0 \le v_t(A) \le 1 \qquad (2.31)$$

is such that μ is decomposed into components v_t concentrated on $\underline{E}_t$, $\underline{E}_t$ being the group of microstructures for which μ has local dimension t and v_t are termed dimension derivate of μ.

The material or measure can also be decomposed into components of differing local dimensions. A number s is an atom of $\bar{\mu}$ if $\bar{\mu}(s)>0$. Let S be the set of atoms of $\bar{\mu}$. The restriction of $\bar{\mu}$ to S is called the atomic part of $\bar{\mu}$ and the restriction of $\bar{\mu}$ to [0,n]\S is the non- atomic part of $\bar{\mu}$.

If μ has the exact dimensional component, μ^s, corresponding to the atoms of $\bar{\mu}$ and the diffuse dimension distribution component μ^D corresponding to the non-atomic part of $\bar{\mu}$, i.e. $\mu^D\{x : Dim_{loc}\mu^D(x=s)=0\ \forall s\}$, then we have the decomposition formula, [11],

$$\mu = \sum_{s\in X}(\mu^s + \mu^D),\ X \subset [0,n],\ s\in S \tag{2.32}$$

Summarising, let A_α be the group of microstructures *x* for which a given measure μ has local dimension α. Studying $\mu(A_\alpha)$ gives information about "dimension decomposition" and looking at dimension of A_α leads to "multi-fractal spectrum" of μ. If this material consists of components (or microstructures) of different dimensions (called a "multi-fractal") then $\dim_{loc}\mu(x)$ may help to find and to describe the differences.

2.3 Stochastic Models Of (Heterogeneous) Materials Microstructures

The characterisations/analyses of random heterogeneous materials microstructures and properties in the stochastic sense entails: stochastic geometry/theory, homogenization theory, the development of governing stochastic differential equations and the use of stereology. Polycrystalline materials can be understood as being a collection of microstructures. These microstructures have random spatial and orientation distributions, the natures of which depend on the type of material under consideration. To better describe these heterogeneous and anisotropic arrangements with great degree of details, stochasticians use the knowledge of field variables. Thus, the term "random variable", when used in this

report might, without loss of generality, stand for "random field variables". These random field variables have the abilities to take values from the (positive), "real lines" thus making it possible to capture the highly detailed local properties. Thus, stochastic micromechanics possess the potential to predict based on the local response of the material. Random field variables for material microstructures depend on spatial and/or temporal parameters, and as such are called a random processes or stochastic processes.

2.3.1 Some aspects of stochastic geometry/theory

The physical features of a random material microstructure in nature may be discrete (such as the number of faces per grain, number of sides per grain, number of vertices/corners per grain), continuous (e.g. sizes of grain/microstructure during growth due to curvature driven grain boundary migration) or a combination of both discrete and continuous (e.g. change of grain size in polycrystalline nanomaterials due to simultaneous curvature driven grain boundary migration and misorientation-angle driven grain rotation coalescence mechanism). Some stochastic quantities that describe these field variables are given here. These notes are approached from the applied perspective targeting the scope of the present project and, hence, cannot be complete. Any one who is inquisitive for broader knowledge may read the numerous textbooks on probability, statistics and random processes.

Most often a 2-D cross-section of a material is sampled and the analysis done on this cross section. The statistical quantities are, thus, functions of the cross-sections' locations in space and the time of the analysis. The homogeneous continuum assumes these cross-section statistics to be the statistics of the entire material. Due to the heterogeneous nature of the material microstructures, stochasticians who apply field variables duel further than does statisticians. It is remarked, in this report, that the random processes and attainable values might be vector quantities, for example, the process $\mathbf{X}(\omega,t) = (X_1(\omega,t), X_2(\omega,t),\ldots, X_n(\omega,t))$

and the value $\mathbf{y} = (y_1, y_2, ...y_n)$. It should also be remarked that the random feature of material microstructure cannot be negative e.g. the random size of a microstructure cannot be smaller than zero.

If a random feature X(ω,t) of a microstructure is discrete, then it is most convenient to specify the probability of the random process by a *probability function*. This is defined as the probability that the random process (or feature) $\mathbf{X}(\omega,t)$ takes on discrete values at a cross section of the material located at ω and at some time point, *t*, given mathematically as

$$\text{Prob}(\mathbf{X}(\omega,t) = \mathbf{y}) = P_{\mathbf{X}}(\mathbf{y}) \text{ where } \mathbf{y} = \mathbf{a_1}, \mathbf{a_2}, \mathbf{a_3}, ... \text{ at time point } t_i,\ \omega \in \Re^n \qquad (2.33)$$

When data are collected from experiments with corresponding frequencies, W_X, then the probability of occurrence, $P_X(\mathbf{y})$, of each *event* can be obtained from $P_{\mathbf{X}}(\mathbf{y}) = W_{\mathbf{X}} \Big/ \left(\sum_{\mathbf{X}} W_{\mathbf{X}} \right)$

Another quantity that deals with either a discrete or continuous random process is the *probability distribution function*. This is the probability that the random process, from some cross-section at ω and at the time point t, takes values that are less than or equal to some value, represented mathematically as

$$Prob(\mathbf{X}(\omega,t) \le \mathbf{y}) = \sum_{\mathbf{y_i} < \mathbf{y}} (P_{\mathbf{X}}(\mathbf{y_i})) = F_{\mathbf{X}}(\mathbf{y}) \qquad (2.34)$$

This probability distribution function has the properties that

$$\lim_{\mathbf{X}(\omega,t) \to 0} F_{\mathbf{X}}(\mathbf{y}) = 0 \quad \text{and} \quad \lim_{\mathbf{X}(\omega,t) \to \infty} F_{\mathbf{X}}(\mathbf{y}) = 1 \qquad (2.35)$$

In most cases, it is convenient to deal with the *probability density function* $\boldsymbol{f_X(y)}$ of the random feature, which is the derivative of the probability distribution function. It has the properties that

$$\int_0^{y} f_{\mathbf{X}}(\mathbf{y}')d\mathbf{y}' = F_{\mathbf{X}}(\mathbf{y}) \quad \text{and} \quad \int_0^{\infty} f_{\mathbf{X}}(\mathbf{y}')d\mathbf{y}' = 1 \tag{2.36}$$

When the observation of a random feature is a combination of both discrete and continuous process, then a natural extension of the above formula is necessary. This can be interpreted as the probability that a continuous process, admitting a countable number of discrete values, takes values less than or equal to some values. This *extended Probability density function* is given as

$$f_{\mathbf{X}}(\mathbf{y}) = f_{\mathbf{X}}^{*}(\mathbf{y}) + \sum_i \left(P_{\mathbf{X}}(\mathbf{y}_i)\delta(\mathbf{y} - \mathbf{y}_i)\right) \tag{2.37}$$

where

$f_{\mathbf{X}}^{*}(\mathbf{y})$ = probability density disregarding the discrete components

$p_{\mathbf{X}}(\mathbf{y}_i)$ = probability function evaluated at $y = y_i$

$\delta(\mathbf{y} - \mathbf{y}_i)$ = Dirac delta function

The extended probability density function has the properties that

$$F_{\mathbf{X}}(\mathbf{y}) = \int_0^{y} f_{\mathbf{X}}^{*}(\mathbf{y}')d\mathbf{y}' + \sum_{\mathbf{y}_i < \mathbf{y}} \left(P_{\mathbf{X}}(\mathbf{y}_i)\right) \text{ and } \int_0^{\infty} f_{\mathbf{X}}^{*}(\mathbf{y}')d\mathbf{y}' + \sum_i \left(P_{\mathbf{X}}(\mathbf{y}_i)\right) = 1 \tag{2.38}$$

2.3.2 Parameters of probability distributions

Most probability distribution (or density) functions are completely characterised by some parameters. These parameters are also the natural quantities of characterising random microstructures of materials. These include:

Mean Value: Given a probability density function, $f_X(y)$, of a "continuous" random process, $\mathbf{X}(\omega,t)$, (or for $\boldsymbol{g}$ a *Borel function* of $\boldsymbol{X}(\omega,t)$) the mean value, $\mu(\omega,t)$, is given by

$$E[\mathbf{X}(\omega,t)] = \mu(\omega,t) = \int_0^\infty \mathbf{y}(\omega,t) f_{\mathbf{X}}(\mathbf{y}) d\mathbf{y} \text{ or } E[\mathbf{g}(\mathbf{X}(\omega,t)] = \int_0^\infty \mathbf{g}(\mathbf{y}(\omega,t) f_{\mathbf{X}}(\mathbf{y}) d\mathbf{y} \quad (2.39)$$

For a discrete random process, it follows that

$$E[\mathbf{X}(\omega,t)] = \mu(\omega,t) = \sum_i \mathbf{X}_i(\omega,t) P_{\mathbf{X}}(\mathbf{y}_i) \quad (2.40)$$

Variance and standard deviation are given respectively as

$$Variance = E\left[(\mathbf{X}(\omega,t) - \mu(\omega,t))^2\right] \quad (2.41)$$

$$standard\ deviation = \sigma(\omega,t) = \sqrt{Variance} = \sqrt{E\left[(\mathbf{X}(\omega,t) - \mu(\omega,t))^2\right]} \quad (2.42)$$

Dispersion or coefficient of variation is given as

$$CV(\omega,t) = \frac{\sigma(\omega,t)}{\mu(\omega,t)} \quad (2.43)$$

Other levels of characterisation that handle the spatial variability (including variations from different cross-sections) and temporal variability of the microstructures (features) in a material are the "auto"- (or "cross")-correlation function, "auto"- (or "cross")-covariance function and the correlation coefficient function (normalized covariance function). Two different expressions are given here; one on spatial variability at constant time and the other one on temporal variability at constant cross-section. The number of expression can be extended by considering simultaneous spatial and temporal variability. Due to the inherent difficulty in preparing samples for experimentations so that data can be collected simultaneously (at an instant) at several cross-sections, not much data on spatial variations at different cross sections are available. Data on temporal variability (e.g. data on grain growth) are easily obtainable and are readily available.

Auto-correlation function is given as

$$\mu_{XX}(\omega_1,t;\omega_2,t) = \Phi_{XX}(\omega_1,t;\omega_2,t) = E\left[\left(X(\omega_1,t)X(\omega_2,t)\right)\right] \tag{2.44a}$$

$$\mu_{XX}(\omega,t_1;\omega,t_2) = \Phi_{XX}(\omega,t_1;\omega,t_2) = E\left[\left(X(\omega,t_1)X(\omega,t_2)\right)\right] \tag{2.44b}$$

Auto-covariance function is given as

$$K_{XX}(\omega_1,t;\omega_2,t) = E\left[\left(X(\omega_1,t)-\mu(\omega_1,t)\right)\left(X(\omega_2,t)-\mu(\omega_2,t)\right)\right] \tag{2.45a}$$

$$K_{XX}(\omega,t_1;\omega,t_2) = E\left[\left(X(\omega,t_1)-\mu(\omega,t_1)\right)\left(X(\omega,t_2)-\mu(\omega,t_2)\right)\right] \tag{2.45b}$$

Auto-correlation coefficient function is given as

$$\rho_{XX}(\omega_1,t;\omega_2,t) = \frac{K_{XX}(\omega_1,t;\omega_2,t)}{\sigma(\omega_1,t)\sigma(\omega_2,t)} \tag{2.46a}$$

$$\rho_{XX}(\omega,t_1;\omega,t_2) = \frac{K_{XX}(\omega,t_1;\omega,t_2)}{\sigma(\omega,t_1)\sigma(\omega,t_2)} \tag{2.46b}$$

As can be noticed, the "auto-functions", e.g. auto correlation functions, give the relationships between a "*particular*" feature at different locations and/or at different time. If the relationships between "*different*" features are needed at different locations and/or at different times then "cross functions" are necessary. Slight modifications of the above expressions give their corresponding "cross-functions". For example, if $\mathbf{X}(w_i,t_i)$ stands for the "size of a grain" and $\mathbf{Y}(w_j,t_j)$ stands for the "number of faces on a grain" at the same (or different) location and at the same (or different) time t, then the cross-correlation function is defined as

Cross-correlation function is given as

$$\mu_{XY}(\omega_1,t;\omega_2,t)=\Phi_{XY}(\omega_1,t;\omega_2,t)=E\left[\left(X(\omega_1,t)Y(\omega_2,t)\right)\right] \tag{2.47a}$$

$$\mu_{XY}(\omega,t_1;\omega,t_2)=\Phi_{XY}(\omega,t_1;\omega,t_2)=E\left[\left(X(\omega,t_1)Y(\omega,t_2)\right)\right] \tag{2.47b}$$

2.3.3 Temporal (time) evolution of the statistics or the stochastic differential equations

The statistical properties/parameters given above are at some time point. This indicates that these properties vary as time changes. This is same with the mechanics of modern materials as the microstructures, for example in nanomaterials, are known to have low stability even at low temperatures or low dispersions in their sizes since they tend to grow more profoundly. It is therefore imperative to study the time evolution of these microstructures and properties. The backbone of this study is the Ito's stochastic differential equations, (generalised) forward and backward Kolmogorov-Fokker-Planck Equations, the Ito's differential rules and equations for moment functions.

Ito's stochastic differential equation

It deals with the expression for the increment of the random process. For a random process, X(w,t), the general (general meaning that it includes both continuous and discrete change) expression for its increment is given as, [16-20]

$$dX(\omega,t)=a(X(\omega,t))dt+b(X(\omega,t))dW(t)+c(X(\omega,t))dV(t) \tag{2.48}$$

where $a(X(\omega,t))$ is drift term, $b(X(\omega,t))$ is diffusion term, $c(X(\omega,t))$ is the jump term, dW(t) and dV(t) are, respectively, the increments of Weiner process (or Brownian Motion) and stochastic counting process within an infinitesimal time interval [t,t+dt], $b(Z(\omega,t))dW(t)$ and $c(X(\omega,t))dV(t)$ respectively account

for the random fluctuation in $X(\omega,t)$ due to the diffusion (continuous) process and the jump (discrete) process.

Generalised Integro-Differential Fokker-Planck equations

The development, with respect to forward time *t*, of the joint probability density function $q_{\{X\}}(y(\omega,t)/y_0(\omega,t_0)) = q_{\{X\}}(y,t/y_0,t_0)$, of the distribution of a random microstructure feature, *X(ω,t),* whose incremental change might be discrete or continuous or both is obtained from the Generalized Integro-differential Forward Fokker-Planck-Kolmogorov Equation, [16-20], given by

$$\frac{\partial}{\partial t}q_{\{\mathbf{X}\}}(\mathrm{y},t/\mathrm{y}_0,t_0) = -\frac{\partial}{\partial y_i}\left[C_i(\mathbf{y},t)q_{\{\mathbf{X}\}}(\mathbf{y},t/\mathbf{y_0},t_0)\right] + \frac{1}{2}\sum_{i,j}\frac{\partial^2}{\partial y_j \partial y_j}\left[D_{ij}(\mathbf{y},t)q_{\{\mathbf{X}\}}(\mathbf{y},t/\mathbf{y_0},t_0)\right] + \int\left[J_{\{\mathbf{X}\}}(\mathbf{y}/\mathbf{x},t)q_{\{\mathbf{X}\}}(\mathbf{x},t/\mathbf{y_0},t_0) - J_{\{\mathbf{X}\}}(\mathbf{x}/\mathbf{y},t)q_{\{\mathbf{X}\}}(\mathbf{y},t/\mathbf{y_0},t_0)\right]dx, \quad (2.49)$$

where C(r,t) and D(r,t) are the first and second derivate moments given from expression (2.48) as, [16],

$$\begin{cases} C(y,t) = a(X(\omega,t)) = a(y,t) \\ D(r,t) = [b(X(\omega,t))]^2 = [b(y,t)]^2 \end{cases} \quad (2.50)$$

and $J_{\{X\}}(y/x,t)$ is the conditional jump probability intensity function given, in accordance with [16], as

$$J_{\{\mathbf{X}\}}(x/y,t) = \sum_{\alpha=1}^{l}\int_{p_\alpha}\delta\left(x-(y+\mathbf{c}_\alpha(y,t)p_\alpha)\right)J_{\{V_\alpha\}}(p_\alpha,t)dp_\alpha \quad (2.51)$$

p_α is the α-component of the mark random variable. By different α-component of a generating source process, it means increment of different microstructure features. Since there exists a relationship between number of faces, number of sides and number corners per grains through the Euler's formula, jump increment

in these microstructure features is as the same component of the generating source process. Thus, the regularity condition holds without loss of generality.

Ito's Differential Rules

Consider an arbitrary function $h(\mathbf{X}(\boldsymbol{\omega},t),t))$ of the microstructure feature, $\mathbf{X}(\boldsymbol{\omega},t),t)$ and of time t. A jump of magnitude p_α in the α-component of $V_\alpha(t)$ of the generating source process at the time t results in jump of $d\mathbf{X}(\boldsymbol{\omega},t) = \mathbf{c}_\alpha(\mathbf{X}(\boldsymbol{\omega},t),t)\,p_\alpha$ of the microstructure feature which impart on the function h a jump of magnitude of, [16-20],

$$
\begin{aligned}
dh(\mathbf{X}(\boldsymbol{\omega},t),t) &= \left(h\left(\mathbf{X}(\boldsymbol{\omega},t)+\mathbf{c}_\alpha(\mathbf{X}(\boldsymbol{\omega},t),t)\,p_\alpha,t\right)-h\left(\mathbf{X}(\boldsymbol{\omega},t),t\right)\right)\\
&= \frac{\partial h(\mathbf{X}(\boldsymbol{\omega},t),t)}{\partial t}dt+\sum_{i=1}^{n}\frac{h(\mathbf{X}(\boldsymbol{\omega},t),t)}{\partial X_i}\left(a_i(\mathbf{X}(\boldsymbol{\omega},t),t)dt+\sum_{\alpha=1}^{m}b_{i\alpha}(\mathbf{X}(\boldsymbol{\omega},t),t)dW_\alpha(t)\right)\\
&+\frac{1}{2}\sum_{i,j}^{n}\frac{\partial^2 h(\mathbf{X}(\boldsymbol{\omega},t),t)}{\partial X_i\partial X_j}\sum_{\alpha=1}^{m}b_{i\alpha}(\mathbf{X}(\boldsymbol{\omega},t),t)b_{j\alpha}(\mathbf{X}(\boldsymbol{\omega},t),t)dt\\
&+\sum_{\alpha=1}^{l}\left\{h\left(\mathbf{X}(\boldsymbol{\omega},t)+\mathbf{c}_\alpha\left(\mathbf{X}(\boldsymbol{\omega},t),t\right)\mathbf{p},t\right)-h(\mathbf{X}(\boldsymbol{\omega},t),t)\right\}dN_\alpha(t)
\end{aligned}
\qquad (2.52)
$$

where $dN(t)$ is the number of jump processes within the infinitesimal time interval [t,t+dt].

Equations for Moments

The moments are obtained by taking the expectation of both sides of the expression of the Ito's Differential Rule above, [16-20], i.e.

$$
\begin{aligned}
\frac{d}{dt}\mathbf{E}\left[h(\mathbf{X}(\boldsymbol{\omega},t),t)\right] &= \mathbf{E}\left[\frac{\partial h(\mathbf{X}(\boldsymbol{\omega},t),t)}{\partial t}\right]+\mathbf{E}\left[\sum_{i=1}^{n}\frac{h(\mathbf{X}(\boldsymbol{\omega},t),t)}{\partial X_i}\left(a_i(\mathbf{X}(\boldsymbol{\omega},t),t)\right)\right]\\
&+\mathbf{E}\left[\frac{1}{2}\sum_{i,j}^{n}\frac{\partial^2 h(\mathbf{X}(\boldsymbol{\omega},t),t)}{\partial X_i\partial X_j}\sum_{\alpha=1}^{m}b_{i\alpha}(\mathbf{X}(\boldsymbol{\omega},t),t)b_{j\alpha}(\mathbf{X}(\boldsymbol{\omega},t),t)\right]
\end{aligned}
$$

$$+\mathbf{E}\left[\sum_{\alpha=1}^{l}\left\{h\left(\mathbf{X}(\boldsymbol{\omega},t)+\mathbf{c}_{\alpha}\left(\mathbf{X}(\boldsymbol{\omega},t),t\right)\mathbf{p},t\right)-h(\mathbf{X}(\boldsymbol{\omega},t),t)\right\}dN_{\alpha}(t)\right] \tag{2.53}$$

2.3.4 Homogenization theory

An issue of great importance during the applications of the theory of random processes is to estimate the characteristics of the material such as the mean and the correlation functions of a physical random process from measurements. The realization of a physical process might be, for example, the microstructure or the features per microstructure. When the ensemble is countably infinite or uncountable, the limited number of sample functions that can be recorded in experiments is generally inadequate to provide reliable estimates. Thus, the fundamental assumption in the stochastic literature is that the media (or cross section or entire materials) are ergodic. Thus, if it can be justified that a random process is stationary then its probabilistic structure is invariant with respect to shift of the origin. As such the mean function, the correlation function, and even higher-order statistical properties can be possibly estimated by the parametric averages using some record of a sample function.

In order for a random measure X(t) to have essentially the same sample mean (*Ergodic in the first moment*) it is simply required that

$$\underset{T\to\infty}{l.i.m}\frac{1}{T}\int_0^T X(t)dt=\left\langle X(t)\right\rangle_t=E\left|X(t)\right|=\mu \tag{2.54}$$

should be a constant. To be Ergodic in correlation it is required that

$$\left\langle X(t+\tau)X(t)\right\rangle=R_{XX}(\tau)=\underset{T\to\infty}{l.i.m}\frac{1}{T-\tau}X(T+\tau)X(t)dt \tag{2.55}$$

should be a function of just τ. That is, E[X(t)] should be constant and E[X(t+τ)X(t)] a function of τ where *T* is the length of the record. The choice of *T*

must be such that further increase of T does not affect appreciably the values of the mean function, correlation function, etc.

3.0 AVERAGING TECHNIQUES

Engineers make use of macroscopic properties. They arise as a result of "averaging in some sense" of the characteristics that are generated from structures at mesoscopic range of length scales. Hence, the most important issue is "how to relate the various mesoscopic characteristics within any material so as to yield the observed macroscopic property".

Different macroscopic quantities given by various measures may correspond to the same single macroscopic material. It has been demonstrated in section (2.2) that if the local dimensions of the measures within a material or the measures of the material microstructures are constant (i.e. exact dimensionality for spherical microstructures) then the dependencies of macroscopic properties of the material on the examined material microstructures characteristics are obtained in power form. However, such simple (or trivial) situations seldom occur in real systems. Typically, local dimensions vary in space and the resulting macroscopic dependencies arise as a result of some sort of spatial averaging.

According to theorems of geometric measure theory, [11], any measure can be decomposed into a family of probability measures and the single measure constituting the spectral density of the currently examined quantity. This has been presented in section (2.2) as "dimension decomposition of measure". The relationship between those probabilistic measures and the probability distributions should follow from the stochastic description of the microstructure. Thus, it is imperative to present the spectral density and some of the averaging techniques that further relate the microstructure characteristics to the macroscopic properties.

3.1 Spectral Density

The spectral density of a measure (or of a macroscopic property), X(t), is obtained from the Fourier Transform of the *correlation function* of the microscopic

characteristics. Consider the integral (or sum – use Dirac delta function for discrete random measures)

$$\overline{X}(\omega) = \frac{1}{2\pi}\int_{-\infty}^{\infty} X(t)\exp(-i\omega t)dt \tag{3.1}$$

which exists in mean square if

$$E[\overline{X}(\omega_1)\overline{X}^*(\omega_2)] = \frac{1}{(2\pi)^2}\int_{-\infty}^{\infty}\int_{-\infty}^{\infty}\phi_{XX}(t_1,t_2)\exp[-i(\omega_1 t_1 - \omega_2 t_2)]dt_1 dt_2 \tag{3.2}$$

is bounded for all values of "ω_1" and "ω_2". The inverse of the above equation in the mean square sense is expressed as

$$E\{\left|X(t) - \int_{-\infty}^{\infty}\overline{X}(\omega)\exp(i\omega t)d\omega\right|^2\} = 0 \tag{3.3}$$

which intuitively states that X(t) may be replaced in the mean square equivalence by a sum of harmonic components, and that $\overline{X}(\omega)d\omega$ is the random complex "amplitude" of the *component* with "frequency ω". In analysis, the LHS of equation (3.2) is easy to determine (i.e. correlation of microscopic characteristics); and when the correlation function $\phi_{XX}(t_1,t_2)$ of the macroscopic property is required, it can be obtained from the inverse Fourier Transform given by

$$\phi_{XX}(t_1,t_2) = \int\int E\left|\overline{X}(\omega_1)\overline{X}^*(\omega_2)\right|\exp[i(\omega_1 t_1 - \omega_2 t_2)d\omega_1 d\omega_2 \tag{3.4}$$

If $\omega_1 = \omega_2$, then the distribution of values of the sample functions over the ensemble of sample functions is the same at any time *t*. In this case, the correlation function of macroscopic measure (or property), $R_{XX}(\tau)$, is obtainable from correlation function of the microscopic characteristics, $\psi_{XX}(\omega)$, through the

inversion formula

$$R_{XX}(\tau) = \int_{-\infty}^{\infty} \psi_{XX}(\omega) \exp(i\omega\tau) d\omega \tag{3.5}$$

By letting $\tau = 0$ in (3.5), the physical significance of the function $\psi_{XX}(\omega)$ is revealed. That is

$$R_{XX}(0) = \int \psi_{XX}(\omega) d\omega \tag{3.7}$$

But $R_{XX}(0) = \mathbf{E}[X^2(t)]$ is the mean-square value of the weakly stationary random process under consideration. *The RHS of (3.7) is the same as the mean square value obtained as sum of the infinitesimal component $\psi_{XX}(\omega)d\omega$. Hence $\psi_{XX}(\omega)$ describes the distribution of the total mean square value over the frequency domain, hence the name* ***mean-square spectral density.*** *$E[X^2(t)]$ is a measure of average energy.* For example in vibration theory, if X(t) stands for random displacement of a single-degree-of-freedom mechanical system, then $E[X^2(t)]$ is proportional to the average potential energy in the system. If X(t) represents the random velocity, then $E[X^2(t)]$ is proportional to the average kinetic energy. In the present project or in micromechanics, if X(t) stands, for example, for the random increment of the microstructure size, then $E[X^2(t)]$ stands for the Gibbs Free energy stored in or released from the system during evolution.

3.2 Poisson Counting Process

When the random feature of a microstructure is discrete, then the Poisson random field is the simplest and most important representation of the point field. Some examples of such heterogeneity are the number of faces per grain, the number of vertices per grain and the number of edges per grain in a polyhedral grain filling aggregate (or in a material).

A random pattern N of number of faces, edges or vertices per grain in a material is a homogenous Poisson Field if:

a) for any integer n and for different grains, $A_1, A_2, A_3, ..., A_n$ in that material, the random variables $N(A_1), N(A_2), \ldots N(A_n)$ characterizing the random number of faces, edges or corners per respective grains $A_1, A_2, \ldots, A_n$ are statistically independent,

b) the number $N(A)$ of faces, corners or edges possessed by any grain A of finite measure $m(A)$ (Lebesgue measure) has the Poisson probability distribution with parameter $\lambda m(A)$, that is

$$P\{N(A) = n\} = \frac{[\lambda m(A)]^n}{n!} \exp[-\lambda m(A)] \tag{3.8}$$

where $m(A)$ is the "volume" of A for a 3-D space or microstructure, "area" of A for a 2- D microstructure or "length" of edge for 1-D microstructure. The parameter λ is called the *intensity* of field N and it characterizes the mean "density" of faces, edges or vertices possessed by the grain A.

An *inhomogeneous Poisson field* is a construct that has a potential to characterize spatial random patterns with variable density defined as follows: N is an *inhomogeneous Poisson field* with mean measure μ if the number $N(A)$ has a Poisson distribution

$$P\{N(A) = n\} = \frac{[\mu(B)]^n}{n!} \exp[-\mu(A)], \quad n = 0,1,.. \tag{3.9}$$

with intensity measure represented as

$$\mu(A) = \int_A \lambda(r) dr \tag{3.10}$$

where $\lambda(r)$ is called the *intensity function*. The function $\lambda(r)$ is estimated from

empirical data.

Poisson-Cox random field, [5], is a generalization of Poisson field obtained by randomising the intensity measure. The Poisson-Cox field originates from a two-step random mechanism: the first, global, is governed by a Poisson-type distribution of microstructure features per grain whereas the second one is associated with randomness of the intensity measure. For more information on the Poisson-Cox random field and other stochastic point fields, the reader is advised to read the work by Sobczyk, [4,5].

3.3 Compound Counting Process

This section relates to the definition of measure from geometric measure theory. For example, grains or microstructures in (nano)-materials do not overlap. Let *N(R)* be the number of microstructures in the (nano)-materials within a sphere of radius *R*. In modelling, it is logical to place the origin of the coordinate axes at the "edge" of the material in such a way that the rest of the material lies within the positive quadrants of the coordinate axes. Also let $\mu(A_i)$ be a measure of the microstructure feature of the ith grain such as the number of faces, number of sides, number of corners on that grain or even the "size" of that grain. The definition of measure, expression (2.19), can be written as, [16],

$$\mu(A) = \mu\left(\bigcup_{i=1}^{N(R)} A_i\right) = \sum_{i=1}^{N(R)} \mu(A_i) \tag{3.11}$$

Here $\mu(A)$ is now called a compound process. Let $dN(R)= N(R+dR)-N(R)$ be the increment of the counting process (or number of grains) within the shell $B(0,R+dR)\backslash B(0,R)$, where *B(0,R)* is a ball or material of radius *R* centred at the origin, 0. If further, the shell $B(0,R+dR)\backslash B(0,R)$ is sub-divided into sub-domains, $B(0,r+dr)\backslash B(0,r)$, each of which corresponds to a single microstructure size, then *dN(r)* is the number of grains in the region of the space occupied by a grain. For

1-D system, $B(0,R+dR)\backslash B(0,R)=[R,R+dR]=[r,r+dr]=B(0,r+dr)\backslash B(0,r)$. Thus, the counting process, *N(r)*, is regular while *N(R)* is not regular. *N(r)* is the same as number of microstructures in sphere or material of radius *r* such that $B(0,r+dr)\backslash B(0,r)$ is the size of a microstructure. Then it follows that the Riemann Stieltjes sum (3.11) can be represented as Riemann Stieltjes integral below, [16]:

$$\mu(A)(r)=\int_0^r \mu(A_i)(y)dN(y) \quad \Leftrightarrow \quad d\mu(A)(r)=\mu(A_i)(r)dN(r) \tag{3.12}$$

It has been observed in most experimental findings that the measure of the features per microstructure is related to the number of microstructures in the material. But if both are assumed to be statistically independent, then the following statistical expressions are obtained

$$\begin{aligned}
&\mathbf{E}[d\mu(A)(r)]=\mathbf{E}[\mu(A_i)(r)]v(r)dr \\
&\mathbf{E}[\{d\mu(A)(r)\}^n]=\mathbf{E}[\{\mu(A_i)\}^n]v(r)dr \\
&\mathbf{E}[d\mu(A)(r_1)d\mu(A)(r_2)]=\mathbf{E}[\{\mu(A_i)\}^2]v(r_1)v(r_2)dr_1dr_2 \quad \text{for } r_1\neq r_2 \\
&\mathbf{E}[\mu(A)(r)]=\mathbf{E}[\mu(A_i)]\int_0^r v(y)dy
\end{aligned} \tag{3.13}$$

where *v(r)* is the mean arrival (or occurrence) rate or mean density of microstructures (or of events). In order to evaluate the higher order statistics of the compound process, the "modified" degeneracy property of higher-degree product density must be taken into account, which takes place within the integration domain, (see part two of this report for detailed examples). Note that the position vector ***r*** used above may be given by $r=(x,y,z)$ in which case $dr=(dx,dy,dz)$.

PART TWO

SPECIFIC DERIVATIONS OR APPLICATIONS

4 MODELLING OF DISPERSED-TYPE RANDOM MICROSTRUCTURE PATTERNS IN TERMS OF GENERAL STOCHASTIC POINT FIELDS

A dispersed-type random microstructure pattern can be stress-free holes, pores, rigid inclusions, etc. Methods of modelling of such random microstructure patterns in terms of Poisson random fields can be found in literature, [4,5,6]. The purpose of the present chapter is to characterise random microstructures using other random point fields. Modelling is done in terms of Erlang renewal fields. The corresponding statistical properties of the stochastic point fields presented are calculated. These statistical properties include the mean functions and the correlation functions of the number of points in a considered region. These statistical properties are expressed in terms of the product density functions characterising the underlying stochastic point fields. From the stochastic characterisation of the number of points in a region, the contact distribution function and the corresponding probability density function are obtained. The contact distribution function represents the probability that there may be at least one point in the region. This function gives the cumulative distribution function of the radial distance from a reference point to the nearest point in the structure (i.e. this is the nearest neighbour distribution function).

4.1 Characterisation In Terms Of Erlang Renewal Process

To characterise the number of points, $N_{B(0,t)}$, in a region B(0,t), the following fact is used

$$N_{B(0,t)} < r \quad \Leftrightarrow \quad \mathrm{S_r} = B(0,r) \supset B(0,t) \tag{4.1}$$

$$\Leftrightarrow \quad S_r = \sum_{i=1}^{r} \{B(0,t_i) \setminus B(0,t_{i-1})\} \quad , \qquad B(0,t_0) = 0$$

where **B**(0,**t**) **=** the ball centred at origin, O, with radius, ***t*** or S_r = the region swept by the position vector of the r^{th} point. Regularity condition is assumed to hold i.e. probability that more than one microstructure have the same absolute value of position vectors or are found at the same location is negligible. Depending on the dimensionality of the vector space under consideration, we have that **B**(0,***t***) = "**length**" if ***t*** belongs to 1-dimensional space, **B**(0,***t***) = "**area**" if ***"t"*** belongs to 2-D, **B**(0,***t***) = "**volume**" if ***"t"*** belongs to 3-D. Note that two points or microstructures with position vectors $\vec{A}$ and $\vec{B}$ is termed consecutive if there exists no microstructure with position vector $\vec{C}$ such that

$$\left|\vec{A}\right| < \left|\vec{C}\right| < \left|\vec{B}\right| \quad \text{or} \quad \left|\vec{B}\right| < \left|\vec{C}\right| < \left|\vec{A}\right|$$

It follows from equation (4.1), that

$$\mathbf{P}(N_{B(0,t)} < r) = \mathbf{P}(S_r \supset B(0,t)) \tag{4.2}$$

$$= 1 - K_r(t) \quad , \quad \text{with } K_o(t) = 1. \tag{4.3}$$

where $K_r(t)$ = cumulative distribution function of S_r.

If the **Renewal Process** is **Poisson Process** of rate ρ, then S_r has Special **Erlang Distribution** with r stages and $N_{B(0,t)}$ has Poisson distribution of mean $\rho\mathbf{B}(0,t)$. If it is supposed, next, that the **Renewal Process** is **Ordinary Renewal Process** with distribution of difference between absolute values of position vectors of two "consecutive " points being of Special Erlangian type with "a" stages, then it follows that $N_{B(0,t)} = r$ if and only if the number of stages completed in the underlying Poisson Process has one of the following values,

$$ra,\ ra+1,\ ra+2,\ \ldots\ ra+a-1$$

Hence, since the stages completed over a set of measure, **B**(0,**t**), follows a Poisson

distribution of mean $\rho B(0,t)$, it follows that

$$\Pr\{N^{(o)}_{B(0,t)} = r\} = \sum_{m=ra}^{ra+a-1} \frac{\rho B(0,t)}{m!} \exp(-\rho B(0,t)) \tag{4.4}$$

To converting equation (4.3) into an equation for the probability generating function of $N_{B(0,t)}$, let

$$\begin{aligned} G\{B(0,t);\xi\} &= \sum_{r=0}^{\infty} \xi^r \Pr(N_{B(0,t)}) \\ &= 1 + \sum_{r=1}^{\infty} \xi^{r-1}(\xi - 1) K_r(t) \end{aligned} \tag{4.5}$$

After applying Laplace Transformation to (4.5) it follows that

$$G^*\{B(0,s);\xi\} = \frac{1}{B(0,t)} + \frac{1}{B(0,t)} \sum_{r=1}^{\infty} \xi^{r-1}(\xi - 1) K_r^*(s) \tag{4.6}$$

where

$$\begin{aligned} K_r^*(s) &= \{f^*(s)\}^r \quad \text{for Ordinary Renewal Process} \\ &= f_1^*(s)\{f^*(s)\}^{r-1} \quad \text{for modified renewal Process} \\ &= \frac{\{1 - f^*(s)\}\{f^*(s)\}}{\mu s} \quad \text{for Equilibrium Renewal Process} \end{aligned}$$

On substituting these specific values of $K_r^*(s)$ and taking Inverse Laplace transformation then

$$G_e\{B(0,t);\xi\} = 1 + \frac{\xi - 1}{\mu} \int_0^{B(0,t)} G_0(u,\xi)\, du \tag{4.7}$$

Or on taking coefficients of ξ^r it follows that

$$\Pr\left[N_t^{(e)}=1\right]=\frac{1}{\mu}\int_0^{B(0,t)}\left\{\Pr\left[N_u^{(0)}=r-1\right]-\Pr\left[N_u^{(o)}=r\right]\right\}du \qquad \text{r}=1,2,3,... \tag{4.8}$$

$$\Pr\left[N_t^{(e)}=0\right]=1-\frac{1}{\mu}\int_0^{B(0,t)}\Pr\left(N_u^{(0)}=0\right)du \tag{4.9}$$

If distribution of the difference of absolute values of the position vectors of two consecutive microstructures (location) is the special Erlangian distribution with "*a*" stages then we have to substitute (4.4) into (4.8) which leads to

$$\Pr\left[N_{B(0,t)}^{(e)}=r\right]=$$

$$\left\{(r+1)\sum_{l=ra}^{ra+a-1}-\frac{\rho B(0,t)}{a}\sum_{l=ra+a-1}^{ra+a-2}-(r-1)\sum_{l=ra-a}^{ra-1}+\frac{\rho B(0,t)}{a}\sum_{l=ra-a-1}^{ra-2}\right\}\frac{\rho B(0,t)}{l!}\exp(-\rho B(0,t))$$

…… (4.10)

Furthermore

$$\Pr(N_{B(0,t)}^{(e)}=0)=\left\{\sum_{l=0}^{a-1}-\rho B(0,t)\sum_{l=0}^{a-2}\right\}\frac{(\rho B(0,t))^l}{l!}\exp(-\rho B(0,t)) \tag{4.11}$$

The distribution of the difference in absolute values of the position vectors of the $(k+1)^{th}$ and k^{th} microstructures (location), $\tau_k = B(0,t_{k+1})\setminus B(0,t_k)$ (it should be noted that τ_k is a measure), that follows gamma distribution has probability density function given as

$$g(\tau_k)=\frac{\nu^k\tau_k{}^{k-1}}{(k-1)!}\exp(-\nu\tau_k) \qquad \text{k}=1,2,3,\ ... \tag{4.12}$$

The mean measure rate of the k^{th} set or microstructure only asymptotically (i.e. as $\tau_k\to\infty$) tends to ν/k. It should be noted that if $k=1$ then the Gamma (Erlang) distribution becomes Poisson distribution of the first (single) set that has rate υ.

To obtain the probability distribution of the number of point, N_{τ_k}, in the k^{th} set that follows Erlang distribution, some important properties of Laplace transform is used which states that: the inverse of Laplace Transform is unique, and hence, two functions that have the same Laplace Transform are considered equivalent if, and only if, they differ only by a set of zero measure, [21]. Hence, the Erlang Distribution is the distribution of sum of independent random variables that have exponential (Poisson) distribution. Hence, the distribution of the number points, N_{τ_k}, in the k^{th} set that has Erlangian distribution is given by equation (4.4). It follows that

$$\Pr\left[N_{\tau_k} = r\right] = \Pr\left[N^{(o)}_{B(0,t_k)} = r\right] = \sum_{n=ra}^{ra+a-1} \frac{\left(\rho B(0,t_k)\right)^n}{n!} \exp\left[-\rho B(0,t_k)\right] \quad (4.13)$$

where ρ is asymptotically related to ν given in equation (4.12) i.e. $\rho \approx \frac{\nu}{k}$, and n is the number of stages completed. From equation (4.13) it follows that

$$\Pr(N_{\tau_k} = 0) = \Pr(N^{(o)}_{B(0,t_k)} = 0) = \sum_{n=0}^{a-1} \frac{\left(\rho B(0,t_k)\right)^n}{n!} \exp(-\rho B(0,t_k)) \quad (4.14)$$

The contact spherical distribution function is given by

$$H_{\tau_k}(q) = 1 - \Pr(N_{\tau_k} = 0) \quad , \quad q \geq 0$$

$$= 1 - \sum_{n=0}^{a-1} \frac{\left(\rho B(0,t_k)\right)^n}{n!} \exp(-\rho B(0,t_k))$$

$$H_{\tau_k}(q) = 1 - \sum_{n=0}^{a-1} \frac{\left(\rho \alpha_l q^l\right)^n}{n!} \exp(-\rho \alpha_l q^l)) \quad (4.15)$$

where l is the dimension of the space under consideration, and $\alpha_l q^l$ is the

Lebesgue measure equivalence of $B(0,t_k)$ and $\alpha_n = \pi^{\frac{1}{2}n} \Big/ \left[2^n \left(\frac{1}{2} n \right)! \right]$ is the volume of n-dimensional ball of diameter 1.

$$B(0,t_k) = \alpha_l q^l$$

Of course, the probability density function, *p.d.f*, $h_s(q)$, corresponding to equation (4.15) is

$$h_s(q) = -\sum_{n=1}^{a-1} \left\{ \frac{\left[\rho\alpha_l q^l\right]^{n-1} \left[l\rho\alpha_l q^{l-1}\right]}{(n-1)!} \exp(-\rho\alpha_l q^l) \right\} + \sum_{n=0}^{a-1} \left\{ \frac{\left[\rho\alpha_l q^l\right]^n}{n!} \left[l\rho\alpha_l q^{l-1}\right] \exp\left[-\rho\alpha_l q^l\right] \right\}$$

…….. (4.16)

But

$$\int_0^{\tau_k} \mathrm{h}_0^{(\mathrm{k})}(u)du = < N_{\tau_k} > = < N^{(o)}_{B(0,t_k)} > = \sum_{m=ra}^{ra+a-1} < N_{B_m(0,t_k)} > \approx a\rho\tau_k \approx \nu\tau_k$$

where $N_{B_m(0,t_k)}$ = number of points in the region $\mathbf{B}(0,\mathbf{t_k})$ during the mth stage.

If $\boldsymbol{B_k}$ and $\boldsymbol{B_l}$ are disjoint sets (i.e. from different stages) and let

$$\Delta N_{t_i} = N_{t_{i+1}} - N_{t_i} = N^{(o)}_{B(0,t_{i+1})} - N^{(o)}_{B(0,t_i)} = \Delta N^{(o)}_{B(0,t_i)}$$

then

$$< N_{\tau_i} N_{\tau_j} > = < \sum_i^\infty \Delta N_{t_i} \sum_j^\infty \Delta N_{t_j} > = < \sum_i^\infty \sum_j^\infty \Delta N_{t_i} \Delta N_{t_j} > = \sum_{i,j}^\infty < \Delta N_{t_i} \Delta N_{t_j} >$$

$$= \sum_{i,j}^\infty < \Delta N^{(o)}_{B(0,t_i)} \Delta N^{(o)}_{B(0,t_j)} > = \sum_{i,j}^\infty \left[f_2(t_i,t_j) \Delta B(0,t_i) \Delta B(0,t_j) \right]$$

and changing Stieltjes sums to Riemann's integral, we have

$$< N_{\tau_i} N_{\tau_j} >= \int_{B(0,t_i)} \int_{B(0,t_j)} \left\{ f_2(t_i, t_j) dB(0,t_i) dB(0,t_j) \right\}$$

5 MODELLING OF THE MICROSTRUCTURAL FEATURES SUCH AS THE NUMBER OF FACES OF GRAINS IN AN AGGREGATE USING THE COMPOUND (MARKED) POINT FIELDS

Most materials are built up by successive addition of inclusion (e.g. grain, pore, or crack) size and/or shape (distribution), [22]. These inclusions are, in general, termed the microstructures in this report.

The characterisation of the overall materials properties, e.g. conductivity, elasticity, permeability, stress, strain, and/or energy from the examinations of the internal microstructures (i.e. establishing relationship between microstructure morphologies and material properties) has been for long a problem of interest and importance to a range of applications in engineering and sciences. A way out is to define a set of morphological (i.e. topological and metric) measures from which one can optimally reconstruct model morphologies and then accurately predict material properties.

Along this line of thought, the following efforts have been devoted. The distribution of microstructures within a material or an aggregate has been modelled using the random point fields, [4,5,6]. The reconstruction of the local stochastic model of microstructure features (e.g. distribution of number of faces per grain and/or sizes of grains) is now known, [4,5,23,24]. Knowledge of the distribution of microstructure features within a material and their cumulative effect(s) to the entire material and/or material's properties remain(s) an issue of interest and importance. In the present chapter, the compound (marked) point process (field) is proposed and the corresponding statistics are determined that appropriately quantify and qualify the cumulative microstructure features within an aggregate. The mark random variable is here a discrete random variable which corresponds to the number of faces per grain and the space counting process, $N(d)$, corresponds to the number of grains in an aggregate.

It should be noted that the distribution of microstructure features within an aggregate is strongly influenced by grain segregation, growth and coarsening mechanisms. The present chapter deals with another attempt to model spatial and temporal evolutions of complex microstructure features in metals that still remain as difficult problems.

Comprehensive analysis and reports about grain growth is dealt with in the subsequent chapters. The facts about grain growth given under this subsection are those that should assist in the understanding of and analysis in the present chapter. Coarsening and grain growth both refer to parasitic surface energy driven evolution of a system of particles to larger mean sizes whereby larger particles absorb smaller ones or grains of with misorientation angles between them rotate and coalesce to eliminate the misorientation angle. In polycrystalline aggregate, in the first case, grains averaging to local mean size surround a particular grain. If the grain size is smaller than the local mean then it shrinks otherwise it grows. Hence, the growth of a grain is always examined by considering its relation to its neighbours (i.e. grain growth or coarsening mechanism), since grains do not grow in isolation.

Scaling state of grains growth: A pattern in either two or three dimensions is in a ***scaling state*** if all of its distribution and correlation functions for all dimensionless quantities are constant in time. The power-law kinetics, [23,25], and several models exist to describe the temporal evolution of the microstructure sizes in the materials. Morhac et al, [26], observed that grain sizes predicted by existing laws and models of grain growth are often far greater than those observed in engineering alloys and even commercially pure materials. Russell, [25], conducted experiments from which it was observed that precipitate coarsening and grain growth in steels (austenite and ferrite) are limited by particle pinning and solute segregation at grain boundaries. Remarkably, Russell also observed that even in the unpinned alloy ***grain growth is much slower*** than that predicted by the simple theory, probably, due to solute drag on the grain boundaries. These lead to other investigations that revealed that the maximum attainable grain size R

during grain growth in a random dispersion of particles is given by the Zener equation. [27], as

$$R = \left[B/(\beta.f^{n})\right]\bar{r} = 1.5\bar{r} \Leftrightarrow A_R = (1.5)^2 A_{\bar{r}} = 2.25A_{\bar{r}} \Leftrightarrow V_R = (1.5)^3 V_{\bar{r}} = 3.375V_{\bar{r}} \quad (5.1)$$

where f is volume fraction of particles, B and n are constants, β is a function of $R/\bar{r}$ and $\bar{r}$ is the mean grain size. From formulation due to Zener and Smith, [28], B=4/3, β=1 and n=1.

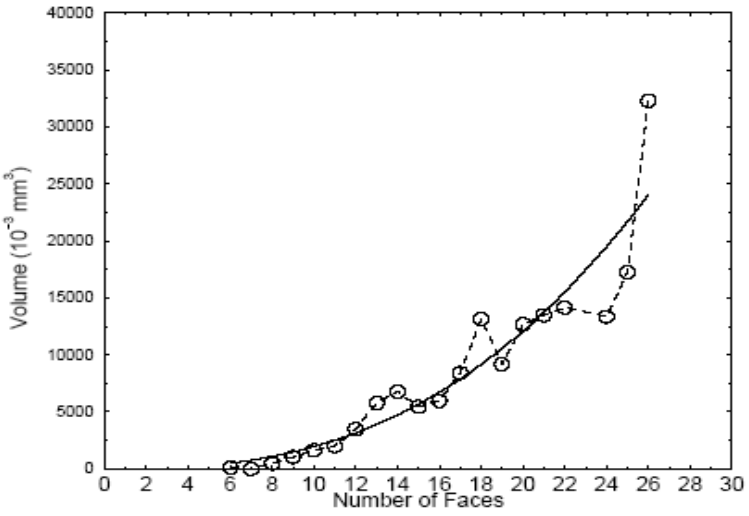

Figure 5.1 *Relationship between grain size and number of faces per grain by Glazier et al*, [29]

It has been found that the average grain growth rate depends linearly on the number of faces [30,31]. Saito, [23], and Glazier et al, [29], observed that the average size of f-faced grain is proportional to the number of faces, Fig.5.1. Morhac et al, [26], found that the effect of the number of faces, F_{ijk}, on the average grain size of f-faced grains for a microstructure is time invariant. It can be concluded that both grain size distributions and distributions of the number of faces, F_{ijk}, of the simulated microstructures become time invariant after a longer time.

Knowing the relationship between the average number of faces of grains adjacent to an f-faced grain (i.e. local critical mean number of faces per grain), $n(F_{ijk})$, and the face number on that grain, F_{ijk} , is important to the modelling of the spatial distribution of the number of faces per grain in the aggregate. This relationship is found to be similar to Aboav-Weaire relation in two dimensions, [23,26],

$$n(F_{ijk}) = C_1 + C_2 / F_{ijk} \tag{5.2}$$

where C_1 and C_2 are constants.

5.1 Proposed Model and Stochastic Analysis

The distribution of random microstructures in space (or in an aggregate) is described by random field variable *N(d)* that characterizes, in general, the number of points (centres of grains) in an aggregate up to a distance *d* from a reference point. The reference point (origin of coordinate axes) might correspond to the centre of mass of the entire structure or a well-chosen point at the edge of the structure such that a defined set of coordinate axes should enclose the aggregate within the positive sector of the axes. The random variable, F_{ijk}, is used to characterise the distribution of number of faces of the grain in an aggregate *located* at a point with position vector $\vec{d}_{ijk}$ from the reference point. The characterisation of number of faces, *V(d),* of a collection of all grains in that aggregate is assumed to follow a compound (marked) stochastic point process, [16], given as

$$V(d) = \sum_{z=1}^{N(d)} {}_{z}F_{ijk} \tag{5.3}$$

where ${}_{z}F_{ijk}$ is the number of faces on the z^{th} grain and *d* is such that $d^2 = d_1^2 + d_2^2 + d_3^2$, i.e. $\vec{d}_{ijk} = (d_i, d_j, d_k)$.

Grain growth/coarsening in a polycrystalline aggregate differs fundamentally from the growth/coarsening of a size of separate particles. For the size of a grain in an aggregate to increase, it is necessary that another grain should decrease in size or disappear from the system [4,5,30,31,32]. Hence, an increase in the number of faces of an average grain (grain growth) brings about a reduction in number of grains in that aggregate since the volume of the entire aggregate is considered constant, [31], during coarsening. In fact, Glazier et al, [33], found that during the growth/coarsening mechanisms, the number of grains in an aggregate decrease as time increases as shown in Fig.5.2.

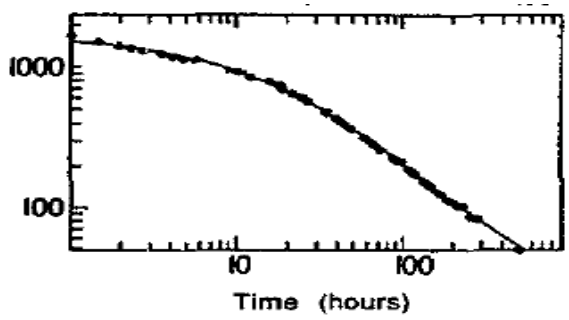

Figure 5.2 *Time evolution of number of grains per unit volume by Glazier J.A. and Weaire D.,* [33]

As a result, in an aggregate, the number of grains per unit volume and the number of faces per grain are physically related. These two variables that play the central role in the present model are assumed to be statistically independent as substantiated by a similar fact that the steady-state displacement x and the velocity $\dot{x}$ response of an oscillator to a Gaussian white noise excitation are statistically independent but physically related as $\dot{x} = dx/dt$. The additional assumptions that $\Pr\{N(0)=0\}=1$ is made. It can be inferred from Aboav-Weaire relation that neither $N(d)$ nor F_{ijk} random variables are necessarily independent nor identically distributed.

To apply the theory of Stieltjes sum or Stieltjes integral, the aggregate is divided into contiguous sub-aggregates. It should be observed that there exists a set of

coordinate points (x_i, x_j, x_k) and $(x_{i'}, x_{j'}, x_{k'})$ with $(i,j,k) \neq (i',j',k')$ such that $d_{ijk} = d_{i'j'k'}$ i.e. two or more grains in the aggregate are located at the same distance from the reference point. Hence, upon application of the theory of Stieltjes sum, the number of initial (radial) sub-regions would/might be lesser than the number of possible microstructure points. Thus, regularity condition does not hold in the usual sense, and hence, modification has to be done. This indicates that integration has to be done with respect to the Cartesian/spherical coordinate variables and not with respect to the radial distance.

After division of the measure of the entire aggregate $B(0,d)$ onto disjoint, contiguous measures of sub-aggregates, $\Delta B(0,d_{ijk}) = B(0,d_{ijk} + \Delta d_{ijk}) \setminus B(0,d_{ijk})$; and also upon division of the measure of sub-aggregate $\Delta B(0,d_{ijk})$ into another (but smaller) contiguous measures of sub-aggregates $\Delta B(0,d_{i'j'k'}) \setminus \Delta B(0,d_{ijk})$ with $(i,j,k) \neq (i',j',k')$ describing coordinates of separate grain-points that have the same distance from the reference point, but which are closer to each other than to any other point as in Voronnoi Tessellations, it follows that *V(d)* in equation (5.3) can be written as the Riemann Stieltjes sum. The limit, in the mean square sense, of the sequence of such sums (5.3), is the mean-square Riemann Stieltjes integral with respect to the counting process *N(d),* [16], i.e. the stochastic integral

$$V(d) = \int_0^{d_1}\int_0^{d_2}\int_0^{d_3} F(s,r,t)\,dN(s,r,t) \Leftrightarrow dV(s,r,t) = F(s,r,t)\,dN(s,r,t) \qquad (5.4)$$

This is the ***master expression*** that represents the random number faces of all the grains in an aggregate or sub-aggregate. The 0 and *d* limits in the above integral correspond to the situation where the origin of the coordinate axes is at the edge of the entire structure. If this origin were within the structure, then the limit of integration would be modified. Since $\Delta B(0,d_{i'j'k'}) \setminus \Delta B(0,d_{ijk})$ represents measure of grain size or "grain volume", regularity condition requires that

$$\sum_{k\geq 2}\Pr\{d[N(s,r,t)]=k\}=O(dt^2) \tag{5.5}$$

This means, obviously, that a grain measure or "grain volume" in an aggregate can only be occupied, with non-zero probability, by one grain or no grain at all. Obviously

$$\sum_{k\geq 2}\Pr\{dN(d_{ijk})=k\}\neq O(dt^2) \quad \text{with} \quad \sum_{k\geq k'}\Pr\{dN(d_{ijk})=k\}=O(dt^2) \tag{5.6}$$

where $dN(d_{ijk})$ represents the number of grains in the sub-aggregate $B(0,d_{ijk}+\Delta d_{ijk})\backslash B(0,d_{ijk})$ and k' is a fixed number . The two expressions in (5.6) state that within a sub-aggregate $B(0,d_{ijk}+\Delta d_{ijk})\backslash B(0,d_{ijk})$, there may be, with non-zero probability, more than one grain; and, there is a finite number of grains in that sub-aggregate.

Since *F(s,r,t)* and *N(s,r,t)* are independent, expression (5.4) gives

$$E[dV(s,r,t)]=E\{F(s,r,t)dN(s,r,t)\}=E\{F(s,r,t)\}\nu(s,r,t)dsdrdt \tag{5.7}$$

And for an average microstructure, and using the regularity condition, then

$$E[dV(s,r,t)^n]=(E[F(s,r,t)])^n\nu(s,r,t)dsdrdt \tag{5.8}$$

where $\nu(s,r,t)$ is the mean rate (sparseness or density) of microstructures/grains in an aggregate. These last two expressions state that the statistics of number of faces of all grains in a sub-aggregate is proportional to the size of the sub-region, the mean rate (or sparseness or density) of grains and the statistics of number of faces per grain in that sub-aggregate. From expression (5.4), it follows that

$$\mu_{V(d)} = E[V(d)] = \int_0^{d_1}\int_0^{d_2}\int_0^{d_3} E\left[F(s,r,t)dN(r,s,t)\right] = \int_0^{d_1}\int_0^{d_2}\int_0^{d_3} E\left[F(s,r,t)\right]\nu(r,s,t)dsdrdt$$

…….…… (5.9)

$$\mu_{VV(d_1,d_2)} = E[V(d_1)V(d_2)] = \int_0^{d_{11}}\int_0^{d_{21}}\int_0^{d_{31}}\int_0^{d_{12}}\int_0^{d_{22}}\int_0^{d_{32}} E\left[F(s_1,r_1,t_1)F(s_2,r_2,t_2)\right]E\left[dN(s_1,r_1,t_1)dN(s_2,r_2,t_2)\right]$$

…….. (5.10)

In order to evaluate this last expression the "modified" degeneracy property of second-degree product density must be taken into account, which takes place within the integration domain. This involves considering the following sets of conditions

$$\left(s_1=s_2=s,\ r_1=r_2=r,\ t_1=t_2=t\right),\ \left(s_1=s_2=s,\ r_1=r_2=r,\ t_1\neq t_2\right),\ \left(s_1=s_2=s,\ r_1\neq r_2,\ t_1=t_2=t\right),$$

$$\left(s_1\neq s_2,\ r_1=r_2=r,\ t_1=t_2=t\right),\left(s_1=s_2=s,\ r_1\neq r_2,\ t_1\neq t_2\right),\left(s_1\neq s_2,\ r_1=r_2=r,\ t_1\neq t_2\right),$$

$$\left(s_1\neq s_2,\ r_1\neq r_2,\ t_1=t_2=t\right),\quad \left(s_1\neq s_2,\ r_1\neq r_2,\ t_1\neq t_2\right) \qquad (5.11)$$

Hence,

$$\mu_{VV(d_1,d_2)} = \int_0^{\min(d_{11},d_{12})}\int_0^{\min(d_{21},d_{22})}\int_0^{\min(d_{31},d_{32})} E[F(s,r,t)^2]\nu(s,r,t)dsdrdt$$

$$+ \int_0^{\min(d_{11},d_{12})}\int_0^{\min(d_{21},d_{22})}\int_0^{d_{31}}\int_0^{d_{32}} E\left[[F(s,r,t_1)][F(s,r,t_2)]\right]\nu(s,r,t_1;s,r,t_2)dsdrdt_1dt_2$$

$$+ \int_0^{\min(d_{11},d_{12})}\int_0^{d_{21}}\int_0^{d_{22}}\int_0^{\min(d_{31},d_{32})} E\left[[F(s,r_1,t)][F(s,r_2,t)]\right]\nu(s,r_1,t;s,r_2,t)dsdr_1dr_2dt$$

$$+ \int_0^{d_{11}}\int_0^{d_{12}}\int_0^{\min(d_{21},d_{22})}\int_0^{\min(d_{31},d_{32})} E\left[[F(s_1,r,t)][F(s_2,r,t)]\right]\nu(s_1,r,t;s_2,r,t)ds_1ds_2drdt$$

$$+ \int_0^{\min(d_{11},d_{12})}\int_0^{d_{21}}\int_0^{d_{22}}\int_0^{d_{31}}\int_0^{d_{32}} E\left[[F(s,r_1,t_1)][F(s,r_2,t_2)]\right]\nu(s,r_1,t_1;s,r_2,t_2)dsdr_1dr_2dt_1dt_2$$

$$+ \int_0^{d_{11}}\int_0^{d_{12}}\int_0^{\min(d_{21},d_{22})}\int_0^{d_{31}}\int_0^{d_{32}} E\left[[F(s_1,r,t_1)][F(s_2,r,t_2)]\right]\nu(s_1,r,t_1;s_2,r,t_2)ds_1ds_2drdt_1dt_2$$

$$+\int_0^{d_{11}}\int_0^{d_{12}}\int_0^{d_{21}}\int_0^{d_{22}}\int_0^{\min(d_{31},d_{32})} E\left[[F(s_1,r_1,t)][F(s_2,r_2,t)]\right]\nu(s_1,r_1,t;s_2,r_2,t)ds_1ds_2dr_1dr_2dt$$

$$+\int_0^{d_{11}}\int_0^{d_{12}}\int_0^{d_{21}}\int_0^{d_{22}}\int_0^{d_{31}}\int_0^{d_{32}} E\left[[F(s_1,r_1,t_1)][F(s_2,r_2,t_2)]\right]\nu(s_1,r_1,t_1;s_2,r_2,t_2)ds_1ds_2dr_1dr_2dt_1dt_2$$

…….. (5.12)

If the second moment of *V(d)* is to be found, then the upper limits of integration in (5.12) with upper limits as the minimum of "two" limits are changed to simple limits i.e. for example $\min(d_{11},d_{12}) = d_{11} = d_1$, $d_{11} \le d_{12}$. From expressions (5.9) and (5.12), it follows that auto-covariance function $k_{VV(d_1,d_2)}$ and the variance function $\sigma^2_{V(d)}$ are obtained as

$$k_{VV(d_1,d_2)} = \int_0^{\min(d_{11},d_{12})}\int_0^{\min(d_{21},d_{22})}\int_0^{\min(d_{31},d_{32})} E[F(s,r,t)^2]\nu(s,r,t)]dsdrdt$$

$$+\int_0^{\min(d_{11},d_{12})}\int_0^{\min(d_{21},d_{22})}\int_0^{d_{31}}\int_0^{d_{32}} E\left[[F(s,r,t_1)][F(s,r,t_2)]\right]\nu(s,r,t_1;s,r,t_2)dsdrdt_1dt_2$$

$$+\int_0^{\min(d_{11},d_{12})}\int_0^{d_{21}}\int_0^{d_{22}}\int_0^{\min(d_{31},d_{32})} E\left[[F(s,r_1,t)][F(s,r_2,t)]\right]\nu(s,r_1,t;s,r_2,t)dsdr_1dr_2dt$$

$$+\int_0^{d_{11}}\int_0^{d_{12}}\int_0^{\min(d_{21},d_{22})}\int_0^{\min(d_{31},d_{32})} E\left[[F(s_1,r,t)][F(s_2,r,t)]\right]\nu(s_1,r,t;s_2,r,t)ds_1ds_2drdt$$

$$+\int_0^{\min(d_{11},d_{12})}\int_0^{d_{21}}\int_0^{d_{22}}\int_0^{d_{31}}\int_0^{d_{32}} E\left[[F(s,r_1,t_1)][F(s,r_2,t_2)]\right]\nu(s,r_1,t_1;s,r_2,t_2)dsdr_1dr_2dt_1dt_2$$

$$+\int_0^{d_{11}}\int_0^{d_{12}}\int_0^{\min d_{21},d_{22})}\int_0^{d_{31}}\int_0^{d_{32}} E\left[[F(s_1,r,t_1)][F(s_2,r,t_2)]\right]\nu(s_1,r,t_1;s_2,r,t_2)ds_1ds_2drdt_1dt_2$$

$$+\int_0^{d_{11}}\int_0^{d_{12}}\int_0^{d_{21}}\int_0^{d_{22}}\int_0^{\min(d_{31},d_{32})} E\left[[F(s_1,r_1,t)][F(s_2,r_2,t)]\right]\nu(s_1,r_1,t;s_2,r_2,t)ds_1ds_2dr_1dr_2dt$$

…….. (5.13)

and

$$\sigma^2_{V(d)} = 7\int_0^{d_1}\int_0^{d_2}\int_0^{d_3} E[F(s,r,t)^2]\nu(s,r,t)dsdrdt \qquad (5.14)$$

The n^{th} order moment is obtained with all possible degeneracies of the joint n^{th}

degree product density taken into account.

5.2 **Applications of Proposed Model**

The distribution of the number of faces per grain in the scaling state is reported to be of varying form e.g. *Weibull, lognormal* or *Rayleigh*, [34], (also see Fig.5.3). It has been observed, [30,31], that during a Pott's model run and *on the scaling state* the mean number of faces per grain is $F_0 = 15.8 \pm 4$. Analyzing data obtained in other research work, [23], resulted in the number of faces per grain in an aggregate to be between **4** and **36**, the mean number of faces per grain in the aggregate of **96.63 grains** being **15.049** with a standard deviation of **5.7257**, the second and third moments of the distribution of number of faces per grain being **259.26** and **5002.11** respectively and the total number of faces in that aggregate being **1454.19**, i.e.

$$F(s,r,t) \in [4.36], \quad \mu = E\left[F(s,r,t)\right] = 15.05, \quad \sigma^2 = E\left[\{F(s,r,t) - \mu\}^2\right] = 32.784, \quad \mu^2 = 259.26$$
$$\mu^3 = E[\{F(s,r,t)\}^3] = 5002.11, \quad N(d) = 96.63 \text{ and } V(d) = 1454.19 \qquad (5.15)$$

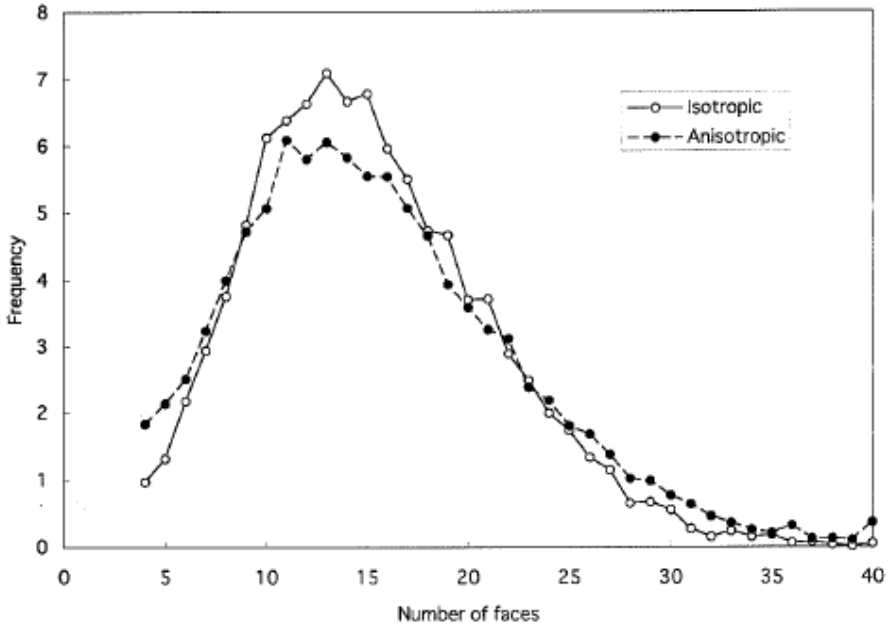

Figure 5.3 *The distribution of number of faces per grain by Saito,* [23]

Since the total number of faces (**1454.19**) in the scaling state is the **mean** of the cumulative number of faces of all the grains in that aggregate, the other corresponding statistics of the cumulative random variable can then be obtained. If grain segregation, growth and coarsening were to occur then the total number of faces in the aggregate and the corresponding statistics would vary when analysed under different time conditions. Such analysis is a subject of future research project.

The total size of the aggregate of grains is used to determine the limit of integrations in the integrals given above: d_i can be obtained from $V_T = \pi \sum_{i=1}^{n} m(a) d_i$, where V_T is the Lebesgue measure (or volume) of the aggregate, $m(a)$ is the Lebesgue constant, n is the order of the Lebesgue measure (i.e. $n=1$ for length, $n=2$ for area, $n=3$ for volume, etc). The "decreasing" relationship between the rate of $N(d)$ and $\langle F_{ijk} \rangle$ may be given by

$$v(s,r,t) = \lambda' e^{-\beta E[F(s,r,t)]} = e^{\lambda - \beta E[F(s,r,t)]} \tag{5.16}$$

where λ' is the density (number per unit volume) of grains corresponding to the minimum mean number of faces per grain, and β is a constant that represents the rate at which $v(s,r,t)$ decreases as $E[F(s,r,t)]$ increases.

Working with an aggregate where the statistical properties of the random variable, F_{ijk}, (whose analytic expression for the probability density function is yet unknown) are not functions of location, it follows that the statistics of F_{ijk} correspond to the statistics of the distribution of faces per grain F_n, Fig.5.3, (F_n is the random number of faces per grain not assigned to any particular location whose statistics have been obtained from other research works) i.e. for example $E[F_{ijk}] = E[F_n]$

Using expression (5.16), expression (5.7 becomes

$$E\left[dV(s,r,t)\right] = E(F_n)v(s,r,t)dsdrdt = E(F_n)e^{\lambda-\beta E[F_n]}dsdrdt \qquad (5.17)$$

Similarly

$$\mu_{V(d)} = E[V(d)] = \int_0^{d_1}\int_0^{d_2}\int_0^{d_3}\left(E[F_n]e^{\lambda-\beta E[F_n]}\right)dsdrdt = \left(E[F_n]e^{\lambda-\beta E[F_n]}\right)_{d_1 d_2 d_3}$$

…… (5.18)

Applying experimental data to an aggregate where $d_1 = d_2 = d_3 = d = \left(3V_T/(4\pi)\right)^{1/3}$ and ***λ`=240*** for the case where grain growth and coarsening are very slow as justified by Russell [25], equation (5.18) simplifies to

$$\mu_{V(d)} = \left(E[F_n].240e^{\beta(4-E[F_n])}\right)d_1 d_2 d_3 = 240\left(E[F_n]e^{\beta(4-E[F_n])}\right)\left(\frac{V_T}{(4/3)\pi}\right)$$

$$\Leftrightarrow e^{\beta(4-15.049)} = \frac{\mu_{V(d)}}{240E[F_n]}\left(\frac{(4/3)\pi}{V_T}\right) = \frac{1454.19}{(240)(15.049}\left(\frac{(4/3)\pi}{100.644}\right) = 0.016757$$

$$\Leftrightarrow \beta = \frac{\ln(0.016757)}{-11.049} = 0.370$$

Expression (5.16) can now be written for the present aggregate as

$$v(s,r,t) = e^{0.370(4-E[F_n])} \qquad (5.19)$$

Obtaining other higher order statistics from experimental data are not trivial issues. However, from expression (5.14), it follows that

$$\sigma^2_{V(d)} = 7\int_0^{d_1}\int_0^{d_2}\int_0^{d_3} E[F_n{}^2]\,240e^{0.370(4-E[F_n])}\,dsdrdt = 7(240)E[F_n{}^2]e^{0.370(4-E[F_n])}d_1d_2d_3$$

$$= 7 \text{ x } 240 \text{ x } 259.258 \text{ x } e^{0.370(-11.049)} \text{ x}\left[\frac{100.644}{(4/3)\pi}\right] = 175504.569$$

$$\Leftrightarrow \quad \sigma_{V(d)} = 418.933 \qquad (5.20)$$

It should be remarked that at scaling state if the standard deviation of the number of faces per grain, which is **5.7527,** is multiplied by the total number of grains, which is **96.63,** then one might have the impression the standard deviation of the cumulative number of faces in the aggregate is **553.275** and not **418.93** as obtained in equation (5.20). The difference in value can be explained mathematically by the degeneracy property of product density of the counting process. Practically, this is due to the fact that, apart from the cumulative mean value, the other higher order cumulative statistics cannot be obtained by simply multiplying the marked random variable's statistics by the total mean number of grain points in the aggregate. It can be clearly seen that if that were the case, then for example

$$N(d).\left[\sigma_{F_{ijk}}\right]^2 = "Var\,[V(d)]"$$

$$= \left[\sigma_{V(d)}\right]^2 = \left[N(d).\sigma_{F_{ijk}}\right]^2 = \left[N(d)\right]^2\left[\sigma_{F_{ijk}}\right]^2 \;\Leftrightarrow\; N(d) = 1 \qquad (5.21)$$

which is true only when N(d)=1 and hence, leading to a contradiction. Hence, the statistics of the **cumulative (compound)** random variable should not be obtained by simple intuition but by utilising the proposed expressions. The spatial evolution of the total number of faces of grains in the aggregate at the scaling state is given by the spatial distribution of the grains (how the aggregate can be traced or covered) and the mean number of faces per grain as proposed by, for example, expressions (5.17) or (5.18). Recall that the mean number of faces per grain may be given as a function of the point of location of the grains and not as constant.

With grain growth being a common feature that affects the temporal distribution of microstructures features within any material, the next task is now to engage in the understanding and analyse of the grain growth processes or mechanisms.

6 STATISTICAL MODEL OF GRAIN GROWTH IN POLYCRYSTALLINE NANOMATERIALS

It has taken about five decades to start apprehending the statement, "*There is plenty of opportunities at the bottom*", made by the American Nobel Prize winner, Prof. Richard P. Feynman, in 1959. Feynman postulated that it would be very interesting if the grains/particles in materials could be reduced to very fine sizes (nano-sizes) whose properties/structures could be analysed and manipulated at atomistic scale to come up with new structures/materials that may exhibit enhanced properties or could lead to the understanding of the entire material itself. Nowadays, nanoscience and nanotechnology are engaged in these studies. Some of the different strategies involved in the production of nanomaterials are the bottom-up methods whereby very fine particles are combined to obtain nano-scale particles and the top-down methods in which case the sizes of coarse particles are reduced to smaller scale ones .

This process of reduction to nano-sizes comes up with the challenges of the instability of the refined grains as they are more vulnerable to growth even at very low temperature which may thus limit their applications. Thus, an interest has been to analyse the grain growth phenomena in nano-crystalline metals. The growth of a single grain in a system of grains was postulated by Hillert in 1965, [35]. His model has always led to the parabolic growth law which holds more correctly for the isotropic case, like the soap froth since grain growth process is considered in his model to be isotropic grain boundary migration mechanism *(GBM) only*. Other experiments on polycrystalline materials have shown deviations from this parabolic law. Apart from Hillert's model, abnormal grain growth has been reported. Recent theoretical and experimental investigations have proven that the growth in the (average) grain size in a system is not only accomplished by GBM. Other processes also involved include grain rotations-coalescence *(GRC)* mechanism, [36,37,38], T2 events in which a small three-sided grain disappears and T1 mechanisms whereby two grains which were

initially neighbours separate along a common grain boundary while, simultaneously, two grains which were initially not neighbours move towards each other to form a new common grain boundary. For more details on T1 and T2 events, interested readers are referred to the original works by the authors in the references, [37,39,40]. Furthermore, there is report, [41], on the release of excess free volumes in the form of vacancies in which during grain growth the less dense GB 'phase' decreases in amount accompanied with the release of excess free volumes that are digested by the GI (or bulk of the materials) in the form of vacancies. Significant efforts have been devoted in this report, [41], to substantiate that the kinematic necessity of the vacancy generation might have an inhibitive effect on grain growth. For more information about the release of excess free volumes in the form of vacancies and its effects on grain growth, one may read the publication by Estrin et al, [41]. Thus, predicting microstructure evolution in materials is important for materials design and processing.

In the present chapter, a statistical model is proposed in order to study grain growth processes in nanomaterials. The effort in the present chapter is aimed at improving on the Hillert's model to account for these new observations. Particular attention has been focused on GBM and GRC mechanisms since both T1 and T2 events are processes that might initiate GBM, grain coalescence or GRC mechanisms. GBM is a process in which the grain size evolves *continuously (diffusion based evolution)* with time and GRC is a *discrete (discontinuous)* process that causes a change in the grain size at some *instant* when the misorientation angle between some adjacent grains *becomes* zero, [38] (see Appendixes **A1** and **A2** for schematics of GRC). Furthermore, the "***stochastic***" approach adopted in this report focuses attention on the "extent" to which the size of a grain will grow after some time interval, and not on how the atoms or groups of atoms in the materials interact to bring out grain growth. A terminology borrowed from Estrin, [41], is that such an approach is "thermodynamic" since the details mechanisms (or chemistry) of, for example, GBM processes and GRC processes are not dealt with. Thus, the "***phase mixture***" approach of the release of excess free volume at the GB that is consumed by the GI is as such not also

dealt with here.

The growth in sizes of individual grains observed in most polycrystalline materials where GBM and/or GRC mechanisms occur may be studied as per the following three cases below:

1. Grain growth by boundary migration only - *GBM*
2. Grain growth by rotation-coalescence only -*GRC*
3. Grain growth by both GBM and GRC simultaneously - *Simultaneous GBM and GRC* (or *Total Process*).

Simultaneous GBM and GRC, a linear combination of both cases 1 and 2, may be given as

$$dr = a_{11} f(r,t)dt + a_{22} G(r,\theta,t)dN(t) \tag{6.1}$$

where the a_{ii}^{s} are the "compensation coefficients" that indicate the proportion in which the two growth mechanisms combine, $f(r,t)=f(r,\theta,t)$ is a curvature driven mechanism, $G(r,\theta,t)$ grain misorientation angle driven mechanism and $dN(t)$ is the increment of the number coalescence mechanisms during an infinitesimal time interval. It is observed that GRC does not affect the curvature of the grain as the grain rotates and GBM does not change the misorientation between two grains while the boundary migrates. Thus, the coefficients, a_{ii}, are considered to be equal to one. Hence, the expression for $f(r,t)$ is taken as an expression similar to that given previously by Hillert, 1965, [35]. To define $G(r,\theta,t)$, note that it reflects the change in the size of the grain, Δr, as the misorientation angle between that grain and its neighbour becomes zero at some time instant *t.* At this instant two grains combine. So, $\Delta r=r$. Thus, $G(r,\theta,t)=r$ (also see the appendix **B** for the alternative derivation of the expression of the GRC process). Hence, the *improved* expression for the change of an *individual* grain size is

$$dr = M_{mig}\left(\frac{1}{r_c} - \frac{1}{r}\right)dt + rdN \tag{6.2}$$

where M_{mig} is the mobility constant for grain boundary migration and r_c is the *local* critical grain size. The local critical grain size is the (exclusive) mean size of the grain surrounding the particular grain and, hence, is related to the global mean size. In fact, references [40,42] state that the ratio μ_r / μ_{r_c} is a constant for a given self-similar distribution as both μ_{r_c} and μ_r scale with same characteristic length of the self-similar distribution. The importance of the local critical grain size is that the grain under consideration will grow if its size is larger than its local critical grain size or, otherwise, it will shrink. Hence, based on the fact that its local critical grain size changes continuously as grains grow, the particular grain may at an instant be seen growing while later it may be shrinking, then followed by growth and so on. This …/growth/shrinkage/growth/… process continues randomly during the growth process. Thus, the grain growth process is geometrically a complex phenomenon. This necessitates that the aggregate be analysed stochastically. The evolution of the grain size may be given by solving the differential expression (6.2). But this does not lead to statistical meaningful results. Hence, it is not pursued as such. Since expression (6.2) holds for *individual* grains and a grain size in an aggregate is random variable leading to the consequence that the effects of the many agents causing grain growth cannot be deterministic as long as the effects of these agents on each grain are not known separately, the stochastic counterpart of this expression is necessary which is given by the addition of fluctuation terms:

$$dr = rdN + M_{mig}\left(\frac{1}{r_c} - \frac{1}{r}\right)dt + a(r,\theta,t)dW(t) + b(r,\theta,t)rdN(t) \tag{6.3}$$

where $a(r,\theta,t)dW(t)$ accounts for the random fluctuation in *r(t)* due to GBM, $b(r,\theta,t)rdN(t)$ does for the random fluctuation in *r(t)* due to coalescence mechanism, $a(r,\theta,t) = a$ is the diffusion term, $b(r,\theta,t) = b$ is the jump term and

d*W(t)* is the increment of the Wiener process. In fact, Zhao, [43], justified that the continuous fluctuation term is a Wiener process.

Based on the stochastic equation, (6.3), the differential equations governing the evolution of the statistical moments of the distribution of the grain size in a system that contains as many grains as possible are derived. Considering the fact many other mechanisms bring about the variations in the grain size, the grain size in the system at any time, *t,* is independent of the number of coalescence mechanisms (stochastic counting processes) up to that time instant. It is known that $E<a\mathrm{d}W(t)>=0$ and $E[brdN(t)] = bE[r]v(t).dt$ where *v(t)* is the mean rate of coalescence events of grains. Since expectation and limit are interchangeable and writing $E[r(t)] = \mu_r = \mu$, it follows that

$$d\mu = M_{mig}\left(E\left[\frac{1}{r_c}\right] - E\left[\frac{1}{r}\right]\right)dt + (1+b)\mu.v(t)dt \tag{6.4}$$

Using expression (6.3) and the Ito's differential rule [16], it follows on writing $E[r^2]=\mu_2$ that

$$d\mu_2 = \left[2M_{mig}E\left[\frac{1}{r_c}\right]\mu - 2M + a^2 + \left[b^2 + 4b + 3\right]v(t)\mu_2\right]dt \tag{6.5}$$

Practical insight is used here and verification is the subject of the next chapter. Many experimental investigations have proven that the distribution of grain size during growth can be approximated more closely by lognormal distribution, [44,45,46]. Thus, the expectations in expressions (6.4) and (6.5) are performed based on the properties of log normal distribution, [47]. Expressions (6.4) and (6.5) are coupled expressions which are then solved simultaneously. Solutions to these expressions reveal information about the evolution of the statistics of grain size during growth.

The mean rate of coalescence of grains, *v(t)*, is determined from the mean rate of

rotation of these grains. The number of coalescence between the a grain and its neighbour is given

$$N(t) = \frac{\theta_2 - \theta_1}{\theta_1} = \frac{\Delta\theta}{\theta_1} \tag{6.6}$$

where θ_1 is the misorientation angle at the initial time, t=0, and θ_2 is the misorientation angle after time, t. Note that for these two grains, θ_1 is a constant, and if $\theta_2 = 0$ at coalescence of the grains then $N(t) = -1$. Therefore

$$\frac{dN(t)}{dt} = \frac{1}{\theta_1}\frac{d\theta}{dt} = \frac{\omega}{\theta_1} \tag{6.7}$$

This is because $N(t) = N(t) - N(0)$ since $N(0) = 0$, where ω the angular velocity of a grain in the aggregate at the instant. Thus, for infinitely small time interval, $\Delta t \rightarrow 0$, and at coalescence it follows that $\theta_1 \cong \theta$ and so

$$v(t) = \frac{dE\left[N(t)\right]}{dt} = E\left[\frac{\omega}{\theta}\right] \tag{6.8}$$

Assuming that the force laws governing GRC processes are viscous rather than conservative by nature, the angular velocity of a rotating grain, ω, relative to its neighbouring grain with respect to an axis through its centre of mass is given by, [37,38] as $\omega = M_{rot}\tau$, where M_{rot} is the rotational mobility of the grain subject to a torque τ. Thus, an expression for the angular velocity between two grains contains information about their rotation mobility. And so the rate of coalescence of the grains has been established to be a function of the rotation mobility. It is then clear that our modified expression, (6.2), and of course (6.3), involve the rotational mobility function (or constant) of that grain.

6.1 Testing Proposed Model of Grain Growth

Prolonged analysis was performed so as to capture the long run behaviour of the statistics. Three types of systems given by *cases 1-3* above were analysed. The parameters employed are $v(t) = H/\mu^6$, $H = 100000$, $M_{mig} = 5$, $\mu_r/\mu_{r_c} = 1.9$, $\mu_{r0} = 1$, $b(r,\theta,t) = r$ and $a(r,\theta,t) = 1000\sqrt{r}$.

It was observed that most statistical properties were higher for the system where both GBM and GRC occur simultaneously. The (normalised) mean size increases faster for the system of simultaneous GBM and GRC mechanisms than for either of GBM or GRC alone as shown in Fig.6.1

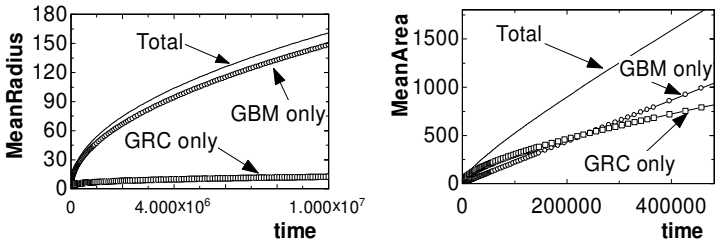

Figure 6.1 *Variation of mean grain size*

It is observed that though GRC had low initial contribution to the increase in mean grain size, its contribution becomes higher (about 85% depending on the initial dispersion of the grains in the polycrystalline material) after a short time while growth was activated. And evolution in the long run is highly dominated by GBM process. This fluctuation indicates an abnormal grain growth. This can be clearly seen if the percentage contributions to the mean size are analysed (Fig.6.2). The evolution of the mean grain area indicates that the inclusion of (different rate of) GRC mechanisms results in departures from the parabolic law of grain growth which has also been observed experimentally, especially in nanomaterials.

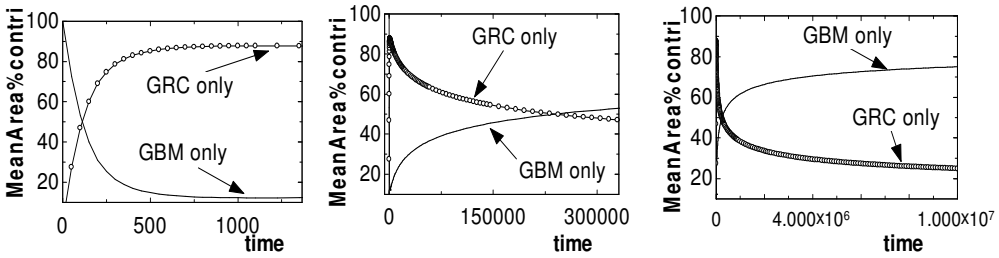

Figure 6.2 *Percentage contributions to mean size*

The evolution of the dispersion of grains sizes are characterised by the coefficients of variation **–** *CV* **-** (Fig.6.3). It is observed that if grain growth is as a result of GBM driven process only, then CV will steadily decay exponentially and homogenises. But for a typical nanomaterial where both GBM and GRC occur simultaneously, it is observed that the CV initially rises steadily and then decays exponentially to homogeneity. This situation, of a less dispersed system becoming more dispersed due to grain growth, has also been reported, [37,38]. This can be explained to be due the fact that with initially no dispersion in grain size, grain growth would still takes place as GRC would trigger grain growth by starting up dispersion which then initiates GBM. We believe that the occurrence/presence of the GRC mechanism is also the reason while nanomaterials are more vulnerable to grain growth even at low temperature. The decay in the dispersion in the long run is due to the fact that as the sizes of the grains become larger, it becomes difficult for them to rotate and, hence, the growth process is dominated by GBM.

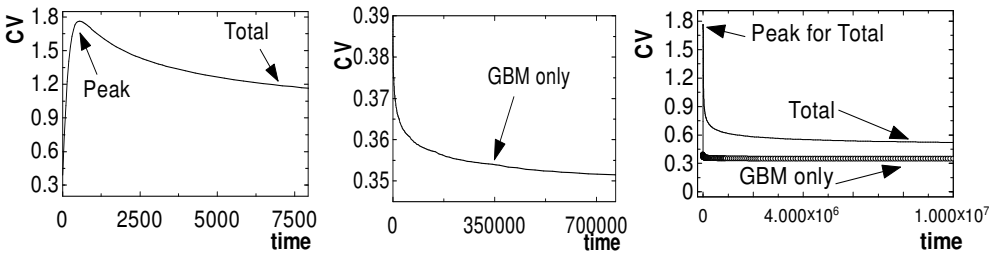

Figure 6.3 *The evolution of the Coefficient of variation (dispersion)*

It can be concluded that the expression for the evolution of the dispersion of the system depends on the growth process under consideration. For GBM process only the CV evolves, [48] and Fig.6.3(b), as

$$CV = 3.5 + (CV_0 - 3.5)\exp(-At) \qquad (\mathbf{6.}9)$$

where *A* is constant. For simultaneous GBM and GRC processes, Fig.(6.3c)

$$CV = \begin{cases} f(t) & 0 < t \le t_a \\ 3.5 + (CV_a - 3.5)\exp[-A(t - t_a)], \;\; CV_a = f(t_a) & t_a < t \le t_f \end{cases} \qquad (\mathbf{6.}10)$$

where *f(t)* is a function that increases and attains a turning point at t_a.

Other parameters of grain growth can be predicted by the asymptotic time dependence (power law kinetics) given as, [23,49,50],

$$\mu_d(t) = \mu_{d0} + K.t^n \qquad (6.11)$$

where $\mu_d(t)$ is the average diameter at time *t*, μ_{d0} is the initial average diameter, *K* is a constant (or function) that is related to the average mobility constant and *n* is a constant which is termed the growth exponent.

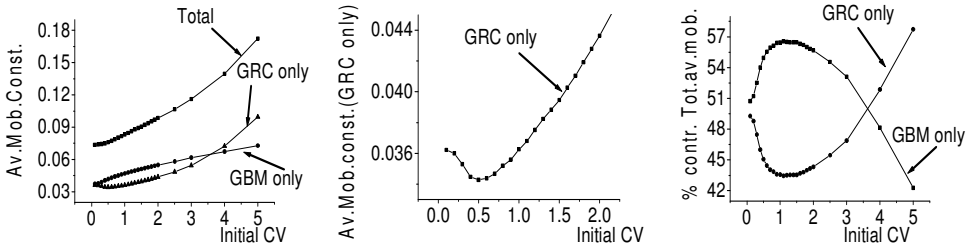

Figure 6.4 *Initial CV versus (a),(b) average mobility and (c) percentage contribution to average mobility*

In the cases where growth is GBM process only and a simultaneous GBM and GRC processes, it is observed (Fig.6.4) that the average mobility increases steadily with increase in the initial dispersion of grain size. The overall result indicates that nanomaterials with highly dispersed grains will grow faster than those with low dispersion. But it is observed that, for GRC only process, the

average rotation mobility is high for very low dispersion which decreases to a minimum and the rises steadily with increasing initial CV. This very high average rotation mobility at very low dispersion also indicates a natural tendency for the grains in nanomaterials to be more vulnerable to growth even at low dispersion. The results also demonstrate that the average rotation mobility which is a consequence of the varying misorientation angle contributes up to about 50% of the overall average boundary mobility, Fig.6.4(c).

Thus, the average mobility constant, *K*, depends on the initial dispersion of grain size and is given by an expression that depends on the growth process under consideration: for GBM, it is approximately by

$$K = K_0 + K_{grad} CV_0 \tag{6.12}$$

and for GRC only and simultaneous GBM and GRC, it can be given as

$$K = K_0^{'} + K_{grad} \left(CV_0 - CV_1\right)^2. \tag{6.13}$$

where K_0 is initial value, K_{grad} is the slope of the curve and CV_1 is the value of initial dispersion at which turning point is attained. CV_1 =0 for simultaneous GBM and GRC.

The variation in the growth exponent is shown in Fig.6.5. This varying growth exponent indicates deviations of results of the present model from the parabolic law (and any growth law) with varying initial CV. A steady decrease demonstrates an increase in the dimensional space where a linear growth law will be obtained. The varying growth exponent has also been experimentally, [49]. The growth exponent may also be assumed to be constant on an average as observed in Fig.6.5C since the variation of slope is small. This constant growth exponent has also been observed experimentally by Kurzydlowski et al [48].

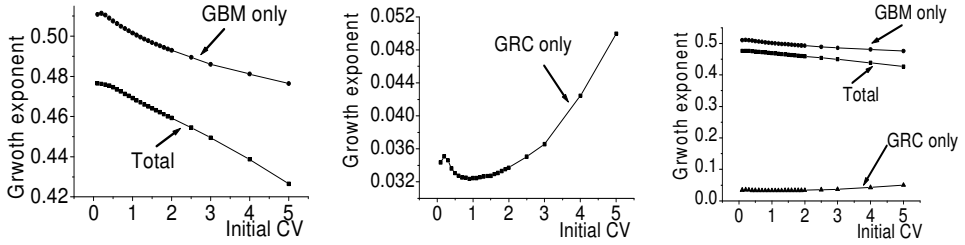

Figure 6.5 *Initial CV versus growth exponent.*

A successful modification of the Hillert's model by incorporating GRC mechanism in the expression for growth of a single grain size which was ignored in the previous model has been achieved and many salient features of grain growth in polycrystalline nanomaterials have thus been revealed. The stochastic counterpart of the improved expression accounts for the random fluctuation in the distribution of the grain size in "dispersed-typed" nanomaterials that have as many grains as possible. The evolution of the probability distribution of the grain size in the material, which is dealt with in the next chapter, can be obtained from information about the evolution of the grain sizes. We should then proceed with studying the time evolution of the probability distribution of the grain size

7 MODELLING OF THE GRAIN SIZE PROBABILITY DISTRIBUTION IN POLYCRYSTALLINE NANOMATERIALS

Nanomaterials are solid materials in which the microstructure elements (such as grains, crystallites, blocks and layers) are refined to have dimensions less than 100nm at least in one direction. This process of refinement comes up with the challenges of the instability of the microstructure elements as they are more vulnerable to growth even at low temperature. Recent investigation, [CHAPTER 6], also indicates that another contributing factor to the low stability of nanomaterials is high rotational mobility of the fine grains more emphatically at low dispersion of grain size.

Theoretical analyses have always resulted in nanomaterials' grain size probability distribution being of varied form: approximately either lognormal, Rayleigh, normal, Weibull, etc. This is because the isotropic Hillert's model of grain growth, [35], which is more suitable for soap froth and which leads to a parabolic law of growth has been previously used to establish these distributions with the hope of approximating experimental observations. But due to deviations from this parabolic law of grain growth in many experimental observations, the model of grain growth developed in CHAPTER 6 which is a modification of the Hillert's model, is used in the present chapter to establish the time evolution of the probability distribution of the grain size in nanomaterials that contains as many grains as possible.

In the modified model, the growth in a grain size in an aggregate is considered to be caused by two mechanisms: curvature driven Grain Boundary Migration process, **GBM**, (a continuous process in which larger grains gradually consume smaller grains) and Grain Rotation Coalescence mechanism, **GRC**, (a discontinuous process whereby two grains instantaneously become one grain only when the misorientation angle between them becomes zero). The modified differential expression for the rate of change of individual grain size in the aggregate as given in CHAPTER 6 can be expressed as

$$\frac{dr}{dt} = M_{mig}\left(\frac{1}{r_c} - \frac{1}{r}\right) + \sum_i r_i \delta(t - t_i) \tag{7.1}$$

where M_{mig} grain boundary mobility constant, r_c is local critical grain size and $r_i \delta(t - t_i)$ reflects the change in grain size as the misorientation angle becomes zero at some particular time point t_i.

Since the grain size in the aggregate is random, the stochastic counterpart of the expression governing the incremental change in individual grain size was obtained by the addition of two fluctuation terms, [CHAPTER 6], to be

$$dr = M_{mig}\left(\frac{1}{r_c} - \frac{1}{r}\right)dt + r dN(t) + a(r,\theta,t)dW(t) + b(r,\theta,t) r dN(t) \tag{7.2}$$

where $a(r,\theta,t)dW(t)$ accounts for the random fluctuation in *r(t)* due to grain boundary migration, $b(r,\theta,t) r dN(t)$ accounts for the random fluctuation in *r(t)* due to the coalescence mechanism, $a(r,\theta,t)$ is the diffusion term, $[1 + b(r,\theta,t)]r$ is the total jump term, d*W(t)* is the increment of the Wiener process and $dN(t) = N(t + dt) - N(t)$ is an increment of a stochastic counting process (i.e. the number of coalescence events) within an infinitesimal time interval.

Based on the (general) stochastic equation, (7.2), the differential equations governing the evolution of the statistical moments of the grain size distribution in the material are derived. These expectations are performed based on the probability distribution that is the subject of the present paper.

The development of the probability density function, $q_{\{r\}}(r, t / r_0, t_0)$, of the grain size distribution with respect to the forward time, *t*, is obtained from the generalized integro-differential forward Fokker-Planck-Kolmogorov equation, [16-20], as

$$\frac{\partial}{\partial t}q_{\{r\}}(r,t/r_0,t_0)=-\frac{\partial}{\partial r}\left[C(r,t)q_{\{r\}}(r,t/r_0,t_0)\right]+\frac{1}{2}\frac{\partial^2}{\partial r^2}\left[D(r,t)q_{\{r\}}(r,t/r_0,t_0)\right]$$
$$+\int\left[J_{\{r\}}(r/x,t)q_{\{r\}}(x,t/r_0,t_0)-J_{\{r\}}(x/r,t)q_{\{r\}}(r,t/r_0,t_0)\right]dx,\quad x>0 \qquad (7.3)$$

where C(r,t) and D(r,t) are the first and second derivate moments given from expression (7.2) as

$$\begin{cases} C(r,t)=M_{mig}\left(\dfrac{1}{r_c}-\dfrac{1}{r}\right) \\ D(r,t)=\left[a(r,\theta,t)\right]^2 \end{cases} \qquad (7.4)$$

and where $J_{\{r\}}(r/x,t)$ is the jump probability intensity function given, in accordance with [16], as

$$J_{\{r\}}(r/x,t)=\int_p \delta\left(r-(x+\left[1+b(x,\theta,t)\right]xp)\right)J_{\{dN\}}(p,t)dp\,,\quad p=1 \qquad (7.5)$$

The function $b(x,\theta,t)$ is assumed as $b(x,\theta,t)=x$ and, so, it is state dependent. A preliminary change of variable has to be performed in order to evaluate the integral in (7.5) with respect to x, [16]. Let $u=x+\left[1+x\right]x$, then $x=-1\pm\sqrt{1+u}$. Since x belongs to the set of grain sizes, it must be greater than or equal to zero. Thus, $x=-1+\sqrt{1+u}$, $dx=du/\left\{2\sqrt{1+u}\right\}$ and equation (7.3) becomes

$$\frac{\partial}{\partial t}q_{\{r\}}(r,t/r_0,t_0)=-\frac{\partial}{\partial r}\left[\left(M_{mig}\left\{\frac{1}{r_c}-\frac{1}{r}\right\}\right)q_{\{r\}}(r,t/r_0,t_0)\right]+\frac{1}{2}\frac{\partial^2}{\partial r^2}\left[(a)^2\,q_{\{r\}}(r,t/r_0,t_0)\right]$$
$$+\int_p\left[q_{\{r\}}(-1+\sqrt{1+r},t/r_0,t_0)\frac{1}{2\sqrt{1+r}}-q_{\{r\}}(r,t/r_0,t_0)\right]J_{\{\sum dN\}}(1,t)dp \qquad (7.6)$$

Equation (7.6) is associated with the pertinent initial and boundary conditions which are determined by the type of material under consideration (i.e. the extent to which grains grow is determined by the type of material under consideration).

Let the domain S_t of the state variable (scalar for the present case- grain size) be confined to the interval]0,d [i.e. for grain growth to occur the size of the grain cannot be zero and indefinite growth is impossible. In general, it is assumed that the 1-dimensional state variable, r(t), is restricted to some domain S_t which may depend on time being influenced by factors affecting grain growth such as the strain hardening effects, impurities, particle pinning and/or solute drag segregations on grain boundaries, [25]. Thus, the necessary initial and boundary conditions are

$$\forall r_0, r \in]0,d[\; : \; q_{\{r\}}(r,t_0 / r_0,t_0) = \delta(r - r_0) \tag{7.7}$$

$$\forall t \in]t_0,t_f[, \quad r_0 \in]0,d[, \quad r = 0 \; : \; q_{\{r\}}(r,t / r_0,t_0) = 0 \tag{7.8}$$

$$\forall t \in]t_0,t_f[, \quad r_0 \in]0,d[, \quad r = d \; : \; q_{\{r\}}(r,t / r_0,t_0) = 0 \tag{7.9}$$

Expression (7.7) states that at a time instant, the probability of a grain to possess two different sizes equals zero. Note, also, that at coalescence of grains due to GRC process, two grains combine to end up with a **unique** size at that instant. Expression (7.8) states that grains cannot "disappear" in the sense that "matter is destroyed". And (7.9) implies that there is a limiting size to which grains grow (i.e. grains do not grow indefinitely or they grow asymptotically).

Equations (7.6), (7.8) and (7.9) are multiplied by $q(r_0 ,t_0)$ and integrated over r_0. The jump process considered here is a counting process only, which means that all mark variables are equal to 1. Consequently, the property of jump probability intensity function is given as $J_{\{dN\}}(1,t) = v(r,t) f_{\{p\}}(p)$ with $f_p(p) = \delta(1-p)$, where $v(r,t)$ is the mean rate of coalescence events of grains (i.e. the rate at which the misorientation angle becomes zero). The evolution of the unconditional probability density function of grains sizes is then given from (7.6) as

$$\frac{\partial}{\partial t}q_{\{r\}}(r,t) = -\frac{\partial}{\partial r}\left[\left(M_{mig}\left\{\frac{1}{r_c}-\frac{1}{r}\right\}\right)q_{\{r\}}(r,t)\right] + \frac{1}{2}\frac{\partial^2}{\partial r^2}\left[(a)^2 q_{\{r\}}(r,t)\right]$$

$$+\left[\frac{1}{2\sqrt{1+r}}q_{\{r\}}(-1+\sqrt{1+r}) - q_{\{r\}}(r,t)\right]v(r,t) \qquad (7.10)$$

with the initial and boundary conditions, (7.8) and (7.9), reducing to

$$\forall\ domain\ S_t =]0,d[\ : q_{\{r\}}(r=0,t) = 0 \qquad (7.11)$$

$$\forall\ domain\ S_t =]0,d[\ : q_{\{r\}}(r=d,t) = 0 \qquad (7.12)$$

$$q_{\{r\}}(r,t)/_{t=0} = q^0{}_{\{r\}}(r) \qquad (7.13)$$

However, from CHAPTER 6, $v(r,t) = dE[N(t)]/dt = -E[\omega/\theta]$ and since in [37,38] it is proved that $\omega = D/r^4$, it is concluded that $v(r,t) = H/r^4$.

Using a Taylor series expansion for $q_{\{r\}}(-1+\sqrt{1+r},t)$ found in expression (7.10) given as

$$q_{\{r\}}(-1+\sqrt{1+r},t) = q_{\{r\}}(r,t) + 2\sqrt{1+r}.\left[\sqrt{1+r}-(1+r)\right]\frac{\partial q_{\{r\}}(r,t)}{dr}$$

$$+\frac{1}{2!}\frac{1}{\frac{1}{2}(\frac{-1}{2})}(1+r)^{3/2}\left[\sqrt{1+r}-(1+r)\right]^2\frac{\partial^2 q_{\{r\}}(r,t)}{\partial^2 r}$$

$$+\ldots+\frac{1}{n!}\frac{2^n}{\prod_{i=1}^{n}(-2i+3)}(1+r)^{(2n-1)/2}\left[\sqrt{1+r}-(1+r)\right]^n\frac{\partial^n q_{\{r\}}(r,t)}{\partial^n r}$$

leads to the main expression in the present chapter which is

$$\frac{\partial}{\partial t} q_{\{r\}}(r,t) = -\frac{\partial}{\partial r}\left[\left(M_{mig}\left\{\frac{1}{r_c}-\frac{1}{r}\right\}\right) q_{\{r\}}(r,t)\right] + \frac{1}{2}\frac{\partial^2}{\partial r^2}\left[(a)^2 q_{\{r\}}(r,t)\right]$$

$$+ H\left[\sum_{n=1}^{\infty}\frac{1}{n!}\frac{2^{n-1}}{\prod_{i=1}^{n}(-2i+3)}\frac{(1+r)^{n-1}\left[\sqrt{1+r}-(1+r)\right]^n}{r^4}\frac{\partial^n q_{\{r\}}(r,t)}{\partial^n r}\right] \qquad (7.14)$$

with the initial conditions (7.11), (7.12) and (7.13). Other authors call a reduced form of equation (7.14) the continuity equation, [45,49].

7.1 Discussions of Solutions of Integro-Differential Equation

The solution of the main expression is obtained numerically. In this report the word "evolution" will stand for "time evolution". To ensure that truncation should be an acceptable operation, the equation (7.14) is multiplied through by r^4 and the evolution in the grain size is normalised with respect to the minimum unattainable grain size, *d,* which can, without loss of generality, be the maximum attainable grain size (i.e. the upper bound). As a consequence, the boundary conditions (7.11)-(7.13) now become

$$\forall\ domain\quad S_t =]0,1[\ : q_{\{r\}}(r=0,t) = 0 \qquad (7.15)$$

$$\forall\ domain\quad S_t =]0,1[\ : q_{\{r\}}(r=1,t) = 0 \qquad (7.16)$$

$$q_{\{r\}}(r,t)/_{t=0} = q^0{}_{\{r\}}(r) \qquad (7.17)$$

Because of this normalisation, the coefficients of the partial derivatives of $q_{\{r\}}(r,t)$ term, $C_n = 2^{n-1}(1+r)^{n-1}\left[\sqrt{1+r}-(1+r)\right]^n \Big/ \left[n!\, r^4 \prod_{i=1}^{n}(-2i+3)\right]$, in the last (summation) terms (4^{th}, 5^{th}, etc) in equation (7.14) attain the maxima given in the Table (7.1) below. It can be seen from the table that C_n decreases rapidly as n increases and, so, higher order terms can be neglected.

Table 7.1 *Maximum values of coefficients of partial derivatives of $q_{\{r\}}(r,t)$*

Values of n	*Maximum attainable value of C_n*
1	0.59
2	0.72
3	0.384
4	0.02304
5	0.00158
6	7.02×10^{-5}
7	2.19×10^{-6}

Most experiments performed are based on initial microstructures that are either Voronoi cells [7,10] or of uniform size, [40]. But the initial probability distributions considered in those papers are either normal, [40], or Rayleigh, [40,50]. The initial grain size obviously has an effect on the evolving microstructure. The present model accounts for this varying initial microstructure by varying the initial dispersion of grain size employed. In this present chapter, the interest is in the initial probability distribution. So, starting with an initial lognormal or normal distribution of grain size in nanomaterials, the solution of the differential equation (7.14) that governs the evolution of the probability density function (*pdf*) of grain size is obtained and the results are plotted. Use is made of the equations (7.18-7.25) when solving the major equation, (7.14). This is because these parameters evolve continuously as the grain growth process progresses.

Since the initial distribution of the grain size is assumed to be lognormal, the probability density function and properties are, [21,47],

$$q_{\{r\}}(r) = \frac{1}{r\sqrt{2\pi\alpha}} \exp\left[-\frac{\{\log(\rho.r)^2\}}{2\alpha} \right] \tag{7.18}$$

$$mean = \rho^{-1} e^{\alpha/2} \tag{7.19}$$

$$\text{Coefficient of variation (CV)} = \sqrt{e^{\alpha} - 1} \tag{7.20}$$

The evolution of the mean grain size can be predicted by the asymptotic time dependence (power law kinetics) given as, [23,49,50]

$$\mu_r(t) = \mu_0 + Kt^n \tag{7.21}$$

where $\mu_r(t)$ is the mean grain size at time, t, μ_0 is the initial mean grain size, K is the average mobility constant and n is the growth exponent. Plots of the evolution of the different parameters in expression (7.21) are found in CHAPTER 6, and hence, will not be repeated here. The corresponding expressions of these parameters are repeated here to facilitate the follow up in the present chapter.

The evolution of the dispersion of grain size depends on the growth process under consideration. For GBM process only the CV evolves as, [48],

$$CV = 3.5 + (CV_0 - 3.5)\exp(-At) \tag{7.22}$$

where A is constant. For simultaneous GBM and GRC processes CV evolves as, [CHAPTER 6]

$$CV = \begin{cases} f(t) & 0 < t \le t_a \\ 3.5 + (CV_a - 3.5)\exp[-A(t - t_a)], \;\; CV_a = f(t_a) & t_a < t \le t_f \end{cases} \tag{7.23}$$

where $f(t)$ is a function that increases and attains a turning point at t_a.

The growth exponent is assumed to be constant on an average in the present chapter, consistent with observations made by Kurzydlowski et al, [48] , though it may vary which is consistent with observations made in CHAPTER 6 and by [50].

The average mobility constant, K, given in expression (7.21) as found in CHAPTER 6 depends on the initial dispersion of the system and given by an expression that depends on the growth process under consideration: for GBM, it is

given as

$$K = K_0 + K_{grad} CV_0 \tag{7.24}$$

and for GRC only and simultaneous GBM and GRC, it can be given as

$$K = K_0^{'} + K_{grad} \left(CV_0 - CV_1\right)^2. \tag{7.25}$$

where K_0 is initial value, K_{grad} is the slope of the curve and CV_1 is the value of initial dispersion at which turning point is attained. CV_1 =0 for simultaneous GBM and GRC.

The following parameters $M_{mig}=8X10^{-4}$, $b(r,t)=r$, $a(r,t)=\sqrt{(r/20)}$ and "$v(r,t)=H/r^4$" are used. The *Initial Coefficient of Variation (CV_0)* is varied to be consistent with experiments. Varying the parameters that are held fixed (e.g. GB mobility varies) as grains grow may surely have an effect on the way the pdf curves evolve, on the limiting distribution or indicate the relationship between the various parameters. Considering solutions for different cases of grain growth suggests how the dominance of each parameter affects the process (see "compared plots" below).

The obtained numerical results are given in Figure (7.1)-(7.3). The plots represent the probability density curves obtained as solution of equation (7.14). The solution for the GBM case only is obtained when only the first two terms on the right hand side of the equation (7.14) are considered. For a simultaneous GBM-GRC process, two more terms (3rd and 4th terms) are included. It can be observed that results from analytical modelling of grain size probability distribution in polycrystalline nanomaterials are different if the effect of GRC mechanism on grain growth process is taken into account and, further, due to the addition of the fluctuation terms. Results also depend on the nature of the fluctuation term, which is a material property as the fluctuation in grain sizes varies from one material to another.

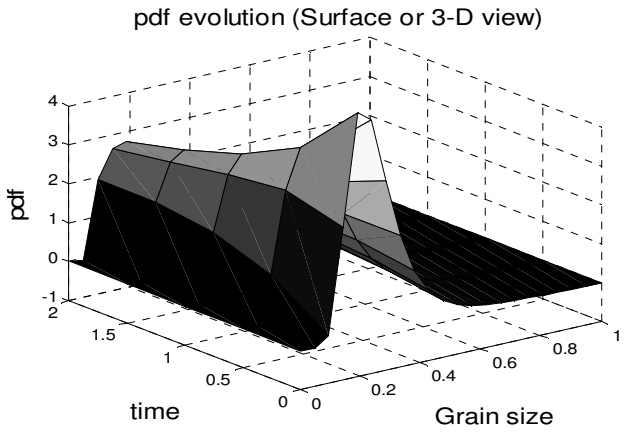

Figure 7.1 *General 3-D view of the evolution of the pdf*

Since from the visual interpretation one cannot tell the exact difference between the curves representing the evolution of the pdf (e.g. between figure (7.2a) and (7.2b)) for different cases of grain growth (i.e. GBM or GBM-GRC), it is not necessary to show all the results for these cases of grain growth. Hence, only one of the corresponding plots is given and discussed. The differences between them are rather compared, (figure (7.3)). The 3-D view, figure (7.1), is not very informative. It only reveals the crest of the surface representation decreasing as time progresses. So, the 2-D views obtained as the intersection at different time instant of a 3-D plot are used to interpret the results.

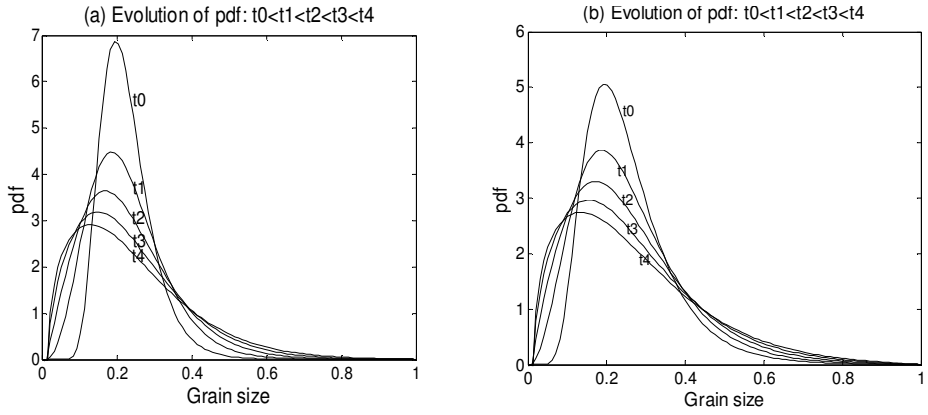

Figure 7.2 *2-D representation of the evolving pdf: (a) GBM only and (b) Simultaneous GBM-GRC*

The plots in figure (7.2a) and figure (7.3a) correspond to the solution of the Fokker-Plank equation (714) when only two terms on the right hand side are considered. It can be seen from figure (7.2) that the true growth process has been revealed: some grains shrink while others grow. This is portrayed by the fact that the curves flatten and the tails become heavier, indicating the creation of more smaller and larger grains at the expense of the initially highly frequent grains. It should be noted that this process of shrinkage-growth does not contradict the fact that the mean grain size increases continuously with time as confirmed by expression (7.21). The flattening of the curves also indicates that the volume of the system is conserved as the areas under the curves are equal. This is achieved by the normalisation of the pdf function.

It can be observed that many of the major attributes of grain growth, such as self similarity (probability density approaching a stationary one), can be predicted by the solution of the Fokker-Planck-Kolmogorov equation. The self-similar behaviours of the system can be clearly seen as the pdf curves evolve. They become closer and closer as time progresses. The peaks decay and the evolution can be represented by a self-similar expression.

The evolution of the pdf depends on the initial dispersion of grain size in the material. One can also see from figure (7.3a) that in nanomaterials, the grain size probability distributions that start with lower dispersion have pdf curves that are correspondingly narrower than those of system with high initial dispersion, figure (7.3a). This, then, reveals that the grain growth rate in such a system with low CV_0 is slower than for system with high CV_0. This is clearly a true practical revelation as grain growth for such a low CV_0 nanomaterials is dominated by GRC process accompanied by little GBM process (for GBM process, larger grains consume smaller grains). For higher initial CV, both mechanisms of growth are present, though GBM is highly favoured.

Comparing grain growth due to GBM mechanism only and a simultaneous GRC-GBM mechanism, it can be observed that nanomaterials having the same initial dispersion in both cases have the pdf curves that are wider for the simultaneous system than for the only one system, figure (7.3b). The curve denoted as "total" represents the solution of the Fokker-Plank equation (7.14) when two more terms are added.

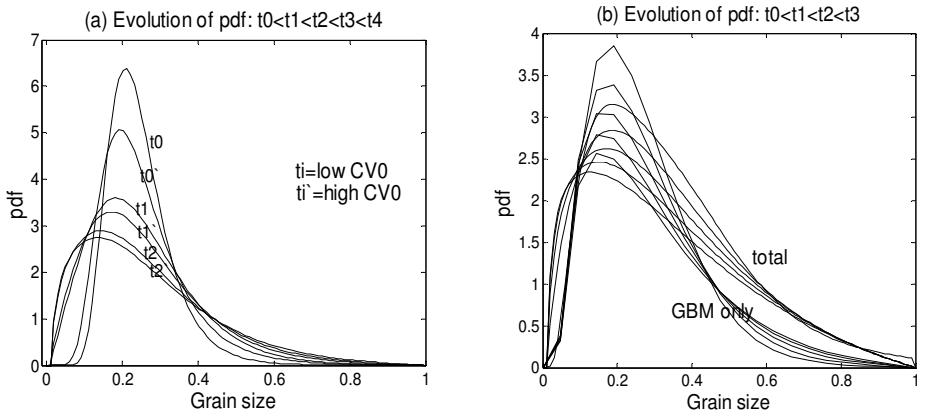

Figure 7.3 *Comparing the evolution of pdf (a) low and high CV_0 for GBM case, and (b) high CV_0 for both GBM and simultaneous GBM & GRC*

7.1.1 GBM only at scaling state

The drift and diffusion terms are not dependent explicitly on time. Since the grain growth due to GBM only homogenises (i.e. dynamical system is asymptotically stable) as $t\rightarrow\infty$, the probability density approaches a stationary one, with the stationary density function $q^{s}_{\{r\}}(r)$ which is independent of time and of the initial density $q^{0}_{\{r\}}(r)$. Hence, equation (7.14) reduces to

$$\frac{\partial}{\partial t}q^{s}{}_{\{r\}}(r) = -\frac{\partial}{\partial r}\left[\left(M_{mig}\left\{\frac{1}{r_c}-\frac{1}{r}\right\}\right)q^{s}{}_{\{r\}}(r)\right] + \frac{1}{2}\frac{\partial^2}{\partial r^2}\left[(a)^2 q^{s}{}_{\{r\}}(r)\right] = 0 \qquad (7.26)$$

Thus,

$$-\left(M_{mig} \left\{ \frac{1}{r_c} - \frac{1}{r} \right\} \right) q^{s}{}_{\{r\}}(r) + \frac{1}{2} \frac{\partial}{\partial r} \left[(a)^2 q^{s}{}_{\{r\}}(r) \right] = Const \; = G_s \tag{7.27}$$

Considering conditions (7.11) and (7.12), the solution to equation (7.27), which is first-order, ordinary non-homogeneous differential equation, is found by means of a standard method, [16], to be

$$q^{s}_{(r)}(r) = \frac{C}{a^2} \exp\left(2 \int_0^r \frac{M_{mig} \left[\frac{1}{y_c} - \frac{1}{y} \right]}{a^2} dy \right) \tag{7.28}$$

where $y_c = Ky$, C is obtained from the normalisation condition of pdf and a can be varied. If $a^2 = r$, then the pdf

$$q^{s}_{(r)}(r) = \frac{C}{r} \exp\left(2 \int_0^r M_{mig} \left[\frac{1}{k} - 1 \right] \frac{1}{y^2} dy \right) = \frac{C}{r} \exp\left(- M'_{mig} . \frac{1}{r} \right) \tag{7.29}$$

is a Weibull distribution. But for constant diffusion term, the expression (7.27) results in a different distribution. Thus, the probability distributions are different as the functional form of "a" varies.

Remarks: Starting with an initial lognormal distribution or normal distribution of grain size, the grain growth parameters have been calibrated such that the grain size pdf evolves as *lognormal distribution* till the scaling (steady) state. At this point, it *cannot* be stated that the initial probability distribution of grain size does not have an effect on the way the pdf evolves and, consequently, the asymptotic pdf. Also, these results are obtained from the specific diffusion and jump terms. This obviously has some influence on the results as it can be testified by the case above, “GBM only at steady state”. This, thus, necessitates research on the types of fluctuation terms that best reflect the result of the process of production/processing of nanomaterials. Also, neglecting higher order terms may,

obviously, have an effect on the results. It could not be stated how many terms have to be considered so that the solution should be accurate enough. Thus, instead of using a Taylor series expansion to simplify the jump probability term, a different approach which might not invoke infinite series and hence, truncation may be more beneficial.

We now have some knowledge of the evolution of the microstructure/grain sizes in nanomaterials. As mentioned in preceding chapter, the grains sizes observed in most experimental works do not attain the sizes predicted by the existing model and laws. Establishing the relationship between the evolution of the internal microstructures and the material properties is an issue of interest in the present project as well as in Materials Science and Engineering. To predict the materials properties more accurately, it is necessary to have a sound knowledge of the microstructure evolution. The next chapter presents another further effort to improve on the correlations between the modelled grain size statistics and experimentally observed data.

8 IMPROVING ON CORRELATIONS BETWEEN MODELLED GRAIN SIZE STATISTICS AND THEIR EXPERIMENTAL COUNTERPARTS DURING GRAIN GROWTH IN NANOMETALS

Observed grains in polycrystalline nanomaterials do not grow to the sizes predicted by existing models. Some models even ignore other grain growth mechanisms that should have additive effects on the modelled grain sizes and, hence, imparting further departures to such models from the experimentally observed grain size evolutions. Isothermal grain growth in polycrystalline nano-materials has been frequently analysed by using the isotropic Hillert's model, [35], to predict the power law kinetics, [23,26]. It has been observed that grain sizes predicted by the power law interpretation of grain growth kinetics are often far greater than those observed in engineering alloys and even commercially pure materials, [23].

These observed departures rationalize the need to modify the existing models. Amongst the modifications is the model developed in CHAPTER 6, which included misorientation angle driven **G**rain **R**otation **C**oalescence mechanism (**GRC**). In this model of CHAPTER 6, while analysing isothermal grain growth by curvature driven **G**rain **B**oundary **M**igration (**GBM**), the GB mobility was considered to be constant. There are many evidences that the energy required to activate isothermal grain growth in polycrystalline nanomaterials increases with increasing grain size. Jiang et al, [51], proved that the dependence of the activation energy, ***Q***, for the GBM process (GB mobility) on grain size is given by

$$Q(r) = Q(\infty)\exp\left(-\frac{2S_{vib}(\infty)}{3R}\frac{1}{r/r_0 - 1}\right) \tag{8.1}$$

where $Q(\infty)$ is conventional activation energy, R is ideal gas (Boltzmann's) constant, $S_{vib}(\infty)$ is vibration part of the over all (conventional) melting entropy S_m, r is grain size and r_0 is radius of a nanoparticle where almost all atoms are

located on the surface. It has been found that except for semiconductors $S_{vib}(\infty)=S_m$, for nanostructured materials r_0=$6h_0$ and for nanometals h_0 is the atomic diameter, [3 and ref. therein].

Due to the Arrhenius type of relationship between the grain boundary mobility and activation energy, the grain boundary mobility decreases during isothermal grain growth i.e. the GB mobility is expressible as a function of Q by the Arrhenius relationship as, [36,51],

$$M(r,T)=M_0^{'}\exp\left[-Q(r)/RT\right] \tag{8.2}$$

where $M_0^{'}$ is the pre-exponential mobility constant. According to Zhao, [3 and ref therein], $Q(r)\boldsymbol{\alpha}RT_m(r)$, $Q(\infty)\boldsymbol{\alpha}RT_m(\infty)$ and $H_m(\infty)=T_m(\infty)S_m(\infty)$, where $T_m(r)$ is the melting temperature of the material with grain size r, $T_m(\infty)$ is the conventional melting temperature and $H_m(\infty)$ is the conventional melting enthalpy (enthalpy of fusion).

In the present chapter, an extension of the previous model of CHAPTER 6, is proposed by studying isothermal grain growth in nanocrystalline aluminium taking into consideration the GB mobility varying with grain size.

Substituting (8.1) into (8.2) will lead to a result that is cumbersome to analyse stochastically. Simplification can be achieved by using homogenisation theory. Since the melting temperatures of materials decrease with grain refinements, [3], nanostructured materials can, without loss of generality, be assumed to be made up of “large” grains. Let $A"=2S_{vib}(\infty)/3R$ and $B"=Q(\infty)/RT$. By twice employing the Taylor series expansion of the exponentials in the result of the above substitution, it follows that

$$M(r,T) = M_0^{'} \exp\left[- B'' \exp\left(- \frac{A''}{r/r_0 - 1} \right) \right]$$

$$= M_0^{'} \exp[- B''] \exp\left(+ \frac{A'' B''}{r/r_0 - 1} \right)$$

$$= \left(M_0^{'} \exp[- B''] \right) \left(1 + B'' \frac{A''}{r/r_0 - 1} \right)$$

And expanding $\left(1 + \frac{B'' A''}{r/r_0 - 1} \right) = \left(1 + A'' B'' \frac{1/r}{1/r_0 - 1/r} \right)$ as function of *1/r* using the Taylor series leads to

$$M(r,T) = M_0(T) \left(1 + \frac{C}{r} \right) \tag{8.3}$$

where $M_0(T) = M_0^{'} \exp[-T_m(\infty)/T]$ and $C = 4H_m h_0 / RT$.

As such, the current modified model of grain growth is then proposed to be

$$dr = M(r,T) \left(\frac{1}{r_c} - \frac{1}{r} \right) dt + B\sqrt{r}\, dW(t) + (A+1) r dN(t)$$

$$= M_0(T) \left(1 + \frac{C}{r} \right) \left(\frac{1}{r_c} - \frac{1}{r} \right) dt + B\sqrt{r}\, dW(t) + (A+1) r dN(t) \tag{8.4}$$

where r_c is the local critical grain size, *A* and *B* are constants, *dW(t)* and *dN(t)* are respectively the increments of the Weiner and the stochastic counting processes within an infinitesimal time interval. On the right hand side of (8.4), the first term is the drift, the second and third (last) terms account for the fluctuations in grain size due to GBM and GRC mechanisms respectively.

The expressions governing the evolution of the statistical moments are then obtained from expression (8.4) using the Ito's Differential Rule and Equations for

Moments, [16-20]. These give

$$\frac{d\langle r\rangle}{dt} = M_0(T)\left\langle 1+\frac{C}{r}\right\rangle\left\langle \frac{1}{r_c}-\frac{1}{r}\right\rangle + (A+1)\langle r\rangle v(\langle r\rangle,t) \tag{8.6}$$

$$\frac{d\langle r^2\rangle}{dt} = 2M_0(T)\left\langle 1+\frac{C}{r}\right\rangle\left\langle \frac{1}{r_c}r-1\right\rangle + B^2\langle r\rangle + (3+4A+A^2)\langle r^2\rangle]v(\langle r\rangle,t) \tag{9.7}$$

where the symbol $\langle ... \rangle$ stands for expected value, *v(<r>,t)* the rate of coalescence events of grains. In obtaining and analysing expressions (8.6) and (8.7), it should be noted that GB mobility is a function of the grain size but statistically independent of that grain size. This is because in an aggregate, a grain is surrounded by neighbours which impose restriction on its evolution (growth). The "effective" GB mobility depends on the "effective" interactions with, and hence, the "effective" size of the neighbours. This effective size of the neighbours is called local critical grain size which, in turn, is also statistically independent of the grain size, [CHAPTER 6]. The lognormal distribution of grain size, [44,CHAPTER 7], is used.

8.1 Application of Proposed Model on Aluminium Sample

The model proposed in this chapter is applied to nanocrystalline aluminium. The parameters employed in testing the model are those possessed by conventional materials. The rate of coalescence events of grains has been established in CHAPTER 6 to be $v(\langle r\rangle,t) = CC\langle 1/r^m\rangle$ where CC=constant and *m* depends, [38], on the type of accommodation under consideration (e.g. *m=5* for accommodation by GB diffusion and *m=4* for accommodation by dislocation motion or lattice diffusion). *m=4* is used in the present work. The properties of aluminium used in computing the simplified forms of expressions (8.6) and (8.7) are gas constant R=8.3145J-K^{-1}-Mol^{-1}, initial mean grain size $< r >_0 = 30\,\text{nm}$,

$h_0 = 0.25\,\text{nm}$, $T_m(\infty) = 933.47\,\text{K}$, $H_m(\infty) = 10.71\,\text{KJmol}^{-1}$, $CV(r)_0 = 0.4$, $M_0^{'} = 0.01\,\text{nm}^2\text{s}^{-1}$, $A = -0.90$, $< r_c >= 1.95 < r >$, CC=12 and $B = 10^{-4}$.

In this report, T_i stands for the condition where the material sample is annealed at temperature "i" Kelvin and T_{inf} for large annealing temperature, thus, leading to constant GB mobility as grains grows (i.e. T_{inf} represents the previous model). Reports are made on different mechanisms of grain growth. The effect of changing the annealing temperature, but still maintaining isothermal conditions, on the grain growth parameters has been tested. It can be observed that the higher the annealing temperature the higher the growth rate, and hence, the maximum attainable grain size after some fixed time interval. In the present work, the annealing temperature has no effect on grain growth due to GRC only. The present results show remarkable departures (reductions) from results of the previous model, and hence justifying the observations made by Morhac et al, [26].

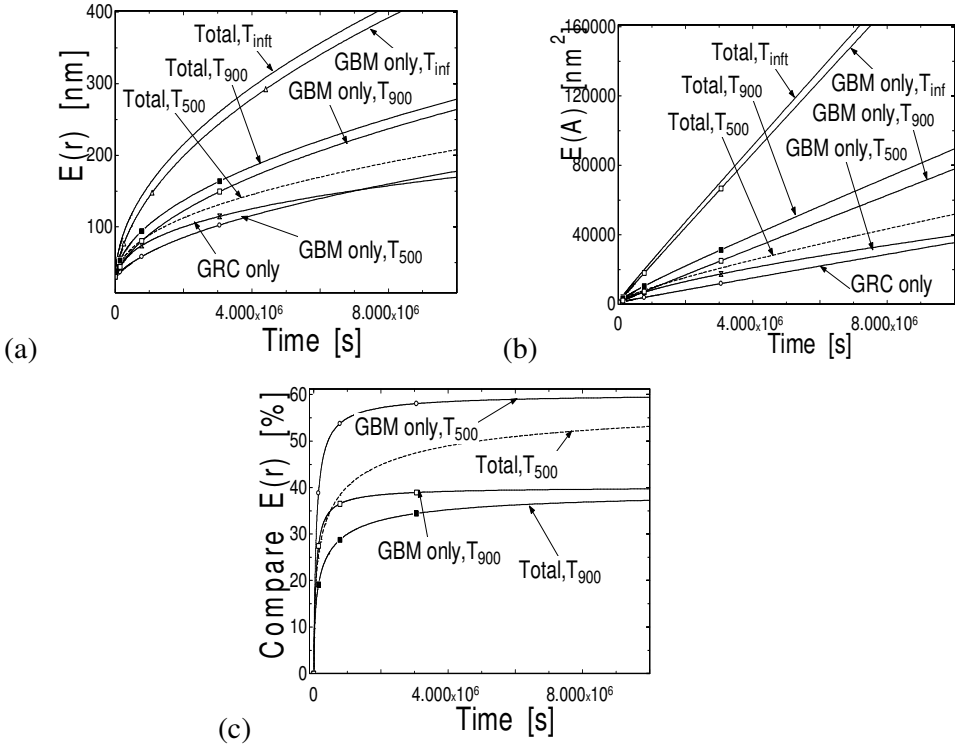

Figure 8.1 *(a) Evolution of mean size, E[r]; (b) mean area, E[A]; (c) comparison with previous model*

At comparatively low annealing temperature, T_{500}, the ratio of "activation energy" – to – "temperature" (energy required to activate GBM) is high leading to low GB mobility. Under such condition, the evolution of the average grain size, E(r), due to GRC only is *initially* higher than that due to GBM only. Maintaining this low annealing temperature and allowing the grain growth process to continue for a very long period leads to a change of situation. The evolution of E(r) due to GBM only *now* becomes larger than that due to GRC only. The physical implication of this is that as the grains grow larger, it becomes difficult for them to rotate. Thus, GRC processes are tremendously slowed down making GBM process to be now dominant, Fig.8.1(a). The evolution of mean grain area, E(A), due to GRC is greater throughout than that due to GBM. This is attributed to the fact that the mean grain area is not given by the square of E(r), i.e. $< (r^2) > \neq (< r >)^2$. The evolution of the E(r) due to simultaneous GBM and GRC (Total) is higher than that of any of the mechanisms alone throughout the period.

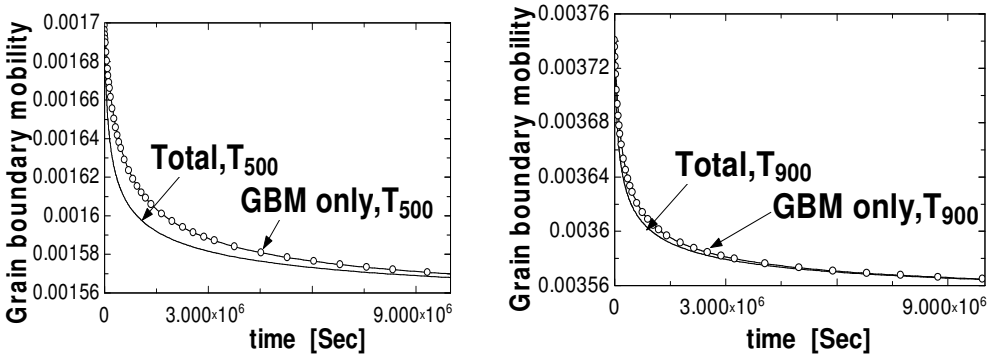

Figure 8.2 *Evolution of grain boundary mobility, (a) at T_{500} and (b) at T_{900}*

When annealing the nanocrystalline aluminium sample at as high as 900K which is much closer to the melting temperature of a conventional aluminium sample, the evolution of the mean grains size is still much smaller, for the present model than for the previous model. But the evolution of E(r) (as well as E(A)) due to GBM is now larger throughout the entire time range than that due to GRC. This is due to higher GB mobility coupled with the inherent difficulty for larger grains to

rotate when the grain sizes become larger. It is observed that as the grains grow, the GB mobility decreases under both temperature conditions though their values corresponding to the same time interval are different, Fig.8.2. The results then show that for practical conditions, there is a great reduction of the extent to which grains grow. See Fig.8.1(c) where results from the present model are compared with those of the previous model. The percentage deviation of E(A) incurred is approximately twice that of E(r). The evolution of the E(A) is not linear for different temperatures. This indicates departure of results of the present model from the parabolic law or any law of grain growth with varying temperature, also see Fig.8.3(b).

Fig.8.1(a) and Fig.8.1(b) indicate that the evolution of the grain size dispersion, CV(r), plays an important role in the characterisation of the microstructure evolution. As can be seen in Fig.8.3(a), overlaying the plots of CV(r) for all of the different mechanisms of grain growth is not quite informative since the range of values for the different mechanisms is wide and the rate of variation of the grain size due to the different mechanisms are not the same, thus, making some plots (Total at T_{inf} and GBM only at T_{inf}) to appear to be linear which are unrealistic, Fig.8.3(b). It can be observed from Fig.8.3(a) that when grain growth is due to GRC only; then CV(r) *rises steadily* to homogeneity. This steady increase in CV(r) due to GRC has also been observed practically, [37,38]. This is because in nanomaterials with little or no dispersion of grain size, the rotation-coalescence of grains can start off dispersion which will increase with more coalescence of grains. When grain growth is due to GBM only, the CV(r) *decreases steadily* to homogeneity. This is because for GBM only larger grains gradually consume smaller grains, thus, decreasing steadily the CV(r). This steady decrease is greater for higher annealing temperature due to the fact that the GBM process is more prominent at higher temperature.

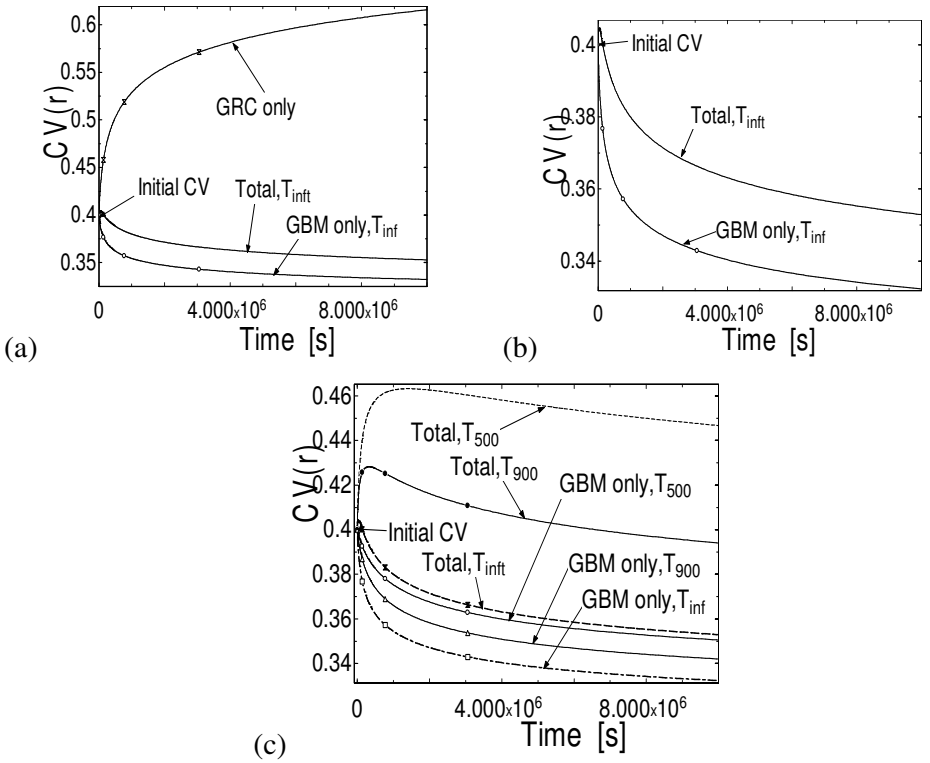

Figure 8.3 *Evolution of CV(r): (a) all mechanisms of grain growth, (b) and (c) Total and GBM only*

Due to the fact that both mechanisms of growth take place simultaneously, there is an *initial* increase in CV(r) of the Total process, followed by a steady decrease to homogeneity. The extent to which the CV(r) rises before decay depends on the amount of contribution made by each mechanism to the total grain size. At low annealing temperature where contribution is mostly due to GRC, there is a comparative greater rise in the CV(r) for the total process before decay.

The characterisation of other grain growth parameters, such as grain growth mobility *K* and grain growth exponent, *n,* can be obtained from the power law kinetics which mostly reports on the time evolution of the E(r), with $E(r)_0$ being the initial mean grain size, given as, [23,26]

$$E(r) = E(r)_0 + \mathrm{K}\, t^n \tag{8.8}$$

In the case of GRC only process at constant $CV(r)_0$, $K = 0.20\text{nm.s}^{-0.4}$ and $n=0.4$. At constant $CV(r)_0$, both K and n strongly depends on the annealing temperature when grain growth is due to GBM only and Total processes. For these two latter processes at low annealing temperature, there is a great difference between the values of the same parameter. They approach each other at high temperature. The variation of n with temperature shows departure of results of the present model from any law of grain growth e.g. parabolic law. It should be observed that as the annealing temperature gets larger, grain growth approaches the parabolic law i.e. n approaches the parabolic law value of 0.5 for both mechanisms of growth. Thus, the relationships between the annealing temperatures and the grain growth mobility as well as the grain growth exponent have been revealed.

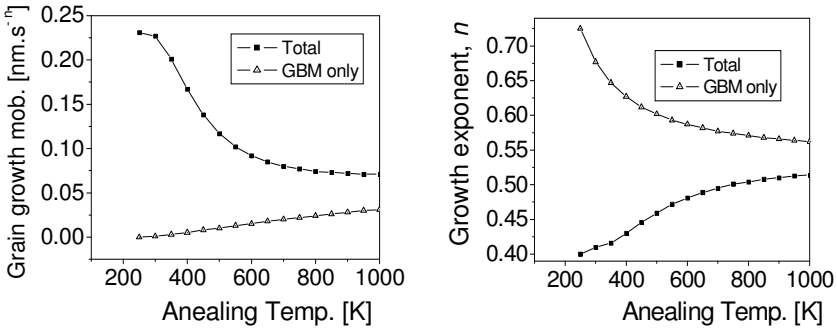

Figure 8.4 *Relationship between annealing temperatures and (a) grain growth mobility, K, (b) grain growth exponent, n*

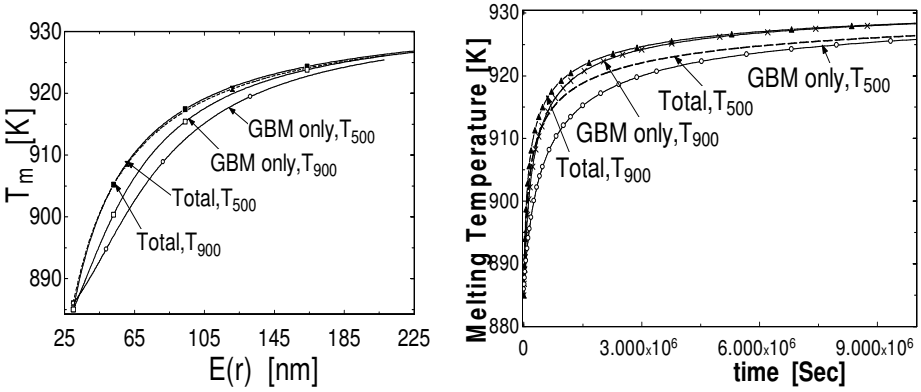

Figure 8.5 *Evolution of material melting temperature, T_m, against (a) mean grain size, E(r) and (b) Time*

A property of a material of interest in nanoscience and nanotechnology is that the melting temperature, $T_m(r)$, of the material decreases as the grain sizes in the material decrease. From the relationship $Q(r) \alpha R T_m(r)$ and expression (8.2), the evolution of $T_m(r)$ is given in Fig.8.5(a) given by

$$T_m(r) = T \ln\left(\frac{M_0^{'}}{M(r,T)}\right) = T_m(\infty) - T \ln\left(1 + \frac{C}{r}\right) \tag{8.9}$$

Note that both the mean grain size and grains size dispersion play vital roles in the determination of the melting temperature of the material. This, thus, establishes the relationship between the melting temperature of the material and the evolving grain size.

A model that reveals improved correlations between the modelled material properties and the experimental data has been proposed and tested. In the following chapters, the efforts of predicting material properties from the knowledge of the evolving microstructure are then be undertaken.

9 THE EFFECT OF GRAIN SIZE DISTRIBUTION ON MECHANICAL PROPERTIES OF NANOMETALS

Predicting material properties from the knowledge of the internal microstructures is attracting significant interest in the fields of Materials Design and Engineering. The most commonly used expression known as Hall-Petch Relationship (HPR) reports on the relationship between flow stress and *average* grain size. On the other hand, there are many evidences that other statistical quantities of grain size distribution in materials may have impacts on the mechanical properties. These could even be more pronounced in the case of grains of the nanometer size, where the HPR is not valid anymore and the Reverse-HPR is applicable. The present chapter seeks to justify that both the mean grain size and grain size dispersion simultaneously play vital roles in the design of the required materials properties.

The mechanisms and impacts of plastic deformation on materials properties are well documented in literature [52,53,54]. It has been observed, [52], that when operating under low strain rate, the initially coarse grains deform mostly by dislocation glide and the dependence of properties on microstructures follows so-called **H**all-**P**etch **R**elationship (**HPR**). Maintaining this low strain rate and refining the grains, in most cases, to the level of 10nm-50nm leads to Reverse-HPR dependence of the properties with deformations being the "Coble Creep" grain boundary diffusion and "Nabarro-Herring Creep" grain interior diffusion and dislocation motion. It is observed that there is a smooth transition of the material properties from HPR to Reverse-HPR i.e. the property curve is a smooth one with no inflexion (sharp) point at the transition point. This can be explained by the fact that at the transition point, the properties become stationary with respect to varying grain sizes as contribution from deformation due to dislocation glide is equal to that from both Coble and Nabarro-Herring Creeps.

As such, a mathematical expression representing this deformation-to-properties phenomenon should be a *single continuous* expression. It has been postulated that the HPR expression that is valid for coarser grains is not more valid for finer

grains because the constant of proportionality in the HPR that depends on the resistance of the grain boundary to dislocation movement is not constant anymore as refinement of the grain sizes continues, [3]. The paper, [3], then arrives at a single modified expression that represents the size-property dependence (both HPR and Reverse-HPR) throughout the entire range of deformation, given as

$$\sigma(\mathbf{d}) = \sigma_0^{'} + A\mathbf{d}^{-1/2} - B(\mathbf{d}^{-1/2})^2 - C(\mathbf{d}^{-1/2})^3 \tag{9.1}$$

where $\sigma_0^{'} = \sigma_0 + K_t$ is the conventional yield (proof) stress, $A = K_d$ is the conventional (or HPR) proportionality constant, $B = K_t\left[2hH_m / RT_r\right]$, $C = K_d\left[2hH_m / RT_r\right]$, $\boldsymbol{d}$ is the grain size, K_t is a constant, h is atomic diameter in the case of metal, H_m is the conventional melting enthalpy, R is ideal gas constant, T_r is the room temperature, $K_d > 100K_t$ and $\sigma_0 > 10K_t$.

These expressions for the dependence of material properties on microstructures (e.g. modified HPR) have previously been reported for average grain size only. However, the average value is not the only statistical quantity that fully represents the grain size distribution in any material, [CHAPTER 6, CHAPTER 7, CHAPTER 8]. The word, "mean", is used on several occasions to indicate that a "change" should indicate an effective change of the statistics. This is because in nanomaterials, a particular grain, at an instant, can be seen to be growing while later it will be shrinking but the statistics of the entire material remains constant. So, it is necessary to extend microstructure-property relationship to take into account more and proper information about the grain size distribution.

During experimentations, the mechanisms of deformations in materials are analysed by monitoring the behaviours along grain boundaries and grain interiors. It is found that nanostructured materials have larger "grain boundary layers"-to-"grain sizes" ratio as compared to conventional materials. Working with a 3-D sample composed of a larger (possibly infinite) number of grains, it is time consuming and, of course, a tedious task to gather accurate information about all

the grains. Hence, it is, without loss of generality, logical to assume that the dependence of materials properties on microstructures holds for "local information about a grain" or for "individual grains", and the knowledge about the grain size distribution then play a vital role. This assumption does not introduce any ambiguity about the microstructures-properties dependence since in polycrystalline nanomaterials the separations between particles/grains are relatively small compared to the case of small particles within a bulk matrix which may, in fact, exhibit different properties dependence where the separations between these grains are relatively large, [55]. The assumption introduces the need to assess the statistics of the materials properties within the materials. In the present chapter, a statistical model of the relationship between flow stress and grain size distribution is proposed.

Expressions for the instantaneous values of the statistics of material properties are obtained from expression (9.1). For example

$$\left\langle \sigma(\mathbf{d}) \right\rangle = \sigma_0^{'} + A\left\langle \mathbf{d}^{-1/2} \right\rangle - B\left\langle \mathbf{d}^{-1} \right\rangle - C\left\langle \mathbf{d}^{-3/2} \right\rangle \tag{9.2}$$

$$\begin{aligned}\left\langle (\sigma(\mathbf{d}))^2 \right\rangle = {} & \sigma_0^{'2} + A^2\left\langle \mathbf{d}^{-1} \right\rangle + B^2\left\langle \mathbf{d}^{-2} \right\rangle + C^2\left\langle \mathbf{d}^{-3} \right\rangle + 2\sigma_0^{'}\left[A\left\langle \mathbf{d}^{-1/2} \right\rangle - B\left\langle \mathbf{d}^{-1} \right\rangle - C\left\langle \mathbf{d}^{-3/2} \right\rangle\right] \\ & - 2\left[AB\left\langle \mathbf{d}^{-3/2} \right\rangle + AC\left\langle \mathbf{d}^{-2} \right\rangle - BC\left\langle \mathbf{d}^{-5/2} \right\rangle\right]\end{aligned} \tag{9.3}$$

$$CV(\sigma) = \sqrt{\left(\left\langle \sigma^2 \right\rangle / \left(\left\langle \sigma \right\rangle\right)^2\right) - 1} \tag{9.4}$$

where the symbol $\langle ... \rangle$ stands for expectation, which are obtained based on the grain size probability distribution under consideration. Thus, knowing the moments of the "grain size", the moments of the "material property" can be found. However, when analysing the time evolution of the statistical moments of the mechanical property, the derivations are different from that of expressions (9.2), (9.3) and (9.4). Analysing this time evolution is the subject of the next chapter.

The probability distribution of grain sizes in nano-crystalline metals is reported to be of varied form: approximately lognormal, normal, Weibull, Rayleigh and so on. The various distributions have different statistical properties. It is acknowledged that their effects on the modelled material properties may be different. The present chapter utilises the lognormal distribution of grain sizes in polycrystalline nanomaterials mostly reported from both theoretical and experimental findings, [45, 46, CHAPTER 7]. Let μ_n be the "n^{th} moment of grain size distribution", $n \in \Re$ i.e. $\mu_n = E[d^n]$. Then, for a lognormal distribution, expressions (9.2) and (9.3) can be simplified by using, (deduced from [47])

$$\mu_n = \mu_1^{n(2-n)} \mu_2^{(n-1)n/2} \tag{9.5}$$

9.1 On the Design of the Required Materials Properties

This proposed model was used to predict mechanical properties in aluminium and copper. The model considers different deformation mechanisms. Room Temperature value of 300K and Gas Constant value of 8.31J-K^{-1}-mol^{-1} with the data of Table 9.1 were used during the analysis. As already remarked earlier, it is unambiguous to report in the present chapter on the variations of the statistical quantities such as mean value and dispersion. The results obtained with the model as indicated in Fig.9.2, Fig.9.3 and Fig.9.4 show that both the mean grain size, E(d), and grain size dispersion, CV(d), together play vital roles in the design of the required/desirable materials properties, σ.

Table 9.1 *Conventional material properties*

Parameters **Metals**	$\sigma_0^{'}$ (MPa), [55]	K_d (MPa.$nm^{1/2}$)	K_t	σ_0 (MPa)	h (nm), [56]	H_m (KJ.mol^{-1})
Aluminium, Al	16.7	1301.77	1.30	15.40	0.250	10.71
Copper, Cu	33	4277.39	2.85	30.15	0.270	13.26

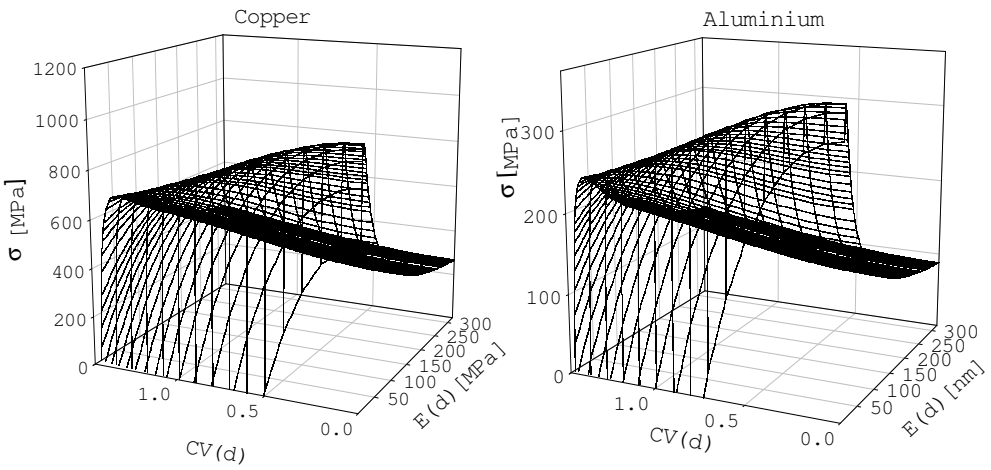

Figure 9.1 *Dependence of mean yield stress on both CV(d) and E(d)*

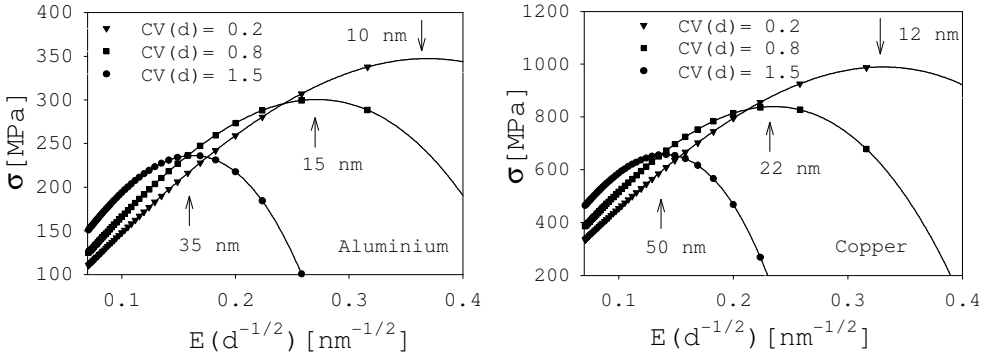

Figure 9.2 *σ versus E(d) at some constant values of CV(d) - CV(r) and E(r) together play vital roles in designing required mechanical properties*

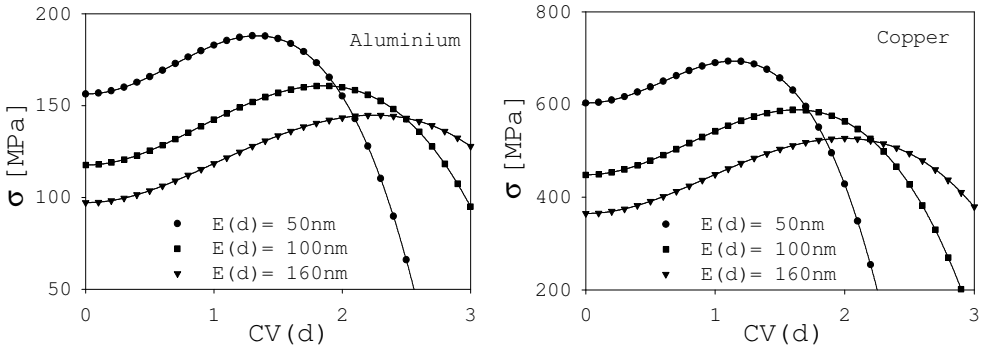

Figure 9.3 *σ versus CV(d) at some constant values of E(d) - CV(r) and E(r) together play vital roles in designing required mechanical properties*

The dependence of materials properties (mean yield stress) on CV(d), (Fig.9.1 and Fig.9.2), is similar to the dependence on E(d), (Fig.9.1 and Fig.9.3), e.g. the evolution from HPR to Inverse-HPR equally holds for CV(d) as it does for E(d). Hence, it is logical to report, in this report, on the dependence of the property on just any one of the variable. It can be seen that for *constant* E(d), the material property *increases* with *decreasing* CV(d) up to a certain value of the CV(d) where the property starts *decreasing* while CV(d) *continues to decrease*, (Fig.9.1 and Fig.9.3). It can also be seen from the figures that the values of the mean grain size at which turning point occurs is not the same for different materials (e.g. for CV(d)≤1.5, it is between 8.5nm-40nm for aluminium and 10nm-60nm for copper) and within a single material these values vary with the dispersion of grain size (in aluminium, for example, it is about 8.5nm at CV(d)≈0 to about 40nm at CV(d)≈1.5).

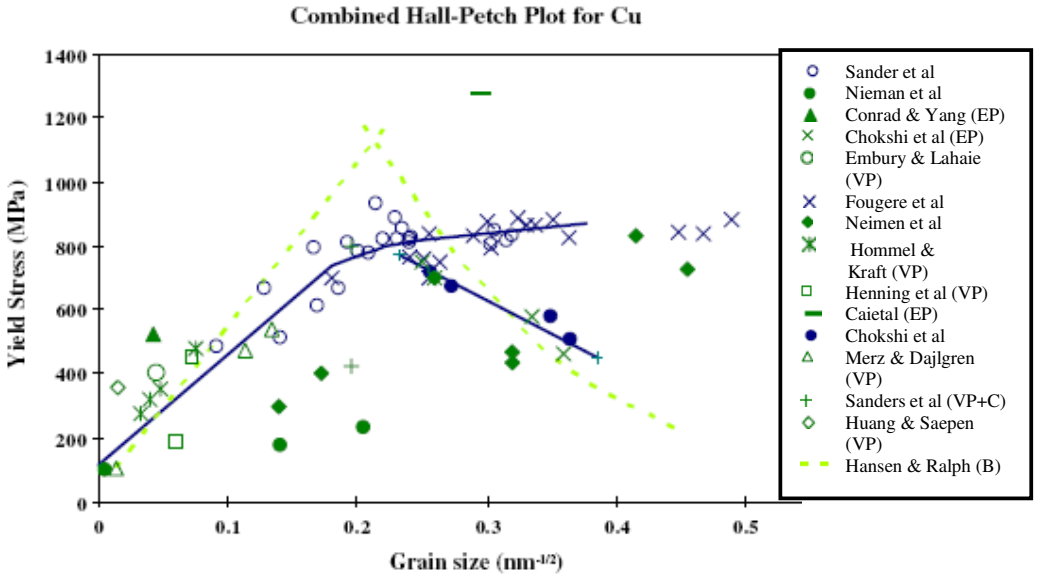

Figure 9.4 *Compiled yield stress versus grain size plot for copper from various sources ranging from coarse to nanograin size by Meyers et al,* [58].

It has, thus, been revealed in the present chapter that materials with *simultaneously* very low dispersion and very low mean grain size (but not too low beyond the region of the turning point with respect to E(r)) have much

better/enhanced mechanical properties. It can be observed from Fig.9.1 and Fig.9.3 that refining samples from the same material type to the same mean grain size by different deformation mechanisms (different mechanisms of deformation results in different, for example, grain size dispersion) can end up with different values for the property. This has been observed experimentally, [52,58], where for a single material, such as copper, different data have been obtained for the dependence of mechanical property on mean size e.g. different fitting constants and differing maximum attainable mechanical properties, see Fig.9.4. These differences in the parameters are attributed to differing strain rates at which deformations take place, [52]; the use of single sample subjected to repeated annealing to change the grain size, [58], and so on.

On the varying strain rate: No Reverse-HPR was observed while deforming copper at high strain rate throughout the entire range of deformation, [52]. It was further observed that the flow stress was larger for higher strain rate for all size ranges, [52]. Considering these two facts and Fig.9.1, one should be able to suggest the effect of strain rate on microstructure characteristics. Higher deformation strain rate has higher tendency to refine the microstructures to have mean size and dispersion values that are constantly located close to the point where the corresponding material yield stress has peak (higher) values, (also see Fig.9.5). It can be said, in other words, that high strain rate has the tendency of effecting *larger changes* (or reduction) in the grain size dispersion in the material compared to low strain rate. When (conventional) material with initially low dispersion is subjected to high deformation strain rate, the constituent size dispersion quickly rises to a maximum value which then decreases progressively as the refinement continues. This is then an open task to find out, both experimentally and theoretically, how the grains size dispersion evolves (varies) with different but specific deformation (strain rate). In the opposite direction of microstructure evolution, grain growth, the above suggestion of the nature of evolution of CV(d) was observed [CHAPTERS 6, CHAPTER 8] and was attributed to the rotation-coalescence mechanisms of grains.

The plot of Fig.9.5 may be represented mathematically as

$$E(d)_{\max} = E(d)_{\max,0} + M\left(CV(d)\right)^n \qquad (9.6)$$

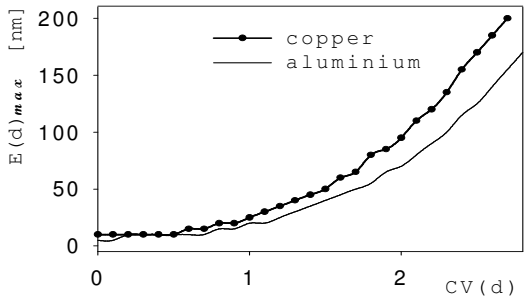

Figure 9.5 *Combination of CV(d) and E(d) values that produce material whose property follows the crest of the plots in Fig.9.1*

where for copper $E(d)_{\max,0} = 9.90$, M=14.46, n=2.61 and for aluminium $E(d)_{\max,0} = 8.58$, M=9.70 and n=2.72. $E(d)_{\max}$ is the corresponding value of the mean grain size required to combine with the given grain size dispersion to produce materials with property on the peak of the surface in Fig.9.1. $E(d)_{\max,0}$ is the minimum grain size below which the material property decreases with decrease in mean size *irrespective* of the grain size dispersion. Interpret Fig.9.5 as follows: *for constant CV(d) and with decreasing mean grain size*, the mechanical property increases above the curve while it decreases below the curve, and *for constant E(d) and for decreasing CV(d)*, the property increases below the curve while it decreases above the curve.

The present study shows that the departures of experimental data from the path predicted by a relationship are due to change of design strategies or inconsistent design procedures. Notice from the Fig.9.3, for example, that at a CV(d)≈2.5, a nanostructured copper with mean grain size 160nm has better mechanical property than the one with mean size 50nm. Maintaining the mean grain sizes in these two samples constant and reducing CV(d) to CV(d)≈0.5 now leads to a reverse situation; where the 50nm mean-grain-size-copper now has better property than

the 160nm one. This actually indicates that there is a crossing point, where the two different samples of Copper have the same mechanical property at the same CV(d). Thus, one can only decide on the fabrication procedure that produces a material with more enhanced property if, in the course of deformation using each procedure, reports are made on simultaneous evolutions of the mean grain size and grain size dispersion.

It has, thus, been demonstrated that all the parameters of the grain size distribution play, generally, vital roles in the design of the desired materials mechanical properties. The next chapter deals with the study of how the material properties evolve with some specific/detailed nature of microstructure evolution.

10 STATISTICAL APPROACH TO CHANGES IN MECHANICAL PROPERTIES OF NANO-CRYSTALLINE MATERIALS INDUCED BY GRAIN GROWTH

Polycrystalline nanomaterials can be produced through different processing routes. The most popular classification of the fabrication methods are the "top-down" and "bottom-up" techniques. Current development enables only the "top-down" method to produce bulk materials. The main process dedicated to the fabrication of nanomaterials by "top-down" techniques is the strain refinement. However, the plastic deformation may be valid in many ways. The consequence of the different processing routes is that, nanomaterials having the same mean grain size may have different grain size dispersion and, hence, different material properties. The present chapter presents further efforts, the results of which will be necessary for use in Materials Science to deduce materials properties from the knowledge of the internal microstructures.

Nano-materials have emerged recently as a new class of solids which are characterized by microstructures belonging to the length scale below 100 nano-metres, called the nanomaterial range of length scale. An important group amongst these materials is nano-crystal. These reduced dimensions impart to nano-crystals special physical, mechanical and chemical properties. Nanocrystalline metals can be produced through different processing routes and conditions. These result in polycrystalline nanometals that have randomly distributed and orientated grains whose sizes are random too. The consequence of different processing routes is that different nanomaterials, in general, having the same mean grain size, E(r), may vary in their grain size dispersions, CV(r). There are many evidences to substantiate that nanomaterials with the same E(r) but having different CV(r) will have ***different*** mechanical properties, [52,59,CHAPTER 9]. It was further demonstrated in CHAPTER 9 that in the course of fabricating nanomaterials through different processing routes, there is a coincidental point (crossing over point) where the different samples having different mean grain size but with the same grain size dispersion will possess ***the***

same materials properties. It is thus imperative to study the impact of detailed microstructure evolutions (i.e. simultaneous evolutions of E(r) and the corresponding CV(r)) on the materials properties.

The impacts of deformation strain rates on the microstructure evolution and mechanical properties are outlined in CHAPTER 9 and in [52]. Here, the summary of the dependence of some of the deformation mechanisms on microstructure sizes is presented. During experimentations, the mechanisms of deformations in materials are analysed by monitoring the activities along grain boundaries (GB) and in grain interiors (GI). A universally acceptable observation is that nanostructured materials have larger GB layer volume fractions whose values increase significantly as the grain sizes decrease through the nanometre range of length scale. Hence, in the nanocrystalline region, the microstructure may be regarded as a dual phase structure of GI and GB layer; and as such can be analysed with the aid of the phase-mixture model.

Engineering materials (having coarse grains) contain large amounts of flaws such as dislocations and micro-cracks in the GI. When subjected to refinement (or loading), such as the Severe Plastic Deformation (SPD), the initially coarse grains deform mainly by motion of dislocation from the GI to the GB with very small diffusion of atoms at GB, [52]. There are further reports that there are dislocation pileups at the GB during the deformation processes as the GBs act as obstacles to dislocation glide, [59]. Dislocations require greater amounts of energy to overcome these barriers to motion. Since dislocations are carriers of plastic deformation, this mechanism manifests itself macroscopically as an increase in material strength as the grain sizes decrease or with increasing dislocation density at the GB and/or increasing opposition to dislocation motion, represented by the HPR.

Further refinement of the materials beyond certain mean grain size, called refinement critical grain size, leads to dominant Coble-Creep GB diffusions of atoms or sliding of atomic planes and minor Nabarro-Herrings GI diffusion with

very little dislocation motions. At very small grain sizes all deformations are accommodated at the GBs that now have larger volume of atoms. This brings about softening due to the weakening effect of the GB and the triple junctions, thus, imposing a limit on how strong the nanocrystalline metals may become. In this case, the material strength decreases with decreasing grain sizes, represented by Reverse-HPR. Others have ascribed the softening of materials with very fine grain sizes to poor sample quality (unrecognized pores in samples) and the suppression of dislocation pileups, [59]. Therefore, the strengthening of conventional engineering materials may be based on appropriate engineering of the microstructures that hinders the formations and propagation of flaws and minimises the GB diffusion/sliding by possibly reducing the GB volume fraction. It has been observed in CHAPTER 9 that this can be achieved by the processing routes that effect greater reductions in grain size dispersion during refinement.

In the present chapter, the impact of detailed microstructure evolution on the mechanical properties of nanocrystalline materials is studied. This deals with microstructure-property relationship induced by grain growth whose driving force is high concentration of internal energy. It is assumed that such relationship (normal/abnormal HPR) holds for individual grains. The assumption rationalizes the need to assess the statistics of the materials properties within the materials. The assessment may lead to the understanding of some key facts about the modelled material properties. The phase mixture model is known that considers the microstructure to be a dual phase structure. Previously, in such a model, the iso-strain or iso-stress, [52], condition of the two phases is assumed, and the complete interactions between different grains are not dealt with. In reality, the hard and soft grains may react differently to the applied load and, furthermore, the larger softer grains might predominantly accommodate the plastic strain in the materials. The interactions between grains may be accounted for in this present approach since the expression governing the increment of the individual grain stress is made up of also local parameters such as local-critical grain size, curvature driven GB mobility function and misorientation angle driven grain rotation-coalescence mobility constant.

A modified expression representing the microstructure-to-properties relationship throughout the entire range of microstructure evolution has been established, [3], to be

$$\sigma(\mathbf{r}) = \sigma_0^{'} + A\mathbf{r}^{-1/2} - B(\mathbf{r}^{-1/2})^2 - C(\mathbf{r}^{-1/2})^3 \qquad (10.1)$$

where $\sigma_0^{'} = \sigma_0 + K_t$ is the starting yield (proof) stress for dislocation movement, $A = K_d$ is the conventional (or HPR) proportionality constant, $B = K_t\left[2hH_m / RT_r\right]$, $C = K_d\left[2hH_m / RT_r\right]$, $\boldsymbol{r}$ is the grain size, K_t is a constant, h is atomic diameter in the case of metal, H_m is the conventional melting enthalpy, R is ideal gas constant, T_r is the room temperature, $K_d > 100K_t$ and $\sigma_0 > 10K_t$.

In our recent model of grain growth developed in CHAPTER 8, a stochastic expression governing the incremental change of individual grain size in nano-materials is given as:

$$dr = M(r,T)\left(\frac{1}{r_c} - \frac{1}{r}\right)dt + D\sqrt{r}dW(t) + (1+a)rdN(t) \qquad (10.2)$$

In this expression, $M(r,t)$ is the GB mobility function, r_c is the local critical grain size, D is constant, a is a constant that is related to the size of the rotating grain, $dW(t)$ is the increment of the Wiener process and $dN(t) = N(t+dt) - N(t)$ is an increment of a stochastic counting process (i.e. the number of coalescence events) within an infinitesimal time interval.

The present chapter, in turn, addresses the evolution of "mechanical" properties of nano-materials undergoing changes in their microstructure. The stochastic differential expressions governing the increment of individual grain yield stress of Nano-Poly-Crystal (NPC) due to grain growth are obtained from expressions (10.1) and (10.2) by the Ito's differential rule [16-20]. It follows that

$$dr^2 = \left\{ 2M_{mig}\left(\frac{r}{r_c} - 1\right) + D^2 r \right\} dt + 2Dr^{3/2} dW(t) + (3 + 4a + a^2) r^2 dN(t) \qquad (10.3)$$

$$d\sigma(r,t) = \left\{ \left(-\frac{A}{2r^{3/2}} + \frac{B}{r^2} + \frac{3C}{2r^{5/2}} \right) M_{mig}\left(\frac{1}{r_c} - \frac{1}{r}\right) + D^2\left[\frac{3A}{8r^{3/2}} - \frac{B}{r^2} - \frac{15C}{8r^{5/2}}\right] \right\} dt$$
$$+ \quad D\left\{ -\frac{A}{2r} + \frac{B}{r^{3/2}} + \frac{3C}{2r^2} \right\} dW(t) + \left\{ \frac{E}{r^{1/2}} - \frac{F}{r} - \frac{G}{r^{3/2}} \right\} dN(t) \qquad (10.4)$$

$$d\sigma^2(r,t) =$$
$$\left\langle 2\left(\sigma_0' + \frac{A}{r^{1/2}} - \frac{B}{r} - \frac{C}{r^{3/2}} \right) \left\{ \left(-\frac{A}{2r^{3/2}} + \frac{B}{r^2} + \frac{3C}{2r^{5/2}} \right) M_{mig}\left(\frac{1}{r_c} - \frac{1}{r}\right) + D^2\left[\frac{3A}{8r^{3/2}} - \frac{B}{r^2} - \frac{15C}{8r^{5/2}}\right] \right\} \right.$$
$$\left. + D^2 \left\{ -\frac{A}{2r} + \frac{B}{r^{3/2}} + \frac{3C}{2r^2} \right\}^2 \right\rangle dt$$
$$+ 2D\left(\sigma_0' + \frac{A}{r^{1/2}} - \frac{B}{r} - \frac{C}{r^{3/2}} \right) \left(-\frac{A}{2r} + \frac{B}{r^{3/2}} + \frac{3C}{2r^2} \right) dW(t)$$
$$+ \left\{ 2\left(\sigma_0' + \frac{A}{r^{1/2}} - \frac{B}{r} - \frac{C}{r^{3/2}} \right) \left(\frac{E}{r^{1/2}} - \frac{F}{r} - \frac{G}{r^{3/2}} \right) + \left(\frac{E}{r^{1/2}} - \frac{F}{r} - \frac{G}{r^{3/2}} \right)^2 \right\} dN(t) \qquad (10.5)$$

where $E = A(b-1)$, $F = B(b^2-1)$, $G = C(b^3-1)$, $b = (2+a)^{-1/2}$ and *dN(r,t)* is the number of coalescence events of grains within an infinitesimal time interval. On the right hand side of expression (10.4), the first term accounts for the change of individual grain yield stress due to curvature driven grain boundary migration (GBM), the second term accounts for the random fluctuation in grain yield stress due to GBM and the last term accounts for the change in grain yield stress due to misorientation angle driven grain rotation coalescence (GRC). Expansions or simplifications of expressions (10.3)-(10.5) are found in appendix **C**.

Assuming that the number of coalescence events of grains is independent of grain size, the evolutions of the statistical moments of grain size and grain yield stress are obtained from expressions (10.2) - (10.5). In deriving these results, one has to

take into consideration the fact that the size of a given grain is independent of the size of its neighbours. Further simplification is made if one takes into account an experimental fact, that the probability distribution of grain size in polycrystalline materials, can be approximated by a lognormal distribution, [44,45,46,CHAPTER 7].

10.1 Salient Features of Mechanical Properties of Nanocrystalline Aluminium Samples

The equations for statistical moment are solved simultaneously. The model was tested on samples of nanocrystalline aluminium with initial mean grain size, $E(r)_0$, 4nm and initial dispersion of grain size, $CV(r)_0$, 0.3. The samples were annealed at the various temperatures as indicated on the plots. The parameters of grain growth and conventional Al sample employed are $H_m(\infty) = 10.71\,\mathrm{KJmol^{-1}}$, $T_m(\infty) = 933.47\,\mathrm{K}$, $T_r = 300\,\mathrm{K}$; R=$8.31\,\mathrm{JK^{-1}mol^{-1}}$, $v(\langle r \rangle, t) = CC\left\langle 1/r^m \right\rangle$, CC=12, $m=4$, $h_0 = 0.25\,\mathrm{nm}$, $M_0^{'} = 0.01\,\mathrm{nm^2 s^{-1}}$, $a = -0.90$, $D = 10^{-4}$, $< r_c >= 1.95 < r >$, $\sigma_0^{'} = 16.7MPa$, $K_t = 1.3$ and $K_d = 1301.77MPa\_nm^{1/2}$.

Since it has been established that the different mechanisms of grain growth impart different and independent nature of evolutions to the mean grain size, E(r), and grain size dispersion, CV(r), [CHAPTER 6, CHAPTER 8], these different mechanisms are considered here to be different processing routes. Since at any instant, a material sample possesses a single value of E(r) as well as a corresponding single value of CV(r), 3-D plots are less informative (does not add any value to the results) and are not dealt with here. Rather, separate plots for the evolution of the mechanical property as functions of each of E(r), CV(r) or time are made, see Fig10.1, Fig.10.2 and Fig.10.3 On these figures $\sigma_{Tot,T}$, $\sigma_{Rot,T}$, $\sigma_{Mig,T}$ $M_{const,T}$ and T_i are respectively the material mechanical properties at temperature T Kelvin due to simultaneous GBM and GRC mechanisms, GRC mechanism only, GBM mechanism only, Total process if it considered that the GB mobility is

constant and Total process where the microstructure evolution is diffusive one only. The temporal evolutions of E(r) and CV(r) are not reported here as comprehensive analyses are found in CHAPTERS 6 & 8. The results obtained from the present model reveal many salient features of the mechanical properties of the aluminium samples. Different mechanisms of grain growth impart different nature of response on the material mechanical properties. The evolutions of the microstructures through different processing routes result in materials that have different properties whose nature of evolution are also different. Observe that the evolution of the material properties through different processing routes intersect each other as E(r), CV(r) or time progresses. Also observe that the value (e.g. of E(r), CV(r) or time) at which the maximum in material property occurs is not constant, and the maximum attainable material properties are not the same through different processing routes. In this project, these values are relatively closer to each other since the original samples had the same values of $E(r)_0$, $CV(r)_0$ and, hence, material property; and the turning points are quickly reached.

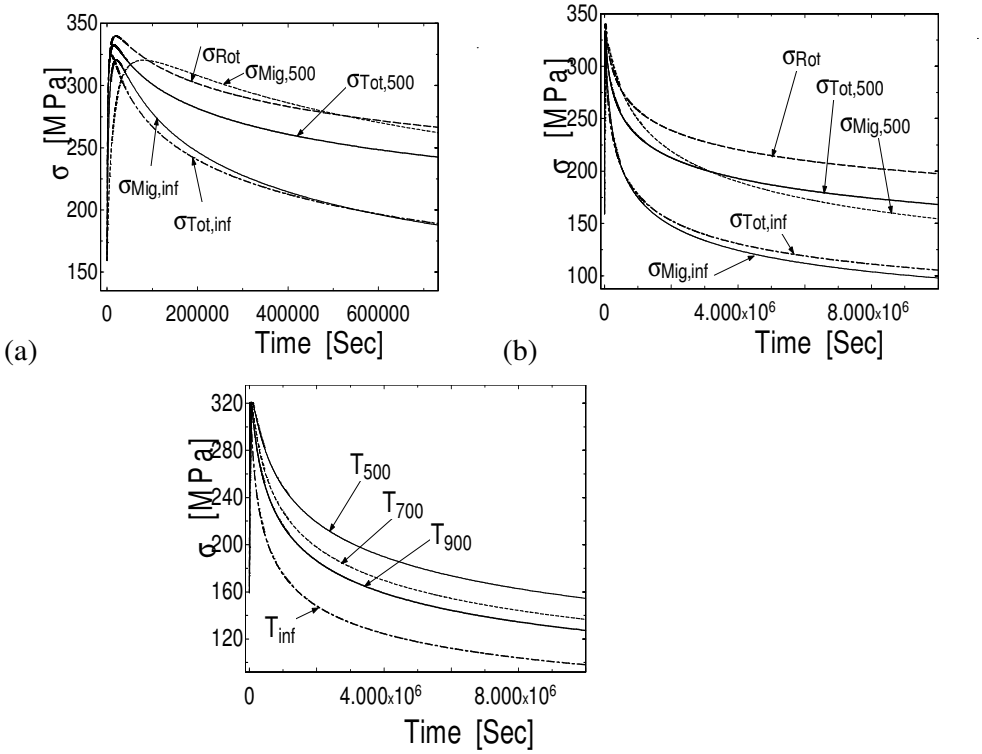

Figure 10.1 *Temporal evolution of material mechanical properties: (a) short period, (b) long period and (c) different annealing temperature*

Observe that the evolution of microstructures due to GRC mechanism results in material with much enhanced yield stress. One might be forced to wrongfully conclude that since the temporal evolution of the microstructure size due to GRC is smaller in most cases than that due to any of the mechanisms [CAHTPTER 6, CHAPTER 8], then it should impart higher value to the mechanical property. But from the evolution of the mechanical property as a function of E(r) or CV(r) (Fig.10.2 and Fig.10.3), one sees that at the same E(r) or CV(r) the material property due to GRC only is higher than that due to any of the mechanisms. It was observed in CHAPTER 8 that the GRC process effects greater changes in CV(r) than any of the mechanisms. Combining these facts and the observations made in CHAPTER 9 and in [52], the GRC process can be said to be as a result of high deformation strain rate. The Total process may be said to be as a result of relatively low deformation strain rate while the GBM process can be compared to the deformation at "varying" strain rate. The evolution of the yield stress due to GRC is higher throughout than that due to Total process, while that due to GBM is initially lower which rises to higher value before falling again to smaller value than those of the other mechanisms.

The temperature dependence of the microstructure-property relationship follows different trends. This has also been observed and explained differently in literature. At higher temperatures, both the GBM and the total processes behave as if they are being operated at the same (low) deformation strain rate.

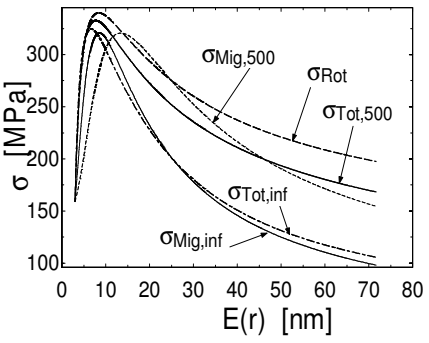

(a)

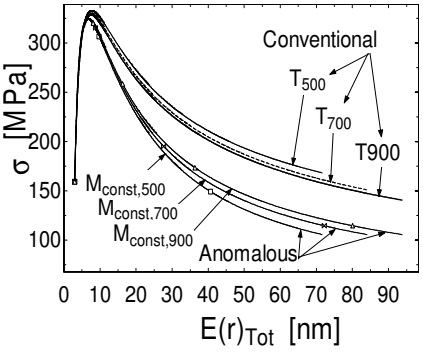

(b)

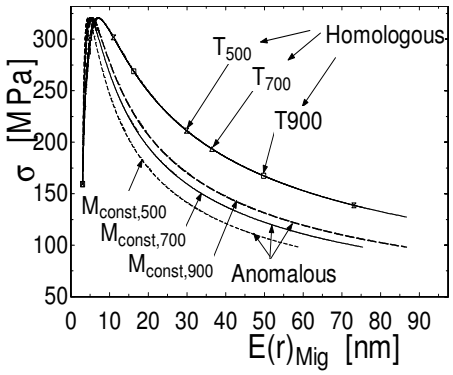

(c)

Figure 10.2 *Variation of mechanical properties, σ, against mean grain size, E(r), (a) all grain growth mechanisms, (b) and (c) Total process and GBM only at varying temperatures*

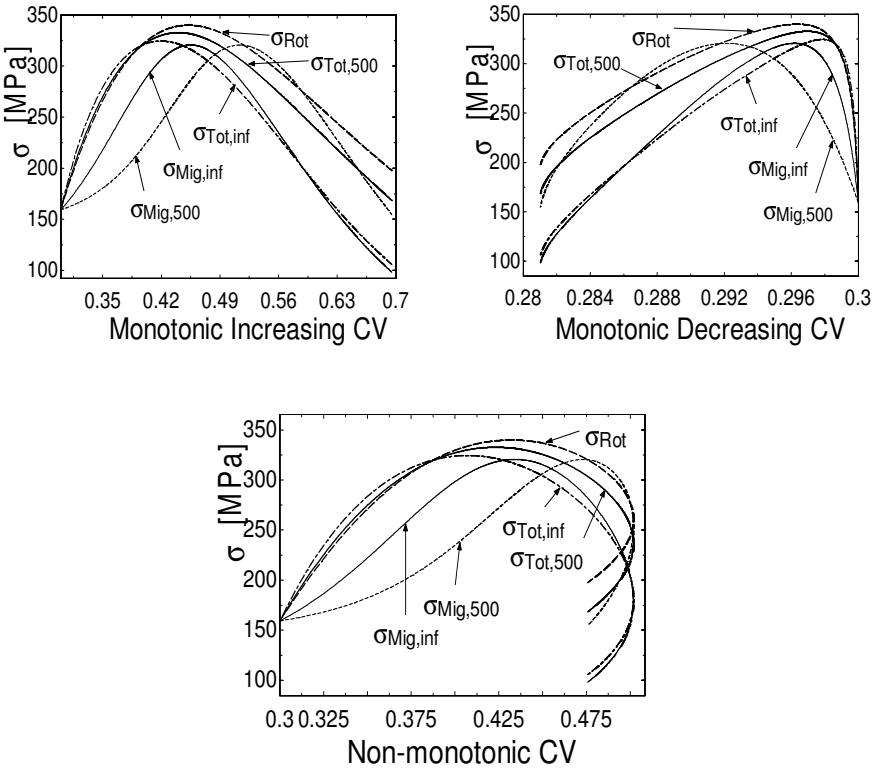

Figure 10.3 *Relationship between σ and grain size dispersion, CV(r)*

10.1.1 Normal temperature dependence of yield stress

For a typical sample (Total process) at elevated temperature, the mechanisms responsible for the strengthening of the material become less fervent. This is because the diffusion activities and speed of dislocation motion are highly favoured. For such a sample, dislocations could cross-slip, and the strength increase observed at low temperatures due to dislocation pile-up would be defeated. It is also possible that the GBs and particle interfaces act as sinks for dislocations at high temperatures, further reducing the dislocation pile-ups. Another school of thought ascribed the decrease in yield stress to decrease in Hall-Petch coefficient which also has large strain rate dependence at elevated temperature, [61]. The conventional/normal temperature dependence occurs for Total process with decreasing GB mobility; see Fig. 10.2 (b) upper curves.

10.1.2 Homologous temperature dependence of yield stress

If the microstructure evolution is diffusive only, T_i, (e.g. deformations by GB and GI diffusions) with no GRC mechanism occurring, then it should be observed that an increase in the temperature leads to no change in the nature of the evolution of the mechanical property as a function of the grain size, see Fig.10.2(c) upper curve. This homologous temperature dependence/behaviour has also been observed by other researchers, [62,63], where at relatively high temperatures, the yield stresses of all their samples fall on the same value. The homologous temperature dependence is observed to occur for the total process where the grain growth is diffusive only and the GB mobility decreases with grain growth.

10.1.3 Anomalous temperature dependence of yield stress

It is observed that if the microstructure evolution is analysed based on the model where the GB mobility is constant with grain growth and at low strain rate, M_{const}, then an increase in the annealing temperature results in an anomalous increase in material property; see Fig. 10.2 (b) lower curves. Several theoretical and

experimental works, [64-68], have been reported on this anomalous temperature dependence. A wide range of mechanisms and phenomena responsible for the anomalous temperature dependence of the yield stress is mentioned in the paper by Morris et al, [66]. The explanation given, [64], for such an anomalous behaviour is that an edge dislocation split into multiple dislocations, the edge dislocation immobilises and the immobilisation causes the mean free path of the edge dislocation to decrease with increasing temperature. Morris et al, [66], gave an explanation based on immobile vacancies with a prerequisite that the sample material be previously well annealed to "relax" any internal structure. It is explained, [65], that this is due to the removal of the thermally activated vacancy. The anomalous temperature dependence has been demonstrated to occur for the grain growth where the GB mobility is constant during growth.

Thus, the conventional, homologous or anomalous temperature dependences of the yield stress have been revealed to be due to different nature of interactions of the microstructures during evolutions. A model of microstructure-property relationship based on the individual/local grain parameters has been established and verified. The evolution of the microstructure through different processing routes results in different materials (i.e. having, for example, the same mean grain size but different grain size dispersion) with ***different*** or ***the same*** mechanical properties.

11 DISCUSSIONS, LIMITATIONS AND CONCLUSIONS

11.1 The Inherent Feature of Nanomaterials Microstructure is Random

Topological randomness of the microstructure means that the number of faces per grain, the number of edges per grain and the number of corners (or vertices) per grain are random variables satisfying the self-consistency relationship. Furthermore, the microstructures in the materials have random spatial distribution. These imply that it is logical to characterise the microstructures and analyse their corresponding characteristics stochastically. The characterisations of the materials microstructures and the analysis of the microstructure characteristics in the stochastic sense entail the use of the random field variables that have the ability to handle continuous spatial variables, thus possessing the potential to capture the highly detailed local properties. Modelling using such an approach in the present project has revealed many prominent features of polycrystalline nanomaterials.

11.2 Averaging Techniques

In order to obtain the observed overall materials properties, the materials characteristics or features measured at the local level have to be averaged. The averaging technique used depends on the type of material property under consideration. When the overall material property is the one (e.g. stress) that is defined per unit value (e.g. per unit area), it has been logical to perform averaging based on the conventional (or first level) "averaging techniques" where, for example, the average of n numbers is obtained by the weighted sum of the n numbers followed by the division of the results by the sum of the weights (or frequencies). If the material property under consideration is such that its value is cumulative (e.g. total number of the faces of all the grain in the material or the total strain incurred during deformation), then higher level of averaging techniques has been employed, which involves the use of compound (marked) point fields. In the marked point field approach, each microstructure has been

assumed to possess some random feature (marked variable) which combines additively with those of the neighbours to form the property of the entire materials.

It is acknowledged that there exists some sort of mathematical relationship between results due to first order averaging and those of higher order averaging e.g. relationship between the strain incurred by a material and the stress. In fact, during conventional experimentations, the strain incurred by the entire material may be measured by means of a strain gauge. The deformation of the strain gauge is then used to infer the strength of (stress in) the material. But in nanoscience and nanotechnology today, the stress applied to and the deformation incurred by each and every microstructure are being "measured". The local strain (or local stress) can then be averaged to obtain the overall strain (or overall stress) by using the knowledge from compound point field (or conventionally).

For example, for composite behaviour, the phase mixture model, [52], and the Shear Lag theory, [62], are known where load (or stress) is assumed to be transferred from one phase to the other through the GB i.e. specifically with the Shear Lag theory, load is assumed to be transferred between high aspect ratio reinforcement and the matrix by means of shear stresses at the particle-matrix interface. In this (and any other) case, the yield stress of the composite depends strongly on the volume fractions (conventional averaging quantity) of the phases which are aspects of the weighted average, and is given, in accordance with [62], as

$$\sigma_y = \sigma_{ym} f\left[1 + \frac{(L+t)A}{4L}\right] + \sigma_{ym}(1-f) \qquad (11.1)$$

where σ_{ym} is the yield stress of the unreinforced matrix, L is the length of the particle perpendicular to the applied stress, t is the length of the particle parallel to the applied stress, A is the particle-aspect ratio, and f is the particle-volume

fraction.

The theorems of compound point processes have been used in this project to model the cumulative number of faces of the grains in the aggregate or material. The approach has proven that the statistics of the cumulative microstructure features cannot be obtained by intuitions by using the expressions that have been established under the chapter. Specifically, it has been found that these statistics of the overall features depend on the statistics of the number of microstructures (i.e. the density of the microstructures), the statistics of the features per microstructure (i.e. statistics of the marked random variable) and the size (i.e. Lebesgue Measure) of the aggregate or material. The result presented under the chapter has been at some time instant. If grain growth, that is a natural phenomenon in nanomaterials, were to occur, then the statistics of the feature per microstructure and consequently the density of the microstructure would evolve. This should lead to evolving cumulative features. Complete information about the evolution of the statistics of the cumulative feature can be obtained from the knowledge of grain growth defined as function of the feature per microstructure only, since the feature per microstructure has been proven to be mathematically related to the density of the microstructure. For example, the knowledge of grain growth depending on the number of faces per grain defined by Glazier et al [29-31] may be used. This is subject to future task.

11.3 Grain Growth Processes or Microstructure Evolutions

Microstructure evolution and its impact on the material stability/property are playing central roles in the design and processing of materials. Knowing the exact nature of this microstructure evolution is thus imperative. Aspects of these evolutions whose mathematical models have been established are the grain growth processes. The detailed microstructure evolution (i.e. the detail evolution of the mean grain size and the corresponding grain size dispersion) due to grain growth is now being modelled.

In the present project, the previously/existing models of grain growth have been improved and tested on aluminium samples. The improvement entails including the Grain rotation Coalescence mechanism (GRC) in the grain growth models that has been previously neglected. The previous model has also been improved by incorporating the fact that, conventionally, the GB mobility is known to decrease with increase in grain sizes. Based on the fact that the grain size in "dispersed-typed" nanomaterials is random, the stochastic counterparts of the improved expressions have been obtained by the addition of the fluctuation terms.

The findings about grain growth, in the present project, reveal

- improved correlations between the results of the proposed model and the experimental data,
- that deviation from the parabolic law of growth may be due to varying initial coefficient of variation of the distribution of sizes of grains in the system, varying rate of rotation of the grains and the annealing temperature,
- that grains in nanomaterials are more susceptible to growth at low temperature and even at low or no dispersion in size distribution as GRC mechanism has a higher mobility at low initial CV and, hence, a higher tendency to trigger growth and, hence, start up dispersion in size distribution,
- that average rotation mobility contributes up to about 50% of the overall average mobility constant depending on the initial CV,
- that for very high annealing temperature, grain growth approaches the parabolic law,
- that the relationships between the annealing temperatures and the grain growth mobility as well as grain growth exponent
- and that though the relationship between grain size and material melting temperature appears to be parabolic (or asymptotic), it should be modelled from the expression given in the project.

Unfortunately, while testing the model proposed in this research project, the rate of coalescence events of the grains has been unaffected by changing the annealing

temperature. This has been due to the fact that two different, but contradictory reports were given in the literature, from the same group of researchers, about the dependence of the rate coalescence of the grains on the annealing temperature (i.e. about the parameter that depends on temperature). In one report, [38], it is stated that this dependence is given by

$$C = A_1 KT \tag{11.2}$$

while in the other, [37], it is given by

$$C = \frac{A_2}{KT} \tag{11.3}$$

where the A_i are defined in the respective papers, K is the Boltzmann constant. The rotational mobility is defined as $M(r) = C/\left(r^n\right)$, where r is grain size and n is constant that depends on the type of GB accommodation mechanism under consideration. It is hoped that when a precise expression for the contradictory dependence (i.e. increasing in one and decreasing in the other) will be known, then further and better improvements will be achieved and more salient features may be revealed.

It has been acknowledged in this report (chapter 6) that, in addition to GRC, other mechanisms of grain growth do take place. This includes the T2 event where a small three-sided grain disappears from the aggregate and the T1 event where grains translate to exchange neighbours. Though motivations have been given under that chapter for considering GBM only and/or GRC only, a careful consideration of other (neglected herein) mechanisms may reveal further useful information about grain growth. Such considerations are going to be subject the author's planned future publications.

The characterizing features of random microstructures such as the ***number of sides or number of triple junctions***, *s*, per grain are mostly used when

undertaking 2-D space analyses; the ***number of faces***, *f*, per grain are usually obtained from/for 3-D experimentations and analyses; and the size ***(radius) of a grain***, *r*, is applicable for all the dimensional spaces i.e. 1-D, 2-D and/or 3-D analyses. The term, "**size**", is used to represent Lebesgue measure which in 1-D size means length, it stands for area in 2-D and for volume in 3-D and so on. Though these random features are highly correlated, the neglect of the explicit expressions for the correlations has frequently resulted in discrepancy in results obtained from both theoretical and experimental investigations of ***grains' structures*** and, hence, ***grains' properties***. It is thus important to investigate the correlations between these random features of nanoparticles. An applicable approach to resolving this problem is to study the correlations between these features during grain growth.

Extensive research has been carried out for decades to analyse the grain growth mechanisms in nanomaterials. It is found in the literature that there are three fundamentally different ways of expressing grain growth phenomena using these three features. Firstly, the Von Neumann-Mullins law, [69-71], exists that expresses the evolution of the ***area*** of grain as a function of the ***triple junctions only*** (i.e. as a function of the ***number of sides*** of the grains only), given as

$$\frac{dA_s}{dt} = J(s - s_0) \tag{11.4}$$

where A_s is the area of an s-sided grain, s is the number of sides on the grain, J is a diffusion constant or triple junction mobility constant and s_0 is a critical constant. This von Neumann-Mullins relationship has been modified, [72],to

$$\frac{dA_s}{dt} = \frac{M_b}{1+\frac{1}{\Lambda}}\left(2\pi - s[\pi - 2\theta]\right) \tag{11.5}$$

where M_b is the reduced grain boundary mobility which is a product of grain boundary mobility with grain boundary surface tension, Λ is the product of the

triple junction mobility and the grain size divided by the grain boundary mobility and θ is the contact angle at a triple junction.

Secondly, in 1965 Hillert suggested the model, [35], which is the expression that predicts how the ***radius (diameter)*** of an individual grain evolves with time as a function of the ***radius*** of the grain alone given as

$$\frac{dr}{\mathrm{dt}} = M\left(\frac{1}{r_c} - \frac{1}{r}\right) \tag{11.6}$$

where M is the grain boundary mobility constant. This has been modified in the present project to

$$dr = M_0(T)\left(1+\frac{C}{r}\right)\left(\frac{1}{r_c} - \frac{1}{r}\right)dt + B\sqrt{r}\,dW(t) + (A+1)r\,dN(t) \tag{11.7}$$

where r is the grain radius, $M_0(T)$ is the temperature dependent part of the grain boundary mobility, C is a constant at constant temperature, r_c is the local critical grain size that restricts the total volume of the sub-aggregate to remain constant during the growth process i.e. the local size of the grain that neither grows nor shrinks, *A* and *B* are constants, *dW(t)* and *dN(t)* are respectively the increments of the Weiner and the stochastic counting processes within an infinitesimal time interval.

And thirdly, J.A. Glazier et al, [29-31], postulated a relationship between the evolutions of the ***grain volume*** as a function of the ***number of faces per grain*** alone, given as

$$V_f^{-1/3}\left[\frac{dV_f}{dt}\right] = k\left(f - f_0\right) \Leftrightarrow \frac{dV_f^{2/3}}{dt} = K(f - f_0) \tag{11.8}$$

where k is a diffusion constant, f is the number of faces of a grain, f_0 is a constant, V_f is the volume of grain having f faces.

An observable fact is that none of the expressions (11.4-11.8) is expressible as a function ***more than one*** of the three random features of the nanoparticles or as a function of a feature other than the one it was originally stated. For example, the evolution of mean grain area has not yet been given as a function of the number of faces per grain, and the evolution of the mean grain volume has not yet been expressible as a function of the number of sides per grain. The issue is that if there exist strong mathematical relations between radius, area and volume, then why is it that one and only one random feature appears in each expression for the evolution of grain size; and that a feature cannot, as yet, be replaced by the other feature in an expression? Answers to this concern may explain the reasons why deviations have been encountered very often while verifying different models of grain growth from both simulations and experiments e.g. while verifying the Von Neumann- Law using the evolution of the mean grain size or evolution of number of faces per grain.

Knowing that these three features of random microstructures (grain size, number of sides per grain and the number of faces per grain) are related by the Euler's equation, we aim in one of our upcoming publications to come up with a unified expression for grain growth that incorporate the Von Neumann-Law, the Hillert's model and the Glazier's model.

To the best of our efforts up to date, no model has been found in literature that predicts the evolution of microstructure sizes with grain refinement. Thus, an effort to predict the evolution of the material property starting with conventional material to nanomaterial was not dealt with. Similar effort has been attempted in the opposite direction of microstructure evolution (grain growth) i.e. the evolution of the material property from nanomaterials to conventional materials.

11.4 Neglecting Grain Size Distribution Parameters or the Probability Density Function, pdf, of Grain Size

The grain size in material is known to be random. This random size can be represented by a probability distribution. From the knowledge of the evolution of the microstructure sizes, the time evolution of the probability density function has been established analytically using the generalised Fokker-Planck Kolmogorov Equation. Findings from the present project reveal that both the mean grain size and the grain size dispersion are vital in the characterisation of the microstructure evolution and consequently, the evolution of the materials properties. Neglecting other grain size distribution parameters during modelling in previous reports has led to loss of vital information about the microstructure characteristics and equally the material properties. The many different properties of "the same type of" material samples given in the literature have been accounted for in the present project where all the grain size distribution parameters have been considered.

Furthermore, the following are some of the results that have been obtained from the analytic modelling of the probability density function, pdf.

- Starting with an initial lognormal distribution or normal distribution of grain size, the grain growth parameters were calibrated such that the grain size pdf evolved as *lognormal distribution* till the scaling (steady) state.
- Results are different when the GRC mechanism is taken into consideration, and further, due to the addition of the fluctuation terms.
- Results also depend on the nature of the fluctuation terms which are determined by the type of material under study.
- The evolution of the pdf depends on the initial dispersion of grain size in the material such that systems with higher initial CV of grain size evolve in such a way that the pdf curves are correspondingly broader than those for system with lower initial CV.
- During grain growth some grains shrink while others get larger.

- Grain growth imparts self-similar behaviour to parameters of grain size distribution.

The following limitations have been encountered during the modelling of the pdf.

- It *cannot* be stated whether the initial probability distribution of grain size does not have an effect on the way the pdf evolves and, consequently, the asymptotic pdf.
- Also, these results are obtained from the specific diffusion and jump terms that may obviously have some influences on the results as can be testified by the case, "GBM only at steady state". This, thus, necessitates research on the types of fluctuation terms that best reflect the result of the process of production/processing of nanomaterials.
- Neglecting higher order terms might, obviously, have an effect on the results. It could not be stated how many terms had to be considered so that the solution could be accurate enough. Thus, instead of using a Taylor series expansion to simplify the jump probability term, a different approach which might not invoke infinite series and hence, truncation may be more beneficial.

11.5 Fabricating or Processing Nanomaterials through Different Processing Routes

The random nature of nanomaterials microstructures may be inherited from the fact that these materials can be produced through different processing routes. Thus, materials with the same mean grain size may differ in their grain size dispersion. It has been demonstrated in the project that the consequence of this is that "these" different materials samples can possess different properties whose nature of evolution can be quite different. It has also been found that different nanomaterial samples can possess the same properties. The basis of the argument is that both the mean grain size and grain size dispersion simultaneously play vital roles in the design of the required or desired material properties. Based on such

considerations and using the lognormal distribution of grain sizes, many salient features of the material properties listed below have been revealed. Letting $\mu_n=E(r^n)$ be the "n^{th} moment of the grain size, *r*" and for lognormal distribution of the grain size, the expressions for the microstructure-property relationship are proposed to be modified so as to incorporate both the mean grain size and the grain size dispersion for the HPR to be

$$\sigma(\mu_1,\mu_2)=\sigma_0+K_d\frac{\mu_2^{3/8}}{\mu_1^{5/4}} \tag{11.9}$$

and for the HPR to Reverse-HPR to be

$$\sigma(\mu_1,\mu_2)=\sigma_0^{'}+A\frac{\mu_2^{3/8}}{\mu_1^{5/4}}-B\frac{\mu_2}{\mu_1^{3}}-C\frac{\mu_2^{15/8}}{\mu_1^{21/4}} \tag{11.10}$$

where the dispersion of grain size is given by

$$CV(r)=\sqrt{\left[\frac{\mu_2-\mu_1^2}{\mu_1^{\,2}}\right]} \tag{11.11}$$

and $\sigma_0^{'}=\sigma_0+K_t$ is the conventional yield stress, $A=K_d$ is the conventional proportionality constant, $B=K_t[2hH_m/RT_r]$, $C=K_d[2hH_m/RT_r]$, K_t is a constant, *h* is atomic diameter in the case of metal, H_m is the conventional melting enthalpy, *R* is ideal gas constant, T_r is the room temperature, $K_d>100K_t$ and $\sigma_0>10K_t$.

11.6 Salient Features of Nanocrystalline Aluminium Sample

A model of microstructure-property relationship based on the individual/local grain parameters was established and verified. The following facts have been revealed from the proposed model.

- The fabrication method that results in a material with more enhanced property can only be decided if, in the course of deformation using each technique, reports are made on simultaneous variations of mean grain size and grain size dispersion.
- The departures of experimental data from the path predicted by a relationship are due to change of (or inconsistent) design strategy.
- The evolution of the microstructure through different processing routes results in materials with different mechanical properties.
- Nanostructured materials with both low CV(r) and low E(r) have the most enhanced material properties.
- The conventional/normal temperature dependence could occur for Total process with decreasing GB mobility.
- The homologous temperature dependence would occur with the process where the grain growth is diffusive only and the GB mobility decreases with grain growth.
- The anomalous temperature dependence has been shown to occur for the grain growth processes where the GB mobility is constant during growth.

11.7 Fractal Theory or Geometric Measure Theory

The theorems of Geometric measure theory could not be applied to analyse the characteristics of the random materials microstructures. This is because, up to date, the apparatus used in the characterisations of the materials microstructures reports on the equivalent radius of the grain sizes (and not the exact undulations). The mathematical characterisations of a random set (grain) necessary for use in the application of the theorems of geometric measure theory cannot, therefore, be achieved in this instant. It should be acknowledged that some detailed characterisations of the microstructure have been achieved and reported in the literature. This includes characterisations of, for example, orientation and elongation distributions.

REFERENCES

[1] Hall, E.O. (1951), *The deformation and aging of mild steel: III discussion of results,* Proc. Phys. Soc., Ser. B, Vol. 64, pp. 747-753.

[2] Petch, N.J. (1953) *The cleavage strength of polycrystasl,* J. Iron and Steel Institute, Vol. 174, pp. 25-28.

[3] Zhao, M. and Jiang (2006), Q., *Reverse Hall-Petch relationship of metals in nanometer size*, Emerging Technologies- Nanoelectronics, IEEE Conference on Vol., pp 472 – 474, (10-13 Jan. 2006)

[4] Sobczyk, K. (2004), *Random material microstructures: methodical background,* AMAS Course on Random Material Microstructures RMM'04, edited by K. Sobczyk, pp 7-48, Warsaw, (February 2-4, 2004).

[5] Sobczyk, K. (2004) *Characterisation of random material microstructures*, Keynote lecture, Proc. SACAM'04 conference, pp. 1-12.

[6] Sobczyk, K.., Kirkner D.J., (2001) *Stochastic Modeling of Microstructures*, Birkhauser.

[7] Fradkov, V.E. and Udler, D. (1994), *Two-dimensional grain growth: topological aspects,* Advances in Physics, Vol. 43, No.6, pp 739-789.

[8] Moller, J. (1989), Random tessellations in R^n, Adv. Appl. Probability, 21, 37-73.

[9] Miles, R.E. (1972), Random division of space, in: Nicholson W.L. (Ed.) Suppl. Adv. Appl. Probability, 243-266.

[10] Stoyan, D. and Stoyan, H. (1994), *Fractals, Random Shapes and Point Fields : methods of geometrical statistics,* John Wiley & Sons.

[11] Falconer, K. (1997), *Techniques in Fractal Geometry*, John Wiley & Sons.

[12] Falconer, K. (1990), *Fractal Geometry*, John Wiley & Sons.

[13] Frost, H. J. (1998), *The microgeometry of dense random packings*, Micromechanics of Granular Materials, edited by M. Satake and J.T. Jenkins, Elsevier Science Publishers B.V., Amsterdam, Printed in The Netherlands, pp 21-30.

[14] Beddow, J.K. (1988) *Morphological analysis of particulate materials,* Micromechanics of Granular Materials, edited by M. Satake and J.T. Jenkins,

Elsevier Science Publishers B.V., Amsterdam, Printed in The Netherlands, pp 11-19.

[15] Kanatani, K. (1988), *Stereological estimation of microstructures in materials,* Micromechanics of Granular Materials, edited by M. Satake and J.T. Jenkins, Elsevier Science Publishers B.V., Amsterdam, Printed in The Netherlands, pp 1-10.

[16] Iwankiewicz, R. and Nielsen, S. R. K. (1999), *Vibration Theory, Vol. 4: Advanced Methods in Stochastic Dynamic of Non-Linear Systems*, Aalborg Tekniske Universitetsforlag.

[17] Gikhman, I.I. and Skorokhod, A.A. (1972), *Stochastic differential equations*, Springer-Verlag.

[18] Arnold, L. (1974), *Stochastic differential equations: theory and applications*, J.Wiley & Sons, New Yok.

[19] Snyder, D.L. (1975), *Random point Processes*, J.Wiley & Sons, New Yok.

[20] Gardiner, C.W. (1985), *Handbook of stochastic methods for physics, chemistry and the natural sciences*. Springer-Verlag.

[21] Cox, D.R. (1967), (David Roxbee), *Renewal Theory, Methuen's monographs on applied probability and statistics*, London: Science paperbooks.

[22] Garboczi, E.J., Synder, K.A., Douglas, J.F., and Thorphe, M.F. (1995), *Geometrical percolation threshold of overlapping ellipsoids*, Phys. Rev. E52, pp. 819-828.

[23] Saito, Y. (1998), *Monte Carlo Simulation of Grain Growth in Three-dimensions*, ISIJ Intern, 38-6, pp. 559-566.

[24] Krill III, C.E. and Chen L.-Q. (2002), *Computer simulation of 3-D grain growth using a phase-field model*, Acta Mat., 50, pp. 3057-3073.

[25] Russell, K.C., *Precipitate Coarsening And Grain Growth In Steels,* Massachusetts Institute of Technology, 77 Massachusetts Avenue, Cambridge, MA 02139-4307.

[26] Morhac, M. and Morhacova, E. (2000), *Monte Carlo Simulation Algorithms of Grain Growth in Polycrystalline Materials*, Cryst. Res. Technol., 35-1, pp. 117-128.

[27] Miodownik, M. A. and Holm E. A., and Hassold G. N. (2001), *3D Massively Parallel Cellular Automaton Simulations of Zener Pinning,* Proc. First Joint International Conference on Recyrstallizaiton and Grain Growth, Aachen, Germany, pp. 347-352.

[28] Smith, C. S. (1948), *Trans. AIME* 175 15.

[29] Glazier, J. A. and Prause, B. (2002), *Current Status of Three Dimensional Growth Laws,* in *Foams, Emulsions and their Applications*, P. Zitha, J. Banhart and G. Verbist editors, Verlag MIT Publishing, Bremen, Germany, pp. 120-127.

[30] Glazier, J.A. (1993), *Grains growth in three Dimensions depends on the Topology,* Phys. Rev. Lett.**,** Vol. 70, No.14, pp.2170-2173.

[31] Weaire, D. and Glazier J.A.(1993), *Relationship between Volume, number of faces and Three dimensional Growth Laws in Cellular Coarsening Patterns*, Philo. Mag. Letters, Vol. 68, No. 6, pp. 363-365.

[32] Suwa, Y. and Saito, Y. (in Japan)*, Movies showing Grain Coarsening in Two-Dimensions, computer simulations of grain growth in two-dimensions* using a technique known as "*phase field" modeling*, University of Cambridge: http://www.msm.cam.ac.uk/phase-trans/abstracts/grain.movies.html cited June 2005 and January 2008).

[33] Glazier, J.**A.** and Weaire, D.(1992), *Review Article: The kinetics of cellular patterns,* J. Phys.: Condens. Matter 4, 1867-1894.

[34] Fayad, W., Thompson, C.V. and Frost, H.J. (1999), *Steady-state grain-size distributions resulting from grain growth in two dimensions*, Scripta Mat. Vol. 40 No.10, 1199-1204.

[35] M. Hillert (1965), *On the theory of normal and abnormal grain growth.* Acta metal. 13, pp.227-38.

[36] Upmanyu M., Srolovitz, D.J., Shvindlerman, L.S. and Gottstein, G. (1999), *Misorientation Dependence on Intrinsic Grain Boundary Mobility: Simulation and Experiment,* Acta Mater. Vol. 47, No. 14, pp. 3901-3914.

[37] Haslam, A.J., Moldovan D., Phillpot, S.R., Wolf, D. and Gleiter, H. (2002), *Combined Atomistic and Mesoscale Simulation of Grain Growth in Nanocrystalline Thin Film,* Comput. Mater. Sc., pp. 15-32.

[38] Moldovan, D., Wolf, D., Phillpot, S.R. and A. J. Haslam (2002), *Role of Grain Growth in a Columnar Microstructure by Mesoscale Simulation,* Acta Materialia 50, pp. 3397 – 3414.

[39] Weare, D. and Rivier N.(1984), Contemporary Phys., Vol.25, p. 59.

[40] Wakai, F., Enomoto, N. and Ogawa, H. (2000), *Three-Dimensional Microstructural Evolution in Ideal Grain Growth- General Statistics,* Acta Mater. 48, pp. 1297-1311.

[41] Estrin, Y. (2001), *Vacancy effect on grain growth*, Recrystallization and Grain Growth, G. Gottstein and D.A. Molodov, Eds., Springer-Verlag, Berlin, pp. 135-144

[42] Pande, C.S., Masumura, R.A. and Marsh S.P.(1997), *Analytic Form of the Sweep Constant in Grain Growth* Acta Mater. Vol. 45, No. 10, pp. 4361-4366.

[43] Zhao, X. (1995), *About the Stochastic Behaviour in Grain growth* Scripta Metallurgica et Materialia, Vol.33, No.7, pp. 1081-1086.

[44] Carpenter. D.T., Codner, J.R., Barmak, K. and Rickman, J.M. (1999), *Issues associated with the analysis and acquisition of thin-film grain size data* Mat. Lett., 41: 296-302.

[45] Pande, C.S. and Rajagopal, A.K. (2002), *Modeling of Grain Growth in Two-Dimensions,* Acta Materialia 50, pp. 3013-3021.

[46] Yu, C.Y., Sun, P.L., Kao, P.W. and Chang, C.P. (2004), *Evolution of Microstructure during Annealing of a severely deformed Aluminium,* Mat. Sc. and Eng. A366, pp. 310-314.

[47] Crow, E.L. and Shimizu, K. (1988), *Lognormal Distributions, Theory and Applications,* M. Dekker New York.

[48] Kurzydlowski, K.J. and Research Team, Warsaw University of Technology, Faculty of Materials Science and Engineering (InMat), Woloska 141 Str., 02-507 Warsaw, Poland.

[49] Fradkov, V.E., and Udler D. (1994), *Two-Dimensional normal grain growth: topological aspects,* Advances in Physics, Vol. 43, No.6, pp. 739-789

[50] Mehnert, K. and klimanek, P. (1996), *Monte Carlo simulation of Grain growth in textured metals using anisotropic grain boundary mobilities*.

Computational Materials Science 7, pp. 103-108.

[51] Jiang, Q., Zhang, S.H. and Li, J.C.(2004), *Grain size-dependence diffusion activation energy of nanomaterials*, Solid State Communications 130, pp. 581-584.

[52] Kim, H.S. and Estrin, Y.(2005), *Phase mixture modelling of strain rate dependent mechanical behaviour of nanostructured materials*, Acta Materialia 53, pp. 765-772.

[53] Veprek, S. (2003), *Superhard and functional nanocomposites formed by self-organization in comparison with hardening of coatings by energetic ion bombardment during their deposition*, Rev. Adv. Mater. Sci. 5, pp. 6-16.

[54] Schiotz, J., Vegge, T. and Jacobsen, K.W. (1998), *Atomic-scale modeling of the deformation of nanocrystalline metals*, arXiv:cond-mat/9812102v1 [cond-mat.mtrl-sci], Condensed Material, p. 1-10.

[55] Davenport, J. *Phase transition in Nanostructured materials,* (1999): http://www.rpi.edu/dept/materials/COURSES/NANO/davenport/nanohtml.html, cited 20 June 2007.

[56] Pullen, W.W.F. (1929), *Engineering tables and data,* 6th ed., Scientific Publishing Co.

[57] Slater, J.C. (1964), *J. Chem. Phys.*, 41, 3199.

[58] Meyers, M.A., Mishra, A. and Benson, D.J. (2006), *Mechanical properties of nanocrystalline materials*, Prog. in Mat. Sc. 51, pp. 427-556.

[59] Krasilnikov, N.A. and Sharafutdiniv, A. (2007), *High strength and ductility of nanostructured Al-based alloy prepared by high pressure technique,* Mat. Science and Engineering A463, 74-77.

[60] Schiotz, J., Di Tolla, F.D. and Jacobsen, K.W. (1998), *Softening of nanocrystalline metals at very small grain sizes,* Nature. 391, pp. 561-563.

[61] Setsuo, T., Kenji, K. and Toshihiro T. (2007), *Hall-Petch Relation At Elevated Temperature For Ultrafine Grained Iron*, To appear in Proc. Of International symposium on Ultrafine Grained, ISUGS 2007, Kitakyushu, (October, 24-26, 2007).

[62] Aikin Jr., R.M. (1997), *The mechanical properties of in-situ composites*, JOM, 49 (8), pp. 35-39.

[63] Takeuchi, S. (2006), *Homologous temperature dependence of the yield stress of icosahedral quasicrystals and its implication,* Philosophical Mag., Vol. 86, No. 6-8, pp. 1007-1013.

[64] Tonda, Hideki, Ando, Shinji, Takashima, Kazuki, Vreeland and Jr. Thad (1994), *Anomalous temperature dependence of the yield stress by (112'2) zone group axes (11'23) secondary pyramidal slip in cadmium crystals. 2: Mechanism,* Acta Metallurgica et Materialia , Vol. 42, No. 8, pp. 2853-2858.

[65] Kupka, M. (2002), *Temperature dependence of yield stress of FeAl alloys,* Material Science and Engineering A336, 320-322.

[66] Morris, D.G. and Munoz-Morris M. A.(2005), *The stress anomaly in FeAl-Fe_3Al alloys,* Intermetallics 13, 1269-1274.

[67] Lahiri, S. K. and Fine, M. E.(1970), *Temperature Dependence of Yield in Fe-1.67 At. Pct Cu and Fe-0.5 At. Pct Au Stress*, Metallurgical Transactions, Vol. 1, 1495-1499.

[68] Sundar, R.S. and Deevi, S.C. (2003), *High-temperature strength and creep resistance of FeAl*, Materials Science and Engineering A357, 124-133.

[69] Von Neumann J. (1952), In: Herring C, editor, Metal Interfaces.Cleveland 7, OH, American Society for Testing Materials, p. 108.

[70] Mullins W.W. (1956), Two dimensional motion of idealized grain boundaries, J. Appl. Phys. 27, p. 900– 904.

[71] Mullins W.W. (2002), Vinals J., Linear bubble model of abnormal grain Growth, Acta Mater 50, p.2945–54.

[72] Gottstein, G., Ma, Y. and Shvindlerman, L.S. (2005), *Triple junction motion and grain microstructure evolution*, Acta Materialia 53, pp. 1535-1544.

BIBLIOGRAPHY

[73] Aggarwal, K.G., Mahanty, J. and Tewary, V.K. (1965), *The Fourier expansion method for computation of the frequency distribution function of crystals*, Proc. Phys. Soc., Vol. 86, pp. 1225-1233.

[74] Aharonov, E. and Sparks, D. (1999), *Rigid phase transition in granular packings*, Physical Review E, Vol. 60, No. 6, pp. 6890-6896.

[75] Bouchaud, J.P., Cates, M.E. and Claudin, P. (1995), *Stress distribution in Granular media and nonlinear wave equation*, J. Phys. I France 5, 639-656.

[76] Butcher, J.C. (2003), *Numerical methods for ordinary differential equations / J.C. Butcher,* J. Wiley.

[77] Chapelle, D. and Darrieulat, M. (2003), *The occurrence of shear banding in millimeter scale (123)[634] grain of an Al-4.5% Mg alloy during phase strain compression*, Material Science and Engineering A347, pp. 32-41.

[78] Cumberland, D.J. and Crawford, R.J. (1987), *The packing of Particles, A Handbook of Powder Technology*, Vol.6, Elsevier.

[79] Daley, D.J. (1988), *An Introduction to Theory of Point Processes*, Springer-Verlag.

[80] Davis, R.E. and Dozier, J. (1989), *Stereological characterization of dry alpine snow for microwave remote sensing*, Adv. Space Res. Vol. 9 No. 1 pp. (1)245-(1)251.

[81] Edwards, S.F. and Grinev, D.V. (1999), *Statistical mechanics of stress transition in disordered granular arrays*, Physical Review Letters, Vol. 82 No. 26, pp. 53975400.

[82] Elias, F., Flament, C., Glazier, J. A., Graner, F. and Jiang (1999), Y., *Foams out of stable equilibrium: cell elongation and side swapping*, Phil. Mag. B, vol. 79, No. 5, pp. 729-751.

[83] Hairer, E. (1996), *Solving ordinary differential equations / E. Hairer, S.P. Nø]orsett, G. Wanner,* 2nd rev. Ed, Springer-Verlag.

[84] Hale, J.K. (1993), *Introduction to functional differential equations,* Springer-Verlag.

[85] Hibbeler, R.C. (1994), Mechanics of materials / R.C. Hibbeler. [multimedia

packages] , Prentice-Hall, 2nd Ed.

[86] Jiang, Y., Mombach, J.C.M and Glazier, J.A. (1995), *Grain growth from homogeneous initial conditions: Anomalous grain growth and special scaling states*, Physical Review E, Vol. 52 No. 4, pp. 3333-3336.

[87] Juneja, O.P. (1985), *Analytic Functions-growth Aspects*, Pitman Advanced Publishing Program.

[88] Kim, H.S. (2001), *Ductility of ultrafine grained copper*, Applied Physics Letters, Vol. 79, No. 25, pp. 4115-4117.

[89] Kupka, M. (2006), *High temperature strengthening of the FeAl intermetallic phase-based alloy*, Intermetallics 14, pp. 149-155.

[90] Krasilnikov, N.A. and Sharafutdiniv, A. (2007), *High stength and ductility of nanostructured Al-based alloy, prepared by high-pressure technique*, Material Science and Engineering A 463, pp. 74-77.

[91] Krishna, M.G., Kapoor, A.K., Prasad, M.D. and Srinivasan, V (2006), *The transition from bulk to nano as a phase transition*, Physica E 33 pp. 359-362.

[92] Langhaar, H.L. (1962), *Energy methods in applied mechanics*, J. Wiley.

[93] Lee, H.N., Ryoo, H.S. and Hwang, S.K. (2000), *Monte Carlo simulation of microstructure evolution based on grain boundary character distribution*, Mat. Sci. and Engineering A281, pp. 176-188.

[94] Leighton, W. (1952), *An Introduction to the Theory of Differential Equations,* Mcgraw-hill.

[95] Li, S., Li, J., Liu, F., Alim, M.A. and Chen, G. (2002) , *The dimensional effect of breakdown field in ZnO varistors*, J. Phys. D: Appl. Phys. 35 pp. 1884-1888.

[96] Lin, Y.K. (1967), *Probabilistic theory of structural dynamics*, McGraw-Hill.

[97] Lewandowska, M., Swiantnicki, W., Piatkowski, A. and Jasienski, Z. (2006), *Microstructure evolution and strain localization in Cu and Cu-8Al single crystal subjected to channel-die compression*, Journal on microscopy, Vol. 223, pp. 275-278.

[98] Ma, N., Kazaryan, A., Dregia, S.A. and Wang, Y. (2004), *Computer simulation of texture evolution during grain growth: effect of boundary*

properties and initial microstructure, Acta Materialia 52, pp. 3869-3879.

[99] Makse, H.A, Gland, N., Johnson, D.L. and Schwartz, L.M. (1999), *Why effective medium theory fails in granular materials*, Physical Review Letters Vol. 83 No. 24, pp. 50705073.

[100] Miodownik, M.A. (2002), *A review of microstructural computer models used to simulate grain growth and recrystallisation in aluminum alloys*, Journal of Light Metals 2. pp. 125-135.

[101] Miodownik, M., Godfrey, A.W., Holm, E.A. and Hughes, D.A. (1999), *On boundary misorientation distribution function and how to incorporate them into three-dimensional models of microstructural evolution*, Acta Mater. Vol. 47, No. 9, pp. 2661-2668.

[102] Moldovan, D., Wolf, D. and Phillpot, S.R. (2003), *Linking atomistic and mesoscale simulations of nanocrystalline materials: quantitative validation for the case of grain growth*, Philosophical magazine, Vol. 83 Nos. 31-34, pp. 3643-3659.

[103] Morris, D.G. and Gunther, S. (1996), *Texture and their evolution during processing of Fe-Al alloys*, Scripta Materialia, Vol. 35, No. 10, pp. 1211-1216.

[104] Morris, D.G., Liu, C.T. and George, E.P. (1999), *Pinning dislocation and the origing of the stress anomaly in FeAl alloys*, Intermetallics 7, 1059-1068.

[105] Pande, C.S. and Masumura, R.A. (2005), *Grain growth and deformation in nanocrystalline materials*, Material Science and Engineering A 409, 125-130.

[106] Park, S.H.C, Sato, Y.S. and Kokawa, H. (2003), *Microstructure evolution and its effect on Hall-Petch relationship in friction stir welding of thixomolded Mg alloy AZ91D*, Journal of Material Science E 38, pp. 4379-4383.

[107] Nemat-Nasser, S. (1999), *Micromechanics: overall properties of heterogeneous materials / Sia Nemat-Nasser, Muneo Hori*, 2nd rev. ed., Elsevier.

[108] Relton, F.E. (1948)*, Applied Differential Equations*, Blackie.

[109] Srinivasan, S.K. (1974), *Stochastic Point Processes And Their Applications*, Griffin.

[110] Steidel, R.F. (1971), *An Introduction To Mechanical Vibrations,* J. Wiley.

[111] Streitenberger, P. and Zoller, D. (2006), *Effective growth law from three-*

dimensional grain growth simulations and new analytical grain size distribution, Scripta Materialia, 55, pp. 461-464.

[112] Stromberg, K.R. (1994), *Probability for analysts / Karl R. Stromberg ; based on lecture notes taken and processed by Kuppusamy Ravindran*, Chapman & Hall.

[113] Suo, Z. (2000), *Evolution of material structures of small features sizes,* International Journal of Solids and Structures 37, pp. 367-378.

[114] Synder, D.L. (1991), *Random Point Processes In Time And Space*, Springer-verlag.

[115] Torquato, S. (2002), *Random heterogeneous materials: microstructure and macroscopic properties / Salvatore Torquato,* Springer.

[116] Wasley, R.J. (1973), *Stress Wave Propagation in Solids*, *An Introduction*, Marcel Dekker.

[117] Williams, W.E. (1980)*, Partial Differential Equations,* Clarendon Press.

[118] Yoo, M.H., Yoshimi, K. and Hanada, S. (1999), *Dislocation Stability and deformations mechanisms of iron aluminides and silicide*, Acta Mater. Vol. 47, No. 13, pp. 3579-3588.

[119] Young*,* B.W (1981), *Energy Methods of Structural Analysis, Theory, Worked Examples And Problems*, The Macmillan Press Ltd, Printed in Hong Kong.

[120] Yu, C.Y., Sun, P.L. Kao, P.W. and Chang, C.P. (2004), *Evolution of microstructure during annealing of severely deformed aluminum*, Mat. Science and Engineering A366, pp. 310-317.

[121] Zhang, H.Y., Hu, Z.Q. and Lu, K. (1995), *Hall-Petch relationship in the nanocrystalline selenium prepared by crystallization from the amorphous state*, J. Appl. Phys. 77 (6), pp. 2811-2813.

APPENDIX A1

SCHEMATICS OF GRAIN GROWTH DUE TO GRC PROCESS

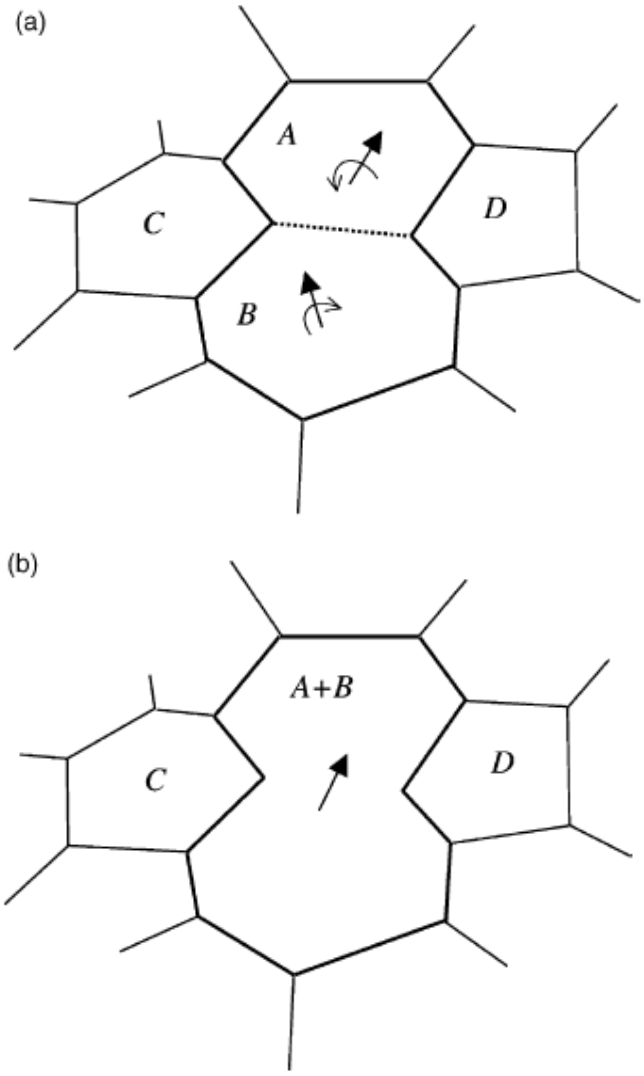

Figure A1 "*Schematic representation of a grain-coalescence event*. In (a), grains A and B sharing a common boundary (dotted line) rotate towards one another until the GB misorientation disappears, leading to the coalescence of the two grain sketched in (b). As can be seen in (b) the coalescence gives rise to topological discontinuity associated with the elimination of two triple junctions", [38].

APPENDIX A2

SCHEMATIC OF THE ELIMINATION OF TWO TRIPLE JUNCTIONS BY A SINGLE ROTATION-COALESCENCE EVENT

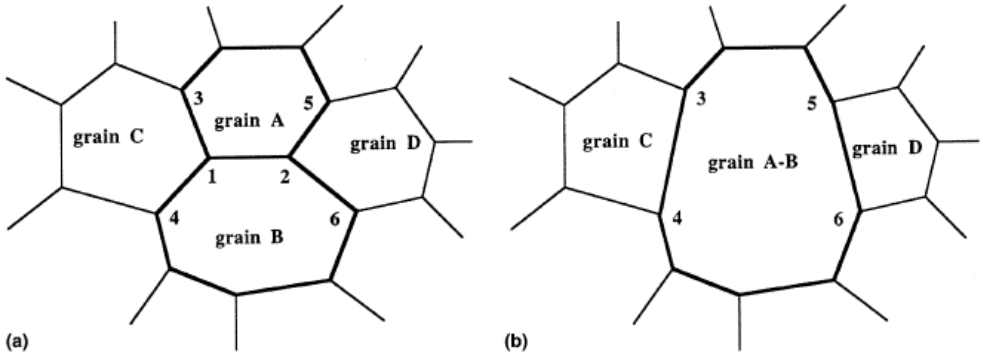

Figure A2 *"Schematic of the elimination of two triple junctions by a single rotation-coalescence event: (a) topology before and (b) after coalescence of grains A and B"*, [37]

APPENDIX B

EXPRESSION FOR CHANGE IN GRAIN SIZE DUE TO GRC PROCESS

If grain growth were due to Grain Rotation Coalescence mechanism only (GRC), then the grain size after a time interval, t, would be given by

$$r(t) = \sum_{i=0}^{N(t)} r_i \tag{B.1}$$

where N(t) is the number of coalescence of grains up to the time t. Since there are infinitely many grains in the aggregate, the entire time interval can be divided into disjoint contiguous infinitesimal time interval. It follows that *r(t)* can be written as the Riemann Stieltjes sum. The limit, in the mean square sense, of the sequence of such sums (B.1), is the mean-square Riemann Stieltjes integral with respect to the counting process *N(d),* [16], i.e. the stochastic integral

$$r(t) = \int_0^t r(s)dN(s) \tag{B.2}$$

and since *s* is a dummy variable, it follows that

$$dr(t) = r(t)dN(t) \tag{B.3}$$

APPENDIX C

INCREMENT OF THE INDIVIDUAL GRAIN SIZE AND GRAIN YIELD STRESS

The modified expression for the HPR that represents the size-property dependence (both HPR and Reverse-HPR) throughout the entire range of deformation as, [3]

$$\sigma(\mathbf{r}) = \sigma_0^{'} + A\mathbf{r}^{-1/2} - B(\mathbf{r}^{-1/2})^2 - C(\mathbf{r}^{-1/2})^3 \tag{C.1}$$

In our recently developed model of grain growth, [CHAPTERS 6, CHAPTER 8], a stochastic expression governing the incremental change of individual grain size in nano-materials is given as :

$$dr = M_0(Rr,T)\left(\frac{1}{r_c} - \frac{1}{r}\right)dt + D\sqrt{r}\,dW(t) + (1+a)r\,dN(t) \tag{C.2}$$

The stochastic differential expressions governing the increment of individual grain yield stress of Nano-Polycrystal due to grain growth are obtained from expressions (C.1) and (C.2) by the Ito's differential rule [16-20]. It follows that

$$dr^2 = \left\{2M_{mig}\left(\frac{r}{r_c} - 1\right) + D^2 r\right\}dt + 2Dr^{3/2}dW(t) + (3+4a+a^2)r^2\,dN(t) \tag{C.3}$$

$$d\sigma(r,t) =$$

$$\left\{M_{mig}\left[-\frac{A}{2}\left(\frac{1}{r_c r^{3/2}} - \frac{1}{r^{5/2}}\right) + B\left(\frac{1}{r_c r^2} - \frac{1}{r^3}\right) + \frac{3C}{2}\left(\frac{1}{r_c r^{5/2}} - \frac{1}{r^{7/2}}\right)\right] + D^2\left[\frac{3A}{8r^{3/2}} - \frac{B}{r^2} - \frac{15C}{8r^{5/2}}\right]\right\}dt$$

$$+ D\left\{-\frac{A}{2r} + \frac{B}{r^{3/2}} + \frac{3C}{2r^2}\right\}dW(t) + \left\{\frac{E}{r^{1/2}} - \frac{F}{r} - \frac{G}{r^{3/2}}\right\}dN(t) \tag{C.4}$$

$$\mathbf{d\sigma^2(r,t)} =$$

$$\left\langle \sigma_0^{'} M_{mig}\left\{-A\left(\frac{1}{r_c r^{3/2}}-\frac{1}{r^{5/2}}\right)+2B\left(\frac{1}{r_c r^{2}}-\frac{1}{r^{3}}\right)+3C\left(\frac{1}{r_c r^{5/2}}-\frac{1}{r^{7/2}}\right)\right\}+D^2\sigma_0^{'}\left\{\frac{3A}{4r^{3/2}}-\frac{2B}{r^{2}}-\frac{15C}{4r^{5/2}}\right\}\right.$$

$$+M_{mig}A\left\{-A\left(\frac{1}{r_c r^{2}}-\frac{1}{r^{3}}\right)+2B\left(\frac{1}{r_c r^{5/2}}-\frac{1}{r^{7/2}}\right)+3C\left(\frac{1}{r_c r^{3}}-\frac{1}{r^{4}}\right)\right\}+D^2A\left\{\frac{3A}{4r^{2}}-\frac{2B}{r^{5/2}}-\frac{15C}{4r^{3}}\right\}$$

$$-M_{mig}B\left\{-A\left(\frac{1}{r_c r^{5/2}}-\frac{1}{r^{7/2}}\right)+2B\left(\frac{1}{r_c r^{3}}-\frac{1}{r^{4}}\right)+3C\left(\frac{1}{r_c r^{7/2}}-\frac{1}{r^{9/2}}\right)\right\}-D^2B\left\{\frac{3A}{4r^{5/2}}-\frac{2B}{r^{3}}-\frac{15C}{4r^{7/2}}\right\}$$

$$-M_{mig}C\left\{-A\left(\frac{1}{r_c r^{3}}-\frac{1}{r^{4}}\right)+2B\left(\frac{1}{r_c r^{7/2}}-\frac{1}{r^{9/2}}\right)+3C\left(\frac{1}{r_c r^{4}}-\frac{1}{r^{5}}\right)\right\}-D^2C\left\{\frac{3A}{4r^{3}}-\frac{2B}{r^{7/2}}-\frac{15C}{4r^{4}}\right\}$$

$$\left.+D^2\left\{\frac{A^2}{4r^{2}}+\frac{B^2}{r^{3}}+\frac{9C^2}{4r^{4}}-\frac{AB}{r^{5/2}}-\frac{3AC}{2r^{3}}+\frac{3BC}{r^{7/2}}\right\}\right\rangle dt$$

$$+2D\left(\sigma_0^{'}+\frac{A}{r^{1/2}}-\frac{B}{r}-\frac{C}{r^{3/2}}\right)\left(-\frac{A}{2r}+\frac{B}{r^{3/2}}+\frac{3C}{2r^{2}}\right)dW(t)$$

$$+\left\langle 2\left\{E\left(\frac{\sigma_0^{'}}{r^{1/2}}+\frac{A}{r}-\frac{B}{r^{3/2}}-\frac{C}{r^{2}}\right)-F\left(\frac{\sigma_0^{'}}{r}+\frac{A}{r^{3/2}}-\frac{B}{r^{2}}-\frac{C}{r^{5/2}}\right)-G\left(\frac{\sigma_0^{'}}{r^{3/2}}+\frac{A}{r^{2}}-\frac{B}{r^{5/2}}-\frac{C}{r^{3}}\right)\right\}\right.$$

$$\left.+\frac{E^2}{r}+\frac{F^2}{r^{2}}+\frac{G^2}{r^{3}}-\frac{2EF}{r^{3/2}}-\frac{2EG}{r^{2}}+\frac{2FG}{r^{5/2}}\right\rangle dN(t) \qquad \text{(C.5)}$$

APPENDIX D

LIST OF PUBLICATIONS

1. **Tengen, T.B. and Iwankiewicz, R. (2006),** *Modelling of the microstructural features such as the number of faces of grains in an aggregate using the compound (marked) point fields***.** In proceeding of the 5th South African Conference on Computational and Applied Mechanics (**SACAM 06**), Cape Town, 16th – 18th January 2006, pages 25-35.
2. **Tengen, T.B., Wejrzanowski, T., Iwankiewicz, R. and Kurzydlowski, K.J. (2007),** *Statistical model of grain growth in polycrystalline nanomaterials***, *Solid State Phenomena***,** Vol 129, pages 157-163.
3. **Tengen, T.B. and Iwankiewicz, R. (2007),** *Modelling grain size probability distribution in nanomaterials*. In proceeding of the Six International Conference on Composite Science and Technology (**ICCST/6**), Durban, 22-24 January 2007. Special issue journal "***Composite Structure***".
4. **Tengen, T.B., Wejrzanowski, T., Iwankiewicz, R. and Kurzydlowski**, **K.J. (2008),** *The effect of grain size distribution on mechanical properties of nanometals***: *Solid State Phenomena*,** Vol. 140 pp 185-190.
5. **Tengen, T.B., Wejrzanowski, T., Iwankiewicz, R. and Kurzydlowski**, **K.J. (2008),** *Stochastic model of grain growth in nanometals*: in the proceedings of SACAM08 (26th-28th March 2008).

UPCOMING PUBLICATIONS

6. **Tengen, T.B., Wejrzanowski, T., Iwankiewicz, R. and Kurzydlowski**, **K.J. (2008),** ***S****tochastic approach to changes in mechanical properties of nano-crystalline materials induced by grain growth*: to be presented at EMRS 2008 (15th-19th September 2008).

7. **T Tengen, T.B., Wejrzanowski, T., Iwankiewicz, R. and Kurzydlowski, K.J.,** *Geometrical aspects of grain growth in polycrystalline materials*.
8. **Tengen, T.B., Wejrzanowski, T., Iwankiewicz, R. and Kurzydlowski, K.J.,** *Modelling of the probability distribution of the mechanical properties within nanomaterials*.